Dehydrogenation of alkanes to alkenes using CO_2 as a mild oxidant; an attractive method of CO_2 utilisation



Yige Gao

St. Cross College

Supervisors

Prof. Peter P. Edwards FRS ML

Prof. Simon Clarke

Prof. Richard G. Compton FRSC MAE

October 2022

A thesis submitted to the Department of Chemistry, University of Oxford for the Degree of Doctor of Philosophy in Inorganic Chemistry

Dehydrogenation of alkanes to alkenes using CO_2 as a mild oxidant; an attractive method of CO_2 utilisation

Yige Gao, St. Cross College

A thesis submitted to the Department of Chemistry, University of Oxford for the Degree of Doctor of Philosophy in Inorganic Chemistry

Abstract

CO_2 reduction has drawn much attention globally in the development of new processes and technology for avoiding the impact of serious climate change. On the other hand, the fossil fuel as energy resources cannot be easily replaced in order to greatly reduce CO_2 emission. CO_2 utilisation has been widely investigated in many manufacture/industries areas. This chemical conversion of CO_2 is not only adding value to the process of CO_2 reduction but also has economic and environmental benefits. Using CO_2 as a feedstock in the synthesis of high-demand chemicals in modern chemical industry would have a high economic value. However, due to the stability of CO_2, a highly effective heterogeneous catalyst is required in order to provide pathways to the synthesis of important chemicals in this way.

In this work, CrO_x-based catalysts supported on ZrO_2 have been developed and investigated for the dehydrogenation of propane using CO_2 with various metal oxides (Zn, Mn, Ca) as promoters. In addition, a different catalyst preparation method the “one-pot synthesis” has been used to develop a more effective catalyst than those in which the metal is added to a support in a conventional way. Another exciting part of the work is the regeneration process of deactivated catalysts for recovering their catalytic ability, thus extending their catalytic lifetime.

Based on this work, we show that the one-pot catalysts provide different catalyst surface morphologies, structures, and catalytic properties as compared to the conventional impregnation catalysts. The dominated ZrO_2 species changed from monoclinic phase in the impregnation catalysts to tetragonal phase in one-pot catalysts. It also reveals a more uniform and highly dispersed catalytically CrO_x active phase in which the CrO_x species can be involved in the reaction more effectively than the corresponding impregnated catalysts. In addition, one-pot catalyst showed an increase amount of the active Cr(VI) species. The introduction of a CaO promoter, the catalyst shows different surface acidity and basicity. In addition, the 2Cr/Ca-ZrO_2 shows an increase in both the overall propane conversion and propylene selectivity. The CaO promoter helps the process to reach 18% of propane conversion with 20% propylene yield and keep for 4-5 hours during the process. After the process, the propane conversion reduces to 10%, 15% product yield but with still about 93% propylene selectivity. Moreover, it also reduces the level of detrimental carbon deposition on the catalyst particles leading to enhanced stability and performance. In addition, the regeneration process can recover the catalytic ability for a continuous CO_2-PDH process which shows the good potential for the long-term stable performance of the one-pot catalysts.

The development of novel catalytic system for CO_2-PDH make this process more attractive and effective not only in reducing net CO_2 emission by using it to produce useful chemical products but also by helping reach the demand for these (propylene in this case). The work suggests that further development of catalysts for this and similar processes is desirable.

The work described in this thesis was performed in the Inorganic Chemistry Laboratory, University of Oxford from October 2018 until October 2022, under the supervision of Professor Peter P. Edwards and Professor Simon Clarke.

I declare that this thesis is entirely my own work, and except where otherwise stated, describes my own research, and has not been submitted previously for any degree at this or any other university.

Yige Gao

St. Cross College

October 2022

Acknowledgements

Thinking back about these 4 years in Oxford, I felt very much appreciated and satisfied. Not only because of what I achieved for my degree, but more about the knowledge I have learned, the experience I have had and the people I have met at this top world-class university. All of these become beautiful, remarkable and tressured memories for my future life.

During my time at Oxford, there are so many people I want to give thanks to. I would like to express my sincerest gratitude to my supervisor, Professor Peter Edwards for his guidance, encouragement and support during my study. His full support and trust have allowed me to complete my research independently. This has allowed me to be an independent young researcher. He also provided financial support for me. This helps me and my family release our pressure and allowed me to focus on my study to finish my degree. Even after his retirement in 2021, he is still giving all his support and care to me. I would also like to thank Prof. Simon Clarke. He became my supervisor after Prof. Peter Edwards' retirement. During these last several months towards finishing my degree, he provided full support and looked after me in the department. I am thankful for his support and efforts in my research and in this thesis. Also many thanks to my second supervisor, Prof. Richard Compton who has always offered the strongest support.

My thanks are extended to Dr. Tiancun Xiao, Prof. Jon Dilworth, Dr. Xiangyu Jie, Dr. Sergio Gonzalez Cortes and Dr. Benzhen Yao for all the generous advice and full support in my research work. Their experience and encouragement have opened my mind and learned a way to be professional during research and learn new laboratory technique skills. To all my colleagues in the PPE group, I am most grateful for all your kind help. Specifically, I must give my special thanks to Ms. Linda Webb who made everything well organised and happen in the group.

To all my friends in Oxford and in China. My roommate Zheying and all my lovely friends, Ally, Yue, Hannah, Yujia and more others in the chemistry department; life in Oxford would be so boring and couldn't be so enjoyable without you. My forever best friends, Amy and Yixue; even if we couldn't meet and talk very often, you are always by my side whenever I needed. Also, Qinyi and Huixin, these two nice and smart young ladies.

There is a special person I would like to thank here, Chengwei 'Cryin' Yuan from China. He is a professional League of Legends (LOL) player from the LPL region. I was impressed and encouraged by his faith, confidence, good personality and his thoughts. He is always passionate and motivated. He put all his effort into his career and always be positive even in a difficult situation. Although he would never be able to know me, I still want to express my thanks to him and all the best wishes to him and his future career. Through him, I also met grateful friends and we often share our life and thoughts with each other in an online chatting room (Mo 泽园后援会). Thanks for their continous encouragement, compliment and trust in me.

Finally and importantly, to my beloved parents Qian Jin and Junhai Gao, there is never enough thanks that can be expressed for all your support, love and trust. You are always my strongest and warmest back up. Your love and faith have always brought me power. For nearly 12 years of studying and living alone, I couldn't imagine how I would be through myself without you. I am most grateful for your wholeheartedly support in my decisions and your contribution is priceless. I would like to express my deepest thanks to my parents for raising me, care me and supporting me and not expecting any return. 爸爸妈妈，谢谢你们一直以来对我的无条件地关心和支持，我爱你们。

- Yige Gao, October 2022, Oxford

Contents

Abstract i

Declaration iii

Acknowledgements iv

Contents vi

List of Figures xi

List of Tables xvi

1 Introduction 1

1.1 The Climate Change Arising from CO_2 1

1.2 Approaches to CO_2 Reduction 6

1.2.1 CO_2 capture and storage (CCS) 7

1.2.2 CO_2 capture and utilisation (CCU) 13

1.2.2.1 Direct utilisation of CO_2 14

1.2.2.2 Conversion of CO_2 16

1.3 Oxidative Propane Dehydrogenation to Form Propylene Using CO_2 as Mild Oxidant 20

1.3.1 Development of propane dehydrogenation 20

1.3.2 Catalyst development for PDH 23

1.3.3 Funamental factors of catalyst design for CO_2-PDH 28

1.4 Thesis objective and research summary 30

2 Experimental Methods 42

2.1 Preparation of Catalysts 42

2.1.1 Impregnation method 43

2.1.2 One-pot synthesis 44

2.2 Catalysts Analysis 45

2.2.1 Reaction system 45

2.2.2 Gas Chromatography (GC) 47

2.2.3 Techniques used for characterisation of catalysts 50

2.2.3.1 X-ray Diffraction (XRD) 51

2.2.3.2 Scanning Electron Microscopy and Energy-dispersive X-ray spectroscopy (SEM-EDS) 53

2.2.3.3 Thermogravimetric Analysis (TGA) 55

2.2.3.4 X-ray Photoelectron Spectroscopy (XPS) 56

2.2.3.5 Temperature-Programme Desorption of Ammonia (NH_3-TPD) 58

2.2.3.6 Brunauer, Emmett and Teller (BET) surface analysis 60

3 The Dehydrogenation of Propane by CO_2 Over ZrO_2-Supported Catalysts Prepared by the Impregnation Method 64

3.1 Introduction 64

3.1.1 Proposed redox cycle of CO_2-PDH 66

3.1.2 Catalyst design for CO_2-PDH 69

3.1.2.1 Promoter effects by mixed metal-oxides catalysts on catalytic performance 72

3.1.2.2 The effect of the support on catalytic performance ... 74

3.2 Chapter Overview 77

3.3 Experimental Methods 79

3.3.1 Preparation of catalysts 79

3.3.2 Catalyst characterisation 80

3.3.3 Catalytic activity tests 80

3.3.3.1 Thermodynamic study of 2Cr-ZrO_2 for CO_2-PDH 80

3.3.3.2 Catalytic performance for CO_2-PDH 81

3.4 Results and Discussion 83

3.4.1 Catalytic performance of 2Cr-ZrO_2 83

3.4.1.1 Characterisations of 2Cr-ZrO_2 83

3.4.1.2 Catalyst activity under different conditions 87

3.4.2 Reactions over ZrO_2-supported CrO_x-based catalysts with different metal oxides as promoters 91

3.5 Conclusion 100

4 One-Pot Synthesis of CrO_x-based Catalysts for CO_2-PDH 108

4.1 Introduction 108

4.2 Chapter Overview 112

4.3 Experimental Methods 113

4.3.1 Catalyst preparation 113

4.3.2 Catalyst characterisation 114

4.3.3 Catalyst activity test 115

4.4 Results and Discussion 117

4.4.1 Catalyst characterisations of impregnated catalyst and one-pot catalysts 117

4.4.2 Catalytic activity tests of one-pot catalysts 134

4.4.3 Post-reaction analysis of one-pot catalysts, 2Cr-ZrO_2 and 2Cr/Ca-ZrO_2 143

4.5 Conclusion 154

5 Reproducibility and Life Cycle Assessment of the One-pot Catalysts 159

5.1 Introduction 159

5.1.1 Catalyst deactivation and lifetime 159

5.1.2 Life cycle assessment (LCA) 163

5.2 Chapter Overview 167

5.3 Experimntal Methods 168

5.3.1 Regeneration process of spent catalysts and catalytic tests of regenerated catalysts 168

5.4 Results and Discussion 170

5.4.1 The regeneration of the spent one-pot catalysts and their catalytic activity after regeneration 170

5.4.2 Environmental and sustainable considerations of the one-pot catalysts 178

5.5 Conclusion 182

6 Conclusions and Outlook 189

6.1 Catalyst Development for CO_2-PDH 189

6.2 CO_2 in Future 194

Appendix : Estimation of Errors 198

List of Figures

Figure 1.1. Carbon dioxide emissions from global fossil fuel combustion and industrial processes from 1750-2020 in billion metric tons....3

Figure 1.2. Diagram of ocean acidification by CO_2....3

Figure 1.3.Gibbs free energy of formation of organic chemicals....6

Figure 1.4. Flow diagram of carbon capture and storage....7

Figure 1.5. Various CO_2 capture methods and materials used currently under investigations....10

Figure 1.6. Diagram of geological and deep ocean storage of captured CO_2....12

Figure 1.7. A summary diagram of carbon utilisation techniques....17

Figure 1.8. Comparison between CCU and CCS....18

Figure 1.9. General flow diagram of propane dehydrogenation process.....23

Figure 1.10. An illustrated schematic of the catalyst for PDH....30

Figure 2.1. Schematic diagram of the micro reactor and online GC....45

Figure 2.2. Picture of the fixed-bed reactor and diagram of the catalysts loading in reactor tube for activity test....46

Figure 2.3. Picture of the flow meter used for flow rate check....47

Figure 2.4. Picture of GC (Perkin Elmer, Clarus 580)....50

Figure 2.5. Schematic diagram of Bragg's law....52

Figure 2.6. Scanning electron microscope column....54

Figure 2.7. Picture of the TA Instrument, SDT Q-600....56

Figure 2.8. X-ray strike of a surface and emission of a photoelectron....58

Figure 3.1. Proposed simplified reaction network for propane oxidative dehydrogenation 67

Figure 3.2. Proposed reaction mechanism of dehydrogenation of C_3H_8 in the presence of CO_2 68

Figure 3.3. Gibbs free energy of formation for selected chemicals..... 70

Figure 3.4. The effect of temperature on equilibrium conversion of propane and carbon dioxide and selectivity of propylene in the presence of propane reforming reaction .71

Figure 3.5. The effect of temperature on equilibrium product composition in the presence of propane reforming reaction 72

Figure 3.6. Catalyst preparation procedure of the widely-used impregnation method 79

Figure 3.7. XRD pattern of 2Cr-ZrO_2 (red), the pure Cr_2O_3 (green) and ZrO_2 (commercial) 84

Figure 3.8. TGA data and derivative plots of temperature programmed oxidation (TPO) of the 2Cr-ZrO_2..... 85

Figure 3.9. XPS peak fitting of Cr species of 2Cr-ZrO_2 86

Figure 3.10. Propane conversion and propylene selectivity over 2Cr-ZrO_2 at various temperatures 88

Figure 3.11. Propane conversion and propylene selectivity over 2Cr-ZrO_2 with different ratios of C_3H_8/CO_2 90

Figure 3.12. (A) The propane conversion and (B) propylene selectivity from the various samples during a 10h reaction 93

Figure 3.13. NH_3 desorption data vs. temperature by NH_3-TPD of (A) 2Cr-ZrO_2, (B) 2Cr/Mn-ZrO_2, (C) 2Cr/Zn-ZrO_2 and (D) 2Cr/Ca-ZrO_2 prepared by impregnation method. 96

Figure 3.14. TGA diagram of four spent impregnated catalysts 97

Figure 3.15. Picture of the four catalysts as their fresh and spent forms 99

Figure 4.1. Catalyst preparation procedure using the one-pot synthesis protocol ... 114

Figure 4.2. XRD pattern of both the impregnation method 2Cr-ZrO_2 (dark green), and the one-pot synthesis 2Cr-ZrO_2 (red) and that with the Ca-oxide promoter, 2Cr/Ca-ZrO_2 (blue) 117

Figure 4.3. XRD pattern of commercial (purple) and one-pot synthesis ZrO_2 118

Figure 4.4. The crystal structure of ZrO_2 (A) monoclinic phase and (B) tetragonal phase 119

Figure 4.5. SEM images of (A) 2Cr-ZrO_2 (imp) catalysts prepared using the impregnation method and (B) 2Cr-ZrO_2. catalysts prepared using the one-pot synthesis method 122

Figure 4.6. SEM images and EDS mapping of the elemental species on the surface of 2Cr-ZrO_2 (imp) samples prepared using impregnation method. (A) SEM (backscattered electron), (B) Cr map, (C) Zr map, (D) O map, and (E) EDS spectrum 123

Figure 4.7.SEM images and Energy-Dispersive X-ray elemental (EDS) mapping of the elemental species on the surface of 2Cr-ZrO_2 samples prepared using one-pot synthesis. (A) SEM (backscattered electron), (B) Cr map, (C) Zr map, (D) O map, and (E) EDS spectrum 124

Figure 4.8. (A)TGA data and (B) derivative plots of temperature programmed oxidation (TPO) of two one-pot catalysts (Blue-2Cr-ZrO_2, Red-2Cr/Ca-ZrO_2) and impregnation catalyst (Yellow-2Cr-ZrO_2) 127

Figure 4.9. XPS peak fitting of Cr species of one-pot synthesis catalyst (A) 2Cr-ZrO_2 and (B) 2Cr/Ca-ZrO_2 129-130

Figure 4.10. NH_3 desorption data vs. temperature by NH_3-TPD of (A) 2Cr-ZrO_2 and (B) 2Cr/Ca-ZrO_2 prepared by one-pot synthesis 133

Figure 4.11. The propane conversion and propylene selectivity from the sample using 2Cr-ZrO_2 prepared by one-pot synthesis in a 10h catalytic test reaction 135

Figure 4.12. Proposed reaction mechanism of dehydrogenation of C_3H_8 in the presence of CO_2 137

Figure 4.13. The propane conversion and propylene selectivity from the various samples (A) 2Cr/Ca-ZrO_2 and (B) 3Cr/Ca-ZrO_2 from one-pot synthesis during a 10h reaction 138

Figure 4.14. Picture of the two one-pot catalysts as their fresh and spent forms. ... 143

Figure 4.15. TGA diagram of two spent one-pot catalysts 144

Figure 4.16. SEM images of spent (A) 2Cr-ZrO_2 and (B). 2Cr/Ca-ZrO_2 prepared by one-pot synthesis 145

Figure 4.17. SEM images and EDS mapping of the elemental species on the surface of spent 2Cr-ZrO_2 samples prepared using one-pot synthesis. (A) SEM (backscattered electron), (B) Cr map, (C) Zr map, (D) O map, (E) C map, and (F) EDS spectrum . 146

Figure 4.18. SEM images and EDS mapping of the elemental species on the surface of spent 2Cr-Ca/ZrO_2 samples prepared using one-pot synthesis. (A) SEM (backscattered electron), (B) Cr map, (C) Zr map, (D) O map, (E) Ca map, (F) C map, and (G) EDS spectrum 148-149

Figure 4.19. XRD patterns of (A) spent and (B) regenerated 2Cr-ZrO_2 (blue) and 2Cr/Ca-ZrO_2(red) catalysts prepared by the one-pot synthesis approach 150

Figure 4.20. XPS peak fitting of Cr species of spent one-pot synthesis catalyst (A) 2Cr-ZrO_2 and (B) 2Cr/Ca-ZrO_2 152-153

Figure 5.1. A general diagram of coke formation on the catalyst surface 161

Figure 5.2. Stages of LCA based on ISO 14040.....165

Figure 5.3. Results obtained for regenerated 2Cr-ZrO_2 catalyst (A) The propane conversions at reaction times of 3h, 6h and 10h during each of six cycles with regeneration between each cycle, (B) the percentage yield and selectivity of propylene after the treatments at the six-hour point during each cycle 172

Figure 5.4. (A) The propane conversions rate at reaction time 3h, 6h and 10h after 6 cycles of regeneration, (B) the percentage yield and selectivity of propylene after the treatments using 2Cr-Ca/ZrO_2 176

Figure 6.1. The experimental procedures diagram of the one-pot synthesis 190

List of Tables

Table 3.1. Summary of the designed CrO_x-based catalysts supported on 10 mmol ZrO_2 80

Table 3.2. Summary of NH_3-TPD data the CrO_x-based catalysts with different promoters 95

Table 4.1. Summarisation of the catalysts used in this chapter 114

Table 4.2. Elemental analysis data of Cr, Zr, Ca and O in catalysts in wt% 125

Table 4.3. Binding energies of the various Cr species for both the impregnation catalysts 2Cr-ZrO_2 (imp) and those from the one-pot synthesis 2Cr-ZrO_2 and 2Cr/Ca-ZrO_2 131

Table 4.4.Summary of catalytic results of four separate 'one-pot' catalysts with 1-3 mmoles of Cr loading 142

Table 4.5. Summary of CO_2 conversion of four 'one-pot' catalysts with 1-3 mmoles of Cr loading 142

Table 4.6. Binding energies and relative proportions of various Cr species of spent catalysts 152

Chapter 1

Introduction

1.1 The Climate Change Arising from CO_2

The global warming issue due to the emission of greenhouse gases has received widespread in the recent decades from the environmental and energy perspective. Among other greenhouse gases, such as CH_4, N_2O, and O_3, CO_2 (derived from fossil fuel and industrial processes) is one of the most well-known and recognised worldwide as a major contributor towards global warming.

As the world's population grows and countries' economies continue to advance, our developing and future demands ensure that energy is now regarded as one of the defining issues of this century.[1] Currently, more than half of the global energy requirement is satisfied by the aerial combustion of fossil fuels, such as petroleum, coal, and natural gas which inevitably give rise to a continuous increase in CO_2 levels in the atmosphere, and this contributes over 60% to global warming.[2–6] Over 40% of the worldwide CO_2 emissions are caused by electricity generation in fossil-fuel power plants. Furthermore, the conversion of raw materials in industries such as aluminium production, textile manufacture, pulp and paper manufacture, refineries, cement, iron, and steel production as well as landfills also result in additional CO_2 emissions to the atmosphere.[7]

It is recognised that global warming is a contributor to climate change and leads to devastating events such as droughts, hurricanes, torrential rains, floods, tornados and

wildfires across the world. These events are responsible for thousands of deaths and have adversely affected the economic development of many countries and the loss of billions of dollars, across the globe.[7] In addition, the increase in global temperature also accelerates the extinction of species on Earth. In Figure 1.1 we show the CO_2 concentration in the atmosphere which has increased rapidly after industrial revolution due to the dominant use of fossil fuels for manufacturing and other industries.[8,9] In recent years (since 2015), the CO_2 concentration has increased by about 4%, and this emission rate has been maintained or even increased. In 2021, atmospheric carbon dioxide levels reached a high of 400 parts per million, in comparison to 1960 levels which stood at about 300 parts per million.[8] In addition, the increase in CO_2 concentration in the atmosphere also leads to marine acidification. In Figure 1.2 we show how CO_2 could cause ocean acidification. Over the last million years, average ocean surface pH has been relatively stable, oscillating between 8.3-8.2. Rapid increases in atmospheric CO_2 levels, CO_2 is partially absorbed by the ocean, causing a decline in pH and ocean acidification. The ocean pH decreased from 8.11 to below 8.06, corresponds to an increase in oceanic acidity of about 30%.[10] In recent decades, ocean acidification has been occurring 100 times faster than during natural events over the past 55 million years. These rapid chemical changes added pressure on marine ecosystems.[11,12]

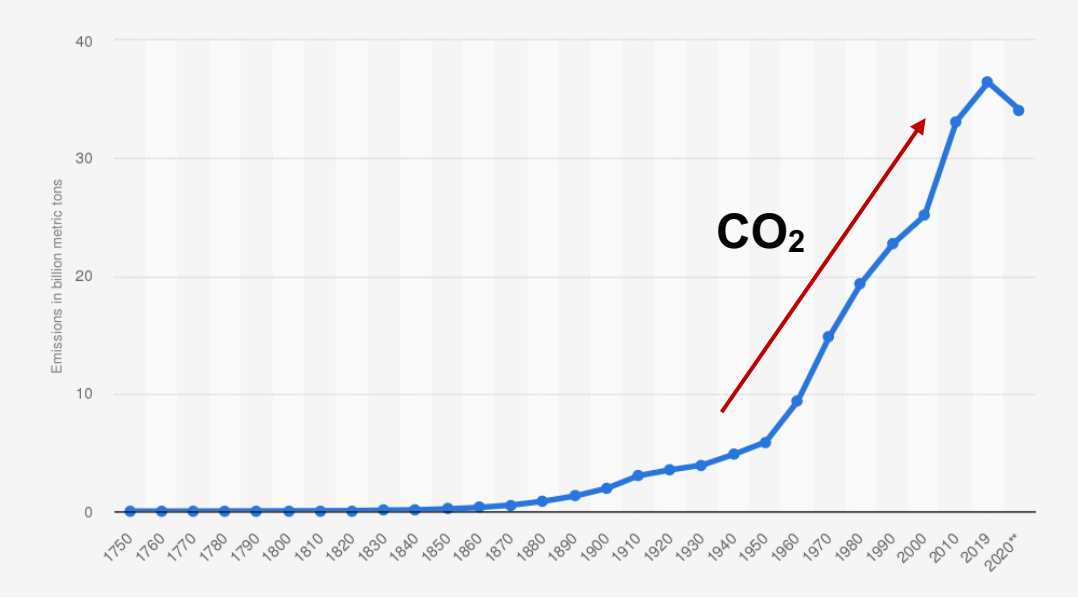


Figure 1.1. Carbon dioxide emissions from global fossil fuel combustion and industrial processes from 1750-2020 in billion metric tons.[9]

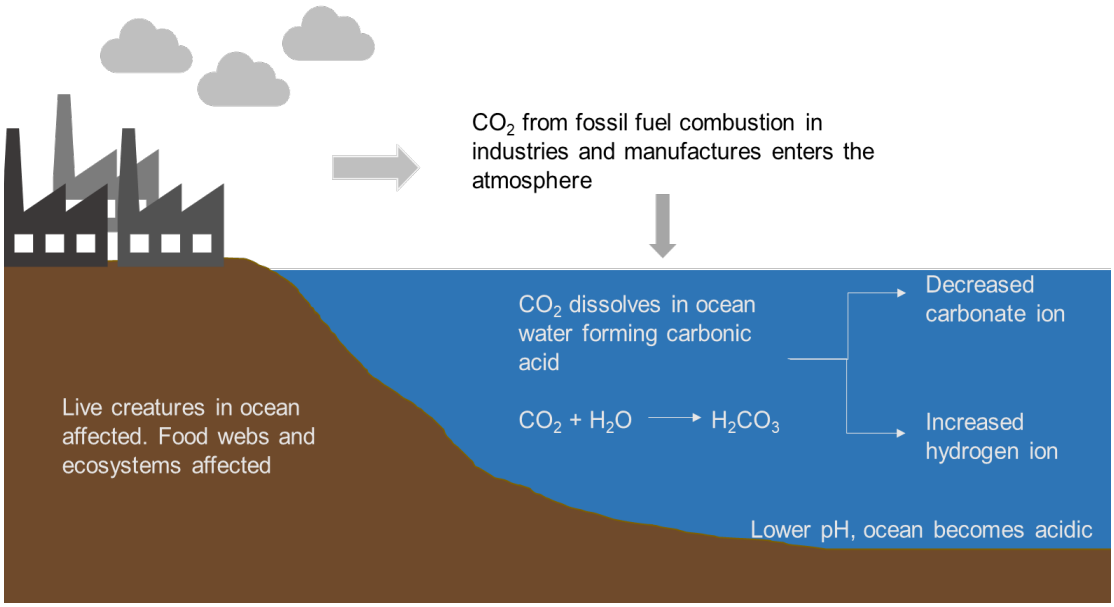


Figure 1.2. Diagram of ocean acidification by CO_2.[13]

To mitigate global warming or at least slow down the greenhouse gas emission rate, especially CO_2 emissions, both the Kyoto Protocol in April 2005 and the Paris Agreement in 2016 have been confirmed and signed by different countries around the world as the official agreements for confronting global climate challenge. These agreements stipulate the average percentage reduction of greenhouse gas for signature countries with the aim of limiting the global temperature increase to 2 °C above the pre-industrial level by 2100.[14] It has been pointed out that to achieve the 2 °C goal, the corresponding CO_2 concentration has to be stabilised at 450 ppm (already reached at 2020) and the carbon emission should be significantly reduced from the current Giga tonne scale.

In fact, the natural removal or the reduction of CO_2 through forests and oceans is simply not enough to remove the excessive amount of CO_2 present in the atmosphere. Several options have been advanced to reduce CO_2 emissions. First, improving the fuel/energy efficiency to reduce the energy demand. Second, renewable energies such as hydropower, wind and solar energy need to be significantly advanced to serve as alternatives to fossil fuels. These energies are widely used to produce electricity. In contrast to all other fuels, renewables used for generating electricity are predicted to grow by almost 7% in 2020.[15] However, these sources, especially solar and wind power largely depend upon geographical, nocturnal, and seasonal variations.[7] For hydropower, the cost of building a large hydro-power station is still a challenge. On the other hand, the efficiency of transporting the produced electricity is also a big challenge.

Hydrogen is recognised as a clean energy resource, through the combustion or oxidation reaction of hydrogen, energy is released as heat or as electricity in fuel cell and water is the only by-product. Hydrogen can be produced from water which is abundant and generously distributed throughout the world.[16] It can also be produced by different methods, such as electrolysis, steam reforming, coal gasification, biomass gasification and so on. The energy resources for hydrogenation production include

both renewable (hydro, wind, solar, geothermal) and non-renewable (coal, natural gas, nuclear) resources.[17] However, the costs of hydrogen production and delivery, hydrogen storage systems, and the cost of hydrogen utilisation systems need to be overcome for large and widespread commercial use. Nowadays, work on renewable energies is still attracting many researchers. Unfortunately, there still exists a large development gap to match the global energy demand. Therefore, a more sensible energy resource management is the prerequisite for the sustainable development and CO_2 reduction of future generations.

Conversely, there are potential commercial applications for CO_2. It has been developed in refrigeration systems to act as a natural cooling agent. It also can be used in fire extinguishers by displacing oxygen or taking oxidising agents away from the fire triangle, and also finds applications in the food and beverage industry.[18]

Converting CO_2 to useful fuels and chemicals can be an attractive possibility. However, the chemical properties of CO_2 still make it difficult to convert to other products as it is almost invariably at the very end of the energy consumption chain both in human life and industry. From the fundamental thermodynamic perspective, CO_2 is a very stable and unreactive gas, as shown in Figure 1.3, at the very bottom line of the energy diagram. This means that any process to convert CO_2 into other chemicals requires a large energy input, and thus is only logical if the energy comes from carbon-emission-free sources such as renewable energy.[19]

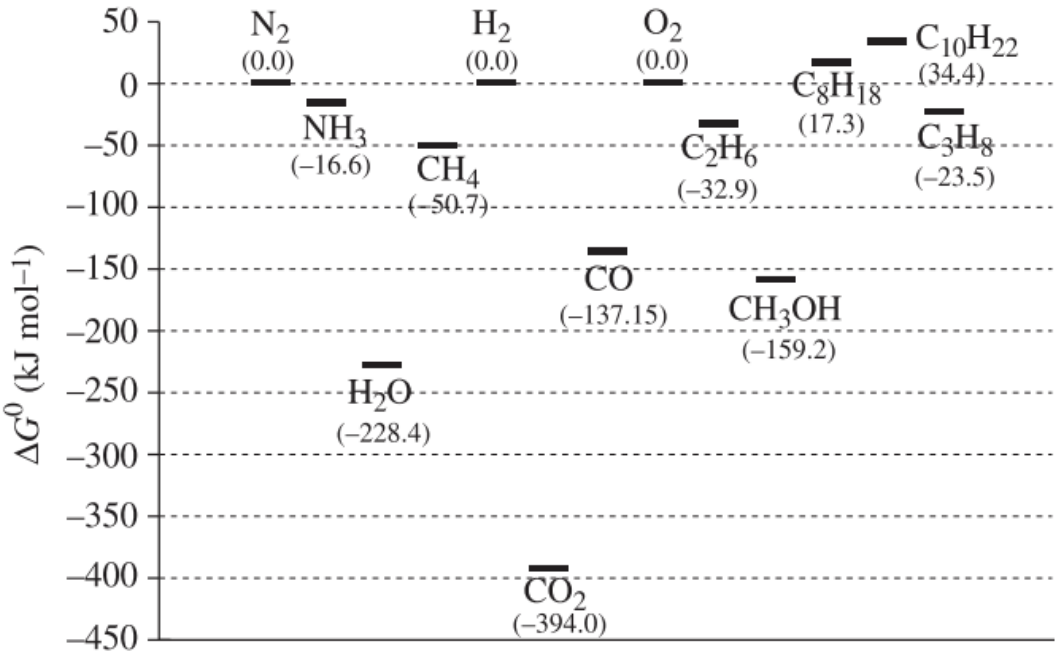


Figure 1.3. Gibbs free energy of formation of organic chemicals.[1]

1.2 Approaches to CO_2 Reduction

CO_2 reduction has drawn much attention globally in new pathways or processes principally for several major reasons. First, the growing recognition that large reductions in global CO_2 emissions are needed to avoid serious climate change impacts. Second, the realisation that large emission reductions cannot be achieved easily or quickly simply by using less energy or by replacing fossil fuels with alternative energy sources that emit little or no CO_2. The reality is that the world today relies on fossil fuels for over 85% of its energy use.[20] Therefore, several different pathways and technologies have been developed and investigated for reducing carbon emissions. Here, we separate these approaches into two large divisions, CO_2 capture and storage (CCS) and CO_2 capture and utilisation (CCU).

1.2.1 CO_2 capture and storage (CCS)

Many current approaches for the reduction of CO_2 emissions are focusing on the technology of carbon capture and storage (CCS), and these have received increasing attention over the past decade.[20,21] It is considered a potential method of limiting atmospheric emissions of CO_2. Energy-economic models show that adding CCS to the suite of other GHG reduction measures significantly lowers the cost of mitigating climate change.[22] Through the CCS process, CO_2 gas from industrial and energy-related sources is separated straight after emission, then captured and transported to a storage location which is long-term isolated from the atmosphere such as a deep geological site, ocean storage and mineral storage.[23] Figure 1.4 shows a simplified flow diagram of CCS process.

As for the CO_2 capture process itself, a one-size-fits-all technology would not be suitable for the numerous and varied industrial processes generating CO_2. For that reason, there are a wide range of CO_2 capturing systems to ensure compatibility with the specific industry or process. For example, power plants and oil refineries are getting closer to implementing CO_2 capturing systems at a large-scale, while the cement and the iron and steel industry will still have to overcome the transition from small-scale demonstration plants to industrial deployment.[6]

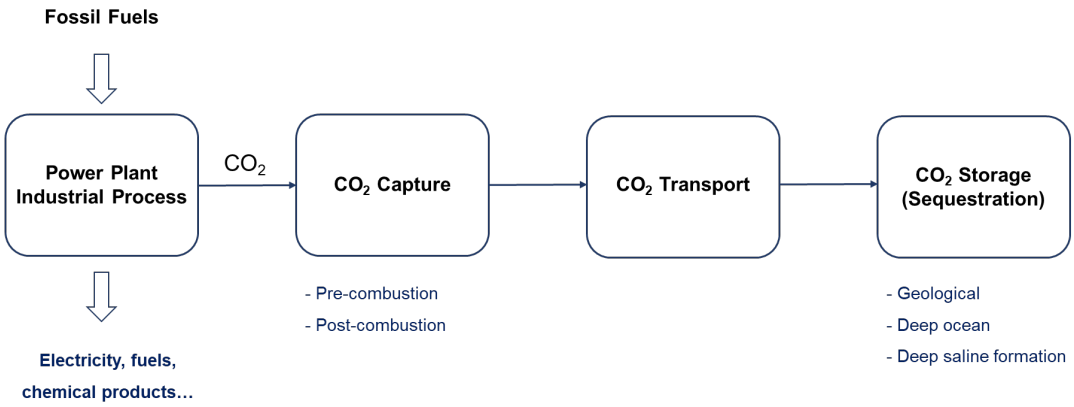


Figure 1.4. Flow diagram of carbon capture and storage.

In the totality of CCS processes, CO_2 can be captured by the pre- or post-combustion method. In the pre-combustion process, the fuels will be pre-treated before combustion. For example, the pre-treatment of fossil fuels will involve a gasification process (partially combusted or reformed) conducted in a gasifier under a limited oxygen level at elevated pressures (typically 30–70 atmospheres). This step allows forming "synthesis gas" which is a mixture of mainly CO and H_2.[24] Then the gas mixture will undergo the water gas shift reaction with steam forming more H_2, while the CO gas will be converted to CO_2.[25] However, this conversion enabling CO_2 capture before fuel combustion may not be available for some processes.

The post-combustion method means that the CO_2 is removed from the gas flow after the combustion process. However, the CO_2 level in combustion flue gas is sometimes quite low (less than 10%). The energy penalty and associated costs for the capture are elevated.[25] To isolate the CO_2 from the flue gas stream before transportation, different physical and chemical processes involving absorption, adsorption, cryogenic capture other advanced concepts have been developed. Oxy-fuel combustion is also used for CO_2 capture, which only is applied to the process involving combustion, such as power plants using fossil fuel. Fuel is burned with pure oxygen to produce flue gas with high CO_2 concentrations. This avoids the need for chemicals or other ways of CO_2 separation from flue gas. The disadvantage is that oxygen is expensive and the environmental impacts, including CO_2 emissions, associated with its production are high because of the energy-intensive air separation processes.[6]

The most developed separation method in the oil and chemical industries involves absorption by chemical or physical solvents.[26] This technology has been used intensively for both post-combustion (with chemical solvents by chemical reaction) and pre-combustion capture (with physical solvents, based on the gas solubility within a solvent).[27] Chemical absorption will be achieved by using aqueous ammonia or amine-based solvents such as mono-ethanolamine (MEA), diethanolamine (DEA), and N-

methyl diethanolamine (MDEA) and also alkaline solutions such as $Ca(OH)_2$ and NaOH. These solvents and solutions are the most commonly used for post-combustion capture in various industries, including cement, iron and steel, power plants and oil refineries.[6,14,28–31]

The well-established commercial physical absorption technologies for pre-combustion CO_2 capture include Selexol, a mixture of diethyl ether of polyethylene glycols, Rectisol and Purisol.[14] Recently, ionic liquids (IL's) have been identified as suitable alternatives to the conventional physical solvents used in the above processes. Their inherent properties include low volatility, low vapour pressure, high thermal stability at elevated temperatures and low regeneration energy requirements to help the CO_2 capture process.[14] Chemical absorption relies upon the regeneration by increasing the temperature of the adsorbent, and therefore, optimal selection of solvents with an optimum combination of thermal and physical properties is important in developing energy-efficient absorption-based CO_2 capture.[14]

In other studies on CO_2 capture, instead of solvents and solution-based processes, various solid materials have been developed, such as zeolites, porous carbons, porous organic polymers, covalent organic frameworks (COFs) and metal-organic frameworks (MOFs).[32] These materials have high surface area and porosity, which allows them to favour CO_2 adsorption. However, some of the materials still require the presence of co-catalysts or electron sacrificial agents during their production which serve to pollute the environment. The current technologies developed or proposed so far are not cost-effective at the current stages. Moreover, the high regeneration temperatures, limited CO_2 adsorption capacities and high production cost of these materials have hindered the development of CCS technologies.

Importantly, no large-scale operation has been fully deployed yet. There are also other CO_2 capture methods, such as membrane separation, chemical looping, hybrid

process and so on. Figure 1.5 shows a summary of currently developed carbon capture methods.

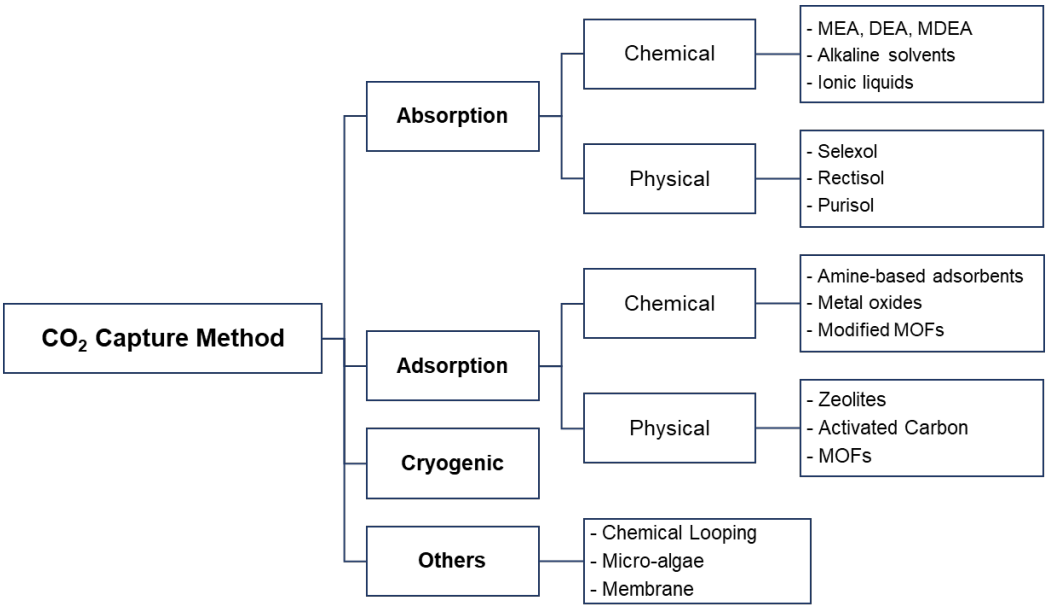


Figure 1.5. Various CO_2 capture methods and materials used currently under investigations.[33–35]

In summary, whilst there has been significant progress within the past few years, most CO_2 capture technologies still have many challenges to become commercially available in all different industries. There needs to be cooperation between materials and chemical scientists and industrial engineers to fill the gap between the characteristics of the materials and process performance. The vision is to build a unique and comprehensive design of capture technologies with high efficiency, cost-effectiveness and a great contribution to reducing CO_2 emissions.

Once the concentrated CO_2 has been captured, it can be transported by pipeline to the storage site. CO_2 can be stored in geological formations such as deep saline aquifers, deep oceans and/or as mineral carbonate/rock in the deep underground which has no other practical use (Figure1.5).[6] The common and widely used storage method is

geological storage, which involves an injection of CO_2 at depths of more than 1 km.[6,24] The CO_2 storage temperatures must be above the critical value (31 °C) with high pressures over 100 atmospheres and above, to give densities of the order of 500 kg/m^3. Geological storage is at present considered to be the most viable and promising option for the storage of the large CO_2 quantities needed to effectively reduce global warming and related climate change.[6,23,25] But the selection of a suitable geological storage site is very important. General requirements for geological storage of CO_2 include appropriate porosity, thickness, and permeability of the reservoir rock, a cap rock with good sealing capability, and a stable geological environment.[25] On the other hand, geological storage also depends on the distance from the source of CO_2, effective storage capacity, pathways for potential leakage and general economic constraints that may limit the feasibility of being a storage site. Deep saline aquifer formations are also being explored for CO_2 storage with a large potential storage capacity of about 700–900 Gt of CO_2.[6] Ocean storage relies on the fact that the ocean bed has a huge capacity to store injected CO_2 at great depths. Yet, ocean storage has never been tested on a large scale even though it has been studied for a long time. The main concerns with CO_2 storage geologically or in the deep ocean are its possible leaks (up to 25 $GtCO_2$ of additional emission in 21st Century[36]) and related damage a concentrated CO_2 stream would cause if it escaped into the environment. The annual leakage rates reported in the literature range from 0.00001% to 1%, depending on the permeability of the geological structure and its faults or defects.[37,38] Moreover, the time of storage and the safety of such a big amount of high-pressure gas storage and transport is also a big question. There are some ongoing CCS projects around the world from the pilot to commercial scale which have been operated more than 10 years.

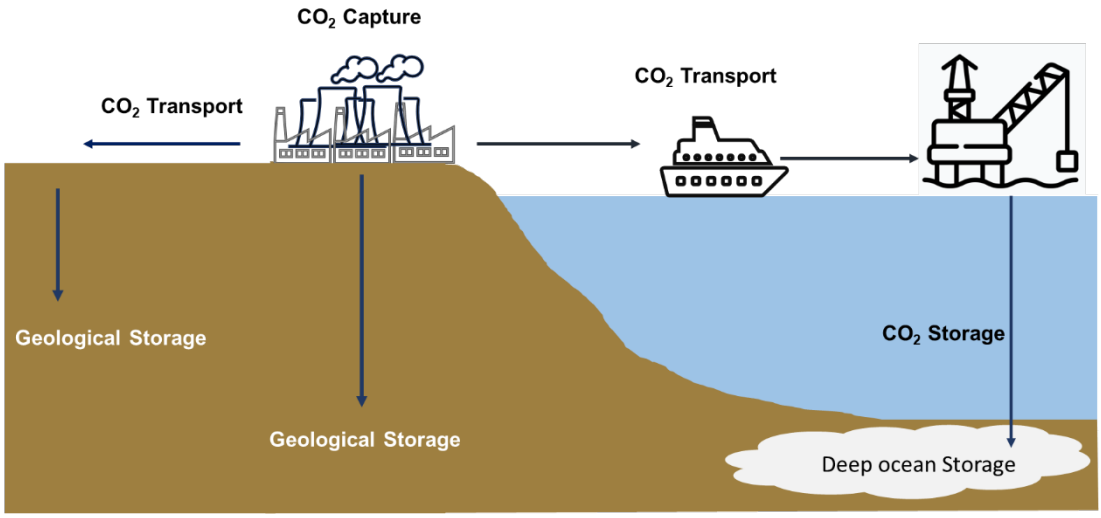


Figure 1.6. Diagram of geological and deep ocean storage of captured CO_2.

In fact, CCS is still not yet fully commercially demonstrated in its primary industrial application even after decades of research and development. CCS still faces a number of significant technical and economic barriers that must be overcome. On the technical side, the main challenge is the uncertainty in CO_2 leakage rates which makes the storage unsafe and violates the initial aim of CO_2 reduction. Also, the leakage can cause some environmental problems, for example, the leakage from deep ocean storage will cause ocean acidification as mentioned before. Besides, the design and build of the CO_2 transportation pipes and storage sites still require more investment and may produce CO_2 during construction. Furthermore, the cost of CCS is relatively high, due mainly to the high cost of CO_2 capture, which includes the cost of CO_2 compression needed for transport and storage. This has prompted a variety of governmental and industrial research focused on developing more cost-effective methods of CO_2 capture. On the other hand, in some countries, CCS is not a viable option as their geological storage capacity is limited or in some cases only available offshore, thus increasing transportation and injection costs. One of the main economic obstacles is the fact that it is an unprofitable activity that requires large capital

investment. In some countries, there are no incentives or subsidies for CCS which is going to make its development and deployment difficult.

1.2.2 CO_2 capture and utilisation (CCU)

Beyond CCS, another strategy involves the capture and subsequent conversion of CO_2 into high-value-added chemicals and fuels. This CO_2 conversion and utilisation (CCU) concept has been gaining significant attention in recent years. The utilisation of CO_2 is varied and can be technological, biological or chemical and all these are seeking to improve or replace traditional processes. This is because of the climate change considerations: the utilisation of CO_2 would be able to reduce CO_2 emissions into the atmosphere and could lead to a reduction in the extraction of CO_2 from fossil fuels.[39] It is also partly because using CO_2 as a feedstock can result in a cheaper or cleaner production process compared with using conventional hydrocarbons. The conversion and utilisation of CO_2 can produce long-term-non-degenerating products such as polymers and small molecule products important for various chemical processes such as methanol, syngas and olefins and so on.

In most of the literature, the term 'CO_2 utilisation' is considered as another extension of CCS and only refers to the use of CO_2, at concentrations above atmospheric levels, directly or as a feedstock in industrial or chemical processes, to produce valuable carbon-containing products.[40] CO_2 utilisation can be classified into direct and indirect uses. Direct use involves using CO_2 at its pure state or suspended in a solution, which directly goes into products. The direct or technological use of CO_2 includes applications such as dry cleaning, water treatment, food industry, and as a solvent for the extraction of compounds with supercritical CO_2 ($scCO_2$), among others.

1.2.2.1 Direct utilisation of CO_2

The current mostly and commercially direct use of CO_2 is in the food and drink industries. CO_2 is commonly used as a carbonating agent for sparkling and soft drinks; for food preservation, packaging gas CO_2 is utilised as a replacement for the toxic elements used for food disinfection (e.g. n-hexane).[39] Moreover, CO_2 can be as a solvent for the extraction of flavours and in the decaffeination process.[6]

In the chemical industry, solvents have been largely used with enormous environmental and economic costs. Traditional organic solvents used in the chemical industry, with their flammability, smog formation, toxicity, and the risk of inhalation, contribute greatly to the environmental and human health impacts.[41,42] The ideal solvent should be non-flammable, non-toxic for both humans and the environment, abundant, renewable, easy to prepare and separate from product, low cost and would not contribute to smog or global warming.[39,41] In this case, CO_2 shows its possibility to be used as a solvent even though it is related to global warming. CO_2 is used as a solvent in both liquid (lCO_2) and $scCO_2$ states. Pure CO_2 gas is in a supercritical state when exceeding its critical value, the temperature is 304.1 K and pressure 7.4 MPa. $scCO_2$ has been largely used in the extraction of functional ingredients for food, beverages and personal care products.[41,43] However, due to the low polarity of CO_2, its use as an extraction solvent is mainly restricted to non-polar components.[43] In spite of the limited solubility of many reactants in $scCO_2$, numerous organic synthetic procedures have been conducted using $scCO_2$.[39,41–43] The reactions where the use of $scCO_2$ has been most developed are hydroformylation, hydrogenation, oxidation, biocatalysts, and polymers synthesis. Even though recycled CO_2 would be used as the solvent, a contribution to global warming would still be generated by using energy to compress the CO_2 to a liquid or supercritical state. This operation involves a generally high cost, which must be taken into account when comparing it with the energy consumption of conventional solvents and as a CCU technique.

Other applications can be found in the pharmaceutical industry where CO_2 can be used as a respiratory stimulant or as an intermediate in the synthesis of drugs and CO_2 can replace the organic solvents in the extraction of compounds.

Enhanced gas or oil recovery (EGR/EOR) is an extension concept of CCS technology. In EGR/EOR process, instead of finding a suitable geological CO_2 storage site, the concentrated and compressed CO_2 may be placed into oil reservoirs to pressurise rock formations and to release any oil/gas that may have been trapped in the formation.[14,24,39,44] Some of the literature classifies this process as CCS, as the CO_2 replaces the ejected oil or gas[6,45,46]; some of the reviews describe EGR/EOR as a direct (physical) utilisation technique of CO_2 and classify it as CCU.[14,26,39,44] In my point of view, I would like to consider the EGR/EOR techniques as a direct utilisation of CO_2 as in this process, CO_2 is involved in oil production and manufacture instead of just being stored like in simple CCS. It has been suggested that the EGR/EOR would be a perfect route to gain the CO_2 mitigation requested in the economical mining of fossil fuels.[47] During the CO_2-EOR process, the injected CO_2 will mix with the oil and release it from its rock formation. This stream will be then pumped to the surface and the CO_2 emerging with the oil is separated and resupplied into the cycle to repeat the process. Most CO_2-EOR systems use naturally occurring CO_2, but lately, research has focused on using CO_2 captured from other different industries and power plant.[14] However, this consumption is likely to be accompanied by further CO_2 emission, and thus will not adequately address the fundamental issue. Despite this, EOR currently contributes to only 3% of CO_2 utilisation. Key drawbacks in such technologies could lie in the energy consumption associated with separation, purification, compression, transportation, and storage processes.[32]

1.2.2.2 Conversion of CO_2

Unlike direct CO_2 utilisation, the indirect CO_2 utilisation focuses on converting CO_2 into chemicals, materials and fuels through different chemical and biological processes.[6,48] CO_2 is a non-toxic and cheap (naturally abundant) feedstock and the demand for fuels is also very high worldwide. The high price of fossil fuels keeps establishing new records. Complete or partial recycling of CO_2 into high-energy-density liquids or gaseous fuels is a very attractive research area.[45] The production of fuels from CO_2 can be achieved through different reaction processes. By reduction or hydrogenation, the C=O bonds are broken to produce chemicals such as methane, methanol, syngas and formic acid; through the Fischer - Tropsch process, CO_2 is used as a feedstock to produce jet fuels and other hydrocarbons.[6,14,26,39,45]

Dry reforming of methane (DRM) is one of the main processes to obtain fuels from CO_2.[1,39]

$$\text{DRM: } CH_4 + CO_2 \leftrightarrow 2CO + 2H_2 \qquad (1.1)$$

$$\Delta H^0_{296} = +247 \text{ kJ/mol}^{49}$$

This reaction (1.1) is a strongly endothermic process where methane (CH_4) is heated in the presence of a metal-based catalyst to produce a gas, commonly called syngas ($CO + H_2$).[18,48,49] Despite its great environmental potential, DRM is not considered an industrially mature process.[14,39] The extremely highly endothermic reaction requires a lot of energy. It also has long reaction time and the requirement of a pure CO_2 supply. These disadvantages make the DRM an impractical process that still needs additional developments and investigations.

CO_2 hydrogenation is another technique in CO_2 utilisation. It is simply defined as the addition of H_2 to CO_2.[50] The direct fixation of CO_2 in the biomass for the biological use is another use of CO_2. To fix CO_2 in biomass, CO_2 can be used to cultivate microalgae

used for the production of biofuels.[51,52] CO_2 could also be employed to produce fine chemicals through carboxylation reactions. The carboxylation reactions use CO_2 as a precursor in the production of organic compounds, such as carbonates, acrylates and polymers.[6,39]

Mineral carbonation of CO_2 or CO_2 mineralisation refers to the reaction of CO_2 with chemical components containing alkaline earth oxides such as CaO and MgO, to produce stable mineral carbonates instead of decomposition of carbonate.[48,53] This applies if the application of the carbonates goes beyond storing CO_2 to be used as a material; for example, in the construction industry. The mineralisation process could able be viewed as a sequestration method because it aims at permanently fixing CO_2. The main advantage of mineral carbonation is the formation of stable carbonates capable of storing CO_2 indefinitely, without the risk of CO_2 leakage as in CCS (geological storage of pure CO_2).[46,51] The carbonates are stable and safe.[46,54] However, this technology is not fully developed for large-scale applications as the energy penalty and costs are still too high.

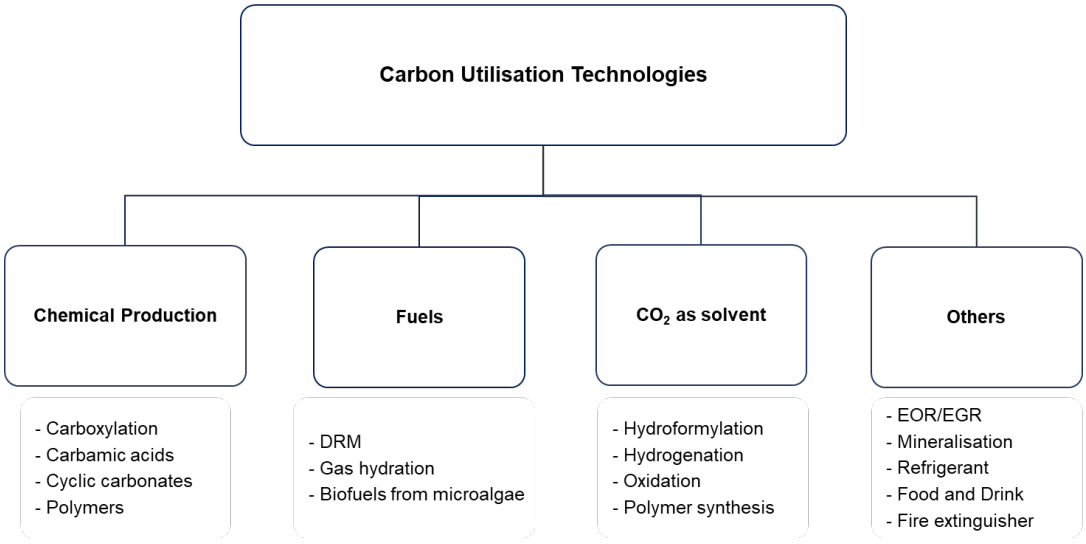


Figure 1.7. A summary diagram of carbon utilisation techniques.

Until now, most carbon resources are based on crude oil, natural gas and coal. CO_2 utilisation is often promoted as a pathway to reduce the net costs or increase the profits of reducing CO_2 emissions or removing CO_2 from the atmosphere. By converting CO_2 into valuable products and fuels, CCU would be able to offer economic benefits while also reducing environmental impacts such as the impact on climate change or fossil resource depletion. In CCU, CO_2 is treated as a valuable feedstock for the production of many value-added chemicals and fuels, which thus provides a solution to both emission-control and energy-supply challenges.[14] However, the disadvantage is that the activation and utilisation of CO_2 is still problematic. This is due to the thermodynamically stability of CO_2 as shown in Figure 1.3. Therefore, energy must be supplied to drive the desired transformation, such as high temperatures, electricity, or the energy from photons may be exploited to carry out carbon dioxide reactions. Consequently, most of the known studies used highly reactive substrates and/or severe reaction conditions to activate CO_2, limiting the application of such methods. Furthermore, chemicals and fuels offer limited storage periods for captured CO_2 because of their short lifetime. Future research efforts should focus on the synthesis of materials and products with longer lifespans. Also, when dealing with the feedstock of the chemical industry, the level of sustainability is still far from satisfactory.

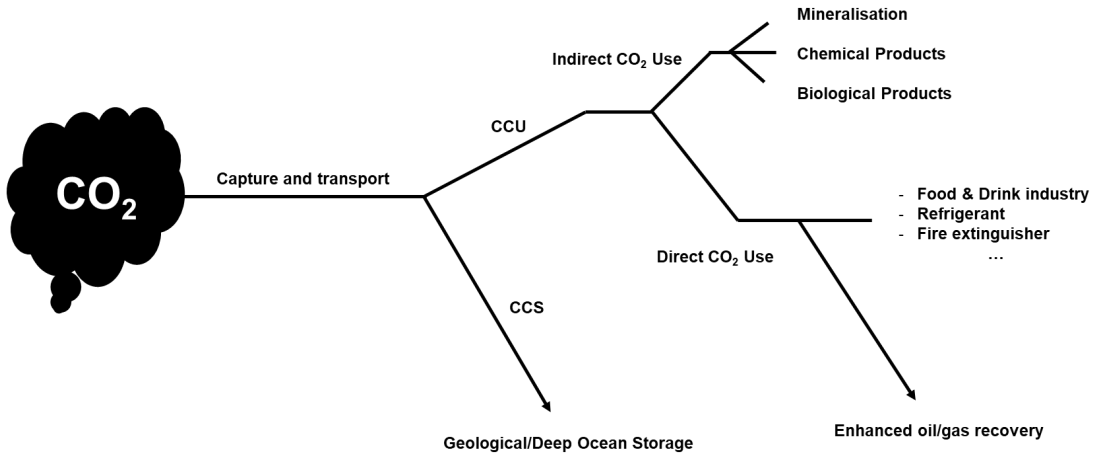


Figure 1.8. Comparison between CCU and CCS.[55]

Carbon dioxide is no doubt a renewable feedstock, and therefore its transformation into useful chemicals is particularly important. Many routes have been proposed recently for the chemical fixation of CO_2, some of which are of great commercial interest with respect to the synthesis of specialised/commodity chemicals. However, those utilisation processes with CO_2 as a raw material are not likely to ease the greenhouse effect to a significant extent if the amount of CO_2 fixed is much smaller compared to the order of magnitude of carbon emissions facing us. Currently, the total amount of global CO_2 utilisation is lower than 200 million tonnes per year.[56] This is much lower compared with the extent of global anthropogenic CO_2 emissions, which is over 32,000 million tonnes per year. In addition, the transformation of CO_2 requires energy input. Thus, product demand, the source of energy and overall net carbon emissions need be taken into consideration. Reorganisation of the present chemical infrastructure, and fundamental research on new CO_2 reactions are both needed. At present, the physical storage and direct use of CO_2 is technically the most feasible direction provided that the associated safety and sustainability issues can be met.

The reduction of global CO_2 emission is an important challenge and many research and investigation projects have paid lots of attention to this area globally. The process of carbon capture followed by storage and utilisation can provide new ideas for solving the carbon emission challenge. Oxidative propane dehydrogenation with CO_2 provides a new CO_2 utilisation pathway and the product, propylene is one of the important chemical feedstocks for chemical manufacture. Therefore, in this thesis, we have focused on the development of propane dehydrogenation using CO_2 as a mild oxidant.

1.3 Oxidative Propane Dehydrogenation to Form Propylene Using CO_2 as Mild Oxidant

1.3.1 Development of propane dehydrogenation

The worldwide development of shale gas is one of the significant energy revolutions in the 21st Century.[57] This brings very high amounts of light alkanes, which account for up to 10% of total shale gas to the market. Thus, the dehydrogenation of these light alkanes to produce light alkenes becomes attractive because alkenes are the most important and basic components in the modern chemical industry to manufacture products such as polyethylene, polypropylene, ethylene oxide, styrene, acetaldehyde, vinyl acetate, ethylene dichloride/dibromide, ethanol, ethylbenzene, and many more chemicals with high selling price in the market.[57–59] The demand for olefins, especially propylene, is increasing rapidly according to recent reports.[60] Propylene is the basic raw material for the production of acrolein, polypropylene, acetone, acrylonitrile, propylene oxide and other industrial products.[61] Steam Cracking (SC) of naphtha and light petroleum and Fluid Catalytic Cracking (FCC) are the conventional propylene production processes. These methods typically provide a range of products including ethene, propene and gasoline, amongst others.[62] Based on analysis by IHS Markit in 2016, these methods accounted for 81% of total propene production in industry.[62] 50% is from steam cracking and 31% is from catalytic cracking. However, these two processes are accompanied by rapid consumption of fossil fuel, vast quantities of emitted CO_2, a large cost for the raw materials and hardly have the capacity to reach the increasing demand.[58,61] In this case, the development of highly efficient, environmental friendly and low-cost process for propylene production is vitally important, both scientifically and economically.[59] In recent studies, there are increasing

developments and investigations on propylene production, such as propane dehydrogenation. Propane dehydrogenation (PDH) is considered a promising catalytic technology utilised for the conversion of propane into propylene which is involved in many industrial applications.[63] This is because the propane dehydrogenation satisfies many principles of green chemistry in comparison to SC and FCC.[64] As illustrated in reaction 1.2, direct propane dehydrogenation is a highly endothermic reaction which requires a large amount of energy input (high reaction temperature over 600 °C) for reaction to occur.

$$\text{Dehydrogenation: } C_3H_8 \rightarrow C_3H_6 + H_2 \qquad (1.2)$$

$$\Delta H^{0}_{296} = +124 \text{ kJ/mol}^{65}$$

At these high temperatures, undesirable side reactions limit the propylene yield and coke formation necessitates frequent catalyst regeneration. The rates of competitive C–C cleavage side reactions will increase, such as hydrogenolysis (1.4) hydrogenation (1.5) reactions; therefore, proper reaction conditions are essential for selective dehydrogenation to occur. In addition, these restrictions lead to great challenges to the dehydrogenation technologies and catalyst design.

$$C_3H_8 \rightarrow CH_4 + C_2H_4 \qquad (1.3)$$

$$C_3H_8 + H_2 \rightarrow C_2H_6 + CH_4 \qquad (1.4)$$

$$C_2H_4 + H_2 \rightarrow C_2H_6 \qquad (1.5)$$

By removing the hydrogen in the form of water from reaction 1.2, oxidative dehydrogenation proceeds to a greater extent than simple catalytic dehydrogenation. The oxidative dehydrogenation of light alkanes is well known and a number of oxidants such as oxygen, nitrous oxide, and carbon dioxide have been introduced as the co-feed in dehydrogenation reactions.[66–70] Thus, the oxidative propane dehydrogenation (OPDH, 1.6) has been introduced O_2 as oxidant.

$$O_2\text{-PDH: } C_3H_8 + ½\ O_2 \rightarrow C_3H_6 + H_2O \qquad (1.6)$$

$$\Delta H^0_{296} = -118 \text{ kJ/mol } [65]$$

By adding O_2 into the reaction stream, the dehydrogenation process becomes exothermic and thermodynamically unrestricted at lower temperatures. Therefore, there is a significant cost saving achieved using molecular O_2.[71–74] In addition, the oxidative dehydrogenation of propane in the presence of molecular O_2, as an oxidising agent, favours low temperature reactions and is exothermic with no thermodynamic limitations. However, the rapid coke generation from side reactions and high operating temperature (over 650-700 °C) sacrifices the propylene selectivity and catalysts' lifetime. On the other hand, overcoming the over-oxidation of propylene is still a challenge for O_2-PDH.

This is considered as a competitive side reaction of propane and propylene to CO and partially CO_2, which often results in loss of propylene selectivity and yield.[75]

It is desirable to use a milder oxidant instead of O_2 for the propane dehydrogenation. Similar to the oxidative dehydrogenation reaction with O_2, the introduction of CO_2 can also act as oxidant in oxidative PDH because the O atom of CO_2 can react with the H atom released from the alkanes to give H_2O.[75,76] In 1972, Fox et al. introduced CO_2 as an alternative oxidant in OPDH (CO_2-PDH, 1.7).[77]

$$CO_2\text{-PDH: } C_3H_8 + CO_2 \leftrightarrow C_3H_6 + CO + H_2O \qquad (1.7)$$

$$\Delta H^0_{296} = +164 \text{ kJ/mol } [65]$$

However, CO_2 is the most stable form of oxidised carbon compound and has a very low Gibbs free energy therefore this reaction is endothermic.[5] This is an intrinsic problem: most of the chemical reactions for CO_2 conversion and utilisation are endothermic reactions, which have large energy costs for the reactions to form valuable chemicals. Nevertheless, CO_2 reacts easily with strong nucleophiles to form

new C–C or C–H bonds.[5] Activation barriers for using CO_2 to produce hydrocarbons are still high and various side reactions also limit this process. So in practical terms, to use carbon dioxide as a mild oxidant in PDH for production of propylene, suitable catalysts for driving the reaction must be developed.

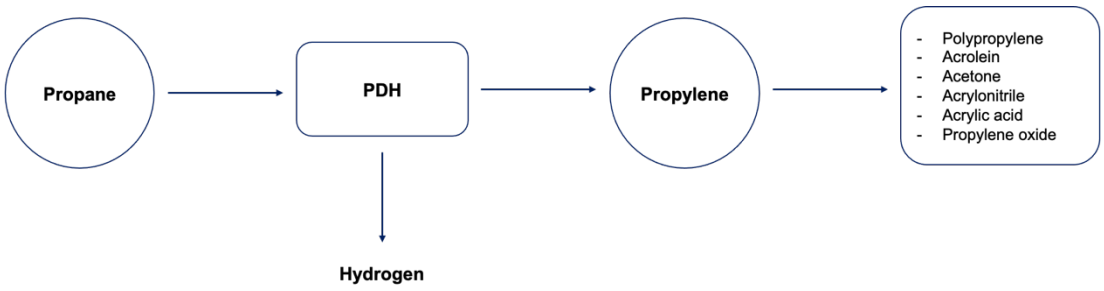


Figure 1.9. General flow diagram of propane dehydrogenation process.

In principle, PDH is a highly atom-economic reaction, does not use toxic reactants and H_2 will be the only by-product (reaction 1.2). But in practice, PDH process (even the alternative processes with O_2 or CO_2 as oxidant – reaction 1.6 and 1.7) will only be an industrially desirable process under certain reaction conditions with minimal side-products and maximum propylene yield. These factors are governed by the choice and design of catalyst. The development of an active, selective and stable catalyst is essential for propane dehydrogenation to be considered as a viable process in the near- and long-term future.

1.3.2 Catalyst development for PDH

The main driving force in the PDH reaction is the cleavage of the C–H bond, therefore, the activation of the first C–H bond of propane is the rate-determining step which determines the catalyst activity.[61,64] The chemical property of incompletely filled d orbitals on transition metals and Lewis acid Metal–O sites on metal oxide surfaces play

important roles in determining the catalytic activities in the PDH process. During catalyst development and design for the PDH process, a large number of heterogeneous catalysts has been investigated, including metal-based catalysts (mainly Pt- based catalysts), metal oxide-based catalysts (such as CrO_x, GaO_x, MoO_x, etc.) and non-oxide-based catalysts (carbides, nitrides, and carbon materials). They are applied for PDH reaction due to their affinity for paraffinic C–H bonds and low activity to C–C cleavage that are needed for high propane conversion performances.

The well-developed commercial/industrial propane dehydrogenation processes are mostly carried out without oxidant (reaction 1.2). The current and successfully implemented industrial PDH processes include Catofin from ABB Lummus Global, UOP-licensed Oleflex, KBR-licensed Superflex, STAR by thyssenkruup Uhde and FCDh from DOW technologies. Particularly, the Catofin and Oleflex processes are two widely applied PDH technologies.

The Catofin process uses a multiple parallel adiabatic fixed-bed catalyst reactor to achieve an appropriate conversion and selectivity with low energy consumption.[63,64] A Chromium oxide catalyst with aluminium oxide as support (CrO_x/Al_2O_3) is commonly used in the Catofin process.[61,63,64] The catalysts contains about 18–20 wt% chromium oxide with 1-2 wt% alkali metal (Na or K) supported on aluminium oxide.[64,72] In this catalytic system, the alkali metal acts as promoter which is able to influence both the activity and selectivity of the catalyst by reducing the surface acidity of aluminium oxide support for suppressing undesired side reactions. Even though improvements in the catalyst design and process conditions have been made for the commercialised Catofin process, challenges still exist relating to their activity, selectivity and stability. The Oleflex process employs alkali metal-promoted Pt–Sn/Al_2O_3 catalysts in a reaction system composed of four moving bed reactors.[72] The typical catalyst in the Oleflex process consists of spherical pellets of γ-Al_2O_3 containing Pt. The Steam Active Reforming (STAR) process employs an Sn-promoted Pt catalyst with about 0.2-0.6

wt%, dispersed on a zinc–aluminate support.[63,64,72] The catalyst used in Dow FCDh technology is comprised of a commercially available Al_2O_3 support that is impregnated with Ga and Pt. In general, most commercialised non-oxidative PDH processes use Pt-based and CrO_x-based catalysts. However, the widely used Pt-based catalysts are limited by their high price, low abundance and serious material sintering caused by high reaction temperature during the catalyst praperation.[78] CrO_x-based catalysts exhibit an outstanding performance in the commercial process, but toxic CrO_x species cause serious environmental pollution and affect human health. Therefore, many research and studies are trying different metal material to replace the toxic CrO_x species. Moreover, the deactivation of the catalysts is also non-negligible. In this case, a possible regeneration pathway could reobtain their catalytic abilities and hence extend their lifetime.

The route of OPDH with O_2 introduced in the reaction 1.6 is exothermic which makes the PDH process more favourable at a lower reaction temperature. As mentioned before, the activation of the C–H bonds is the rate-determining step for propylene production during OPDH. Hence, the potential in catalysts development is the efficiency in C–H bonds cleavage. Thus, the aim is to have a highly selective catalyst and an optimised reaction process for OPDH. So far, there are various catalytic systems which have been reported for OPDH. Like the commercialised catalysts, most of them contain transition metals or transition metal oxides. Apart from CrO_x-based catalysts, vanadia, molybdena, and gallium oxides have also been investigated for OPDH process. Vanadium oxides are known to be active for many hydrocarbon oxidation reactions, including dehydrogenation.[71] Research on vanadium-based dehydrogenation catalysts started in the 1980s, although at that time the focus was on oxidative dehydrogenation using vanadium−magnesium mixed oxides.[68,79] The nature of the vanadium present on the catalyst depends to a large extent on the type of support, the support surface area, the metal loading, and the oxidation state of

vanadium.[80] Therefore, a combination of V−O-support, V−O−V, or V-O moieties may be obtained, each having different catalytic activity. GaO_x-based catalysts have been studied for OPDH reactions for several years. However, the active sites of Ga-based catalyst have been debated and are strongly affected by the types of supports, preparation methods, and loading amounts.[81] Studies have shown that the active site of Ga_2O_3 is the Lewis acid site provided by coordinatively unsaturated Ga^{3+}.[82,83] Heteroatom-doped nanocarbon materials as metal-free catalysts have been approved for oxidative dehydrogenation reactions. More recently, the ODHP reaction has even been introduced into the realm of boron nitrides and metal–organic frameworks.[70,84–86]

CO_2 as a milder oxidant is introduced to replace O_2. It has been show that the CO_2 could help to inhibit the massive coke deposition that often deactivates the catalytic system during the direct propane dehydrogenation and O_2-assisted propane dehydrogention.[87] CO_2 is a waste and greenhouse gas and its utilisation has attracted much attention in recent years. However, as the most thermodynamically stable form of carbon, CO_2 activation is difficult. Hence, the challenges for developing an efficient catalyst to catalyse CO_2-PDH involves the activation of CO_2 during the dehydrogenation.[65]

Several types of catalysts have been extensively explored for PDH reaction with some promising results that could bring the process one step closer to commercialisation.[75] Catalyst studies among metal oxide catalysts have investigated various metals including Cr, Pd, Ga and Ce. Cr-based catalysts are one of the common metal choices used for this reaction. In 1998, Takahara investigated the CO_2/propane dehydrogenation over Cr_2O_3 on SiO_2.[88] From then on, various catalysts were investigated. In fact, the heterogeneous catalysts normally have two parts, the metal oxides and supports. In general, the metal oxide is the redox agent for the reaction, the supports also affect the catalytic activity but are not normally directly involved in the reaction. The most widely used supports are TiO_2, AlO_2 and ZrO_2. The factors that

affect catalytic efficiency will be discussed later. To improve the catalytic behaviour during the light alkane dehydrogenation with CO_2, mixed metal oxides with optimum metal ratios also have been studied. Zhu et al. showed that a catalyst with Mn doped $NaWO_4$ loaded into a SiO_2 support for were effective for ethane dehydrogenation with CO_2.[89] In more recent research, Co-Al_2O_3 by Sun et al. and WO_x-VO_x-SiO_2 by *Ascoop et al.* were also investigated in the propane dehydrogenation process.[90,91]

CrO_x-based catalysts generally have good performance in propane dehydrogenation, but are strongly influenced by the nature of the support.[92] In Xian Du's D.Phil study, it has been found that the conversion of propane can be changed by modifying the acidity and basicity on the catalyst surface with different supports. It has been written that 'the reactivity was decreased over Cr_2O_3/Al_2O_3 but increased over Cr_2O_3/SiO_2'.[93] To improve the catalytic performance, many materials have been investigated as supports. In recent research, zeolites have been established as catalytic supports in the CO_2-dehydrogenation of propane. A range of porous crystalline materials such as ZSM-5, MCM-41 and SBA that are widely used for the petrochemical industries and for pollution control.[94–96] Because of their three-dimensional porous structure, controllable acidity and large specific surface area, they are a good supports for metal oxide catalysts. ZSM-5 and MCM-41 have been widely investigated in the CO_2-PDH reaction as catalyst supports. A ZSM-5-supported Cr_2O_3 catalyst was found to be an efficient catalyst for the oxidative dehydrogenation of propane in the presence of CO_2.[75,92,97] Further details on these catalytic systems are introduced and described in details in Chapter 3.

Oxidative dehydrogenation of propane through CO_2 mild oxidation is also an energy-efficient and environmentally promising approach to convert propane to propylene, also adding high value to the propane-rich shale gas.[57] Moreover, such activation of CO_2 under mild conditions can lead to syngas production, which is the basic building block for fuel and chemicals. Therefore, using of CO_2 for an environmentally benign

process leads to the production of industrially useful chemicals. However, increasing the propane conversions and propylene selectivity is still a major challenge for this process. This requires the development and investigation of different catalysts. A valuable catalyst for CO_2-PDH should have good activity and stability, long life cycle (reusability), be environmental friendly and inexpensive to produce.

Unfortunately, this process has not yet been implemented in an industrial/commercial-scale application, because several undesirable over-oxidation reactions result in a low yield of propylene and a moderate propane conversion. Also, the reaction conditions such as the ratio between propane and CO_2, reaction temperature and feed gas flow rate would affect the catalyst performance during PDH process. In general, the current productivities, especially in catalysts development, seem not high enough to be of interest for industrial application due to the low selectivity of many metal oxide catalysts. As a result, it is of great significance to synthesize a series of advanced catalysts possessing an eco-friendly character, cost-effective nature, excellent anti-coking properties, long-term stability and robust recyclable life, which are beneficial for further practical applications.[78]

1.3.3 Fundamental factors of catalyst design for CO_2-PDH

Although during the catalyst development for PDH, the various metal-based and metal oxide-based catalysts has been investigated based on their catalytic activity and propylene selectivity, it is still very important to understand how we could improve their catalytic performance, what kind of factors affect catalyst's activities during the process. A number of review papers about the catalysts for PDH have been published.[50,64,98–100] Chen et al. and Yang et al. have done deep research and detailed summaries on the catalysts for propane dehydrogenation and also their prospective in future design.[61,78]

In catalysis, the active sites, promoter, and support are the basic factor that usually constitute a catalyst performance for a particular application.[101] Figure 1.10 shows an illustration structure of a catalysts. The active sites are the main catalytic centres of the system. Oxidative propane dehydrogenation is facilitated on oxide and oxide-supported catalysts of transition metals, with lattice oxygen species as the major active site.[98] These active sites are widely considered to be reactive oxygen species present in different structural forms on the surfaces of the catalysts. The catalyst should possess active sites which can selectively cleave the C–H bond with limited C–C cleavage at high activity and which provide good CO_2 adsorption.[102] The acidity and basicity of the catalyst are important. The high acidity is known to reduce the propylene selectivity due to the competitive side reactions including C−C cleavage, desorption of propylene and deep dehydrogenation of propylene. These reactions can be regulated by the adsorption of propyl intermediate via promoter and support effects.[100] On the other hand, the high basicity will result the excessive CO_2 adsorption that could lead to blockage of the active sites for C–H bond cleavage. Therefore, the balance between acid and basic sites is important, especially when both the propane and CO_2 are activated on different active components.[98,102] Availability of both acidic and basic sites is beneficial to CO_2-PDH catalysts, and the acid sites should be composed of medium and high strength acid sites.[102] Supports and promoters, in these case, play an important role to help balance the catalyst surface acidity and basicity.

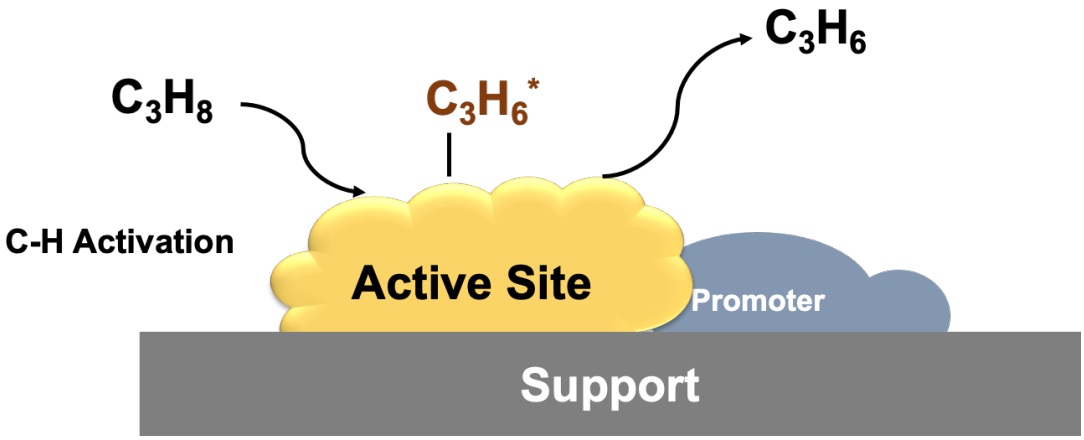


Figure 1.10. An illustrated schematic of the catalyst for PDH.[100]

Promoters are added to enhance the catalytic activity and are not themselves the catalyst. In the catalytic system, the addition of different kind of promoters will be able to affect the catalyst surface structure, hence influence their catalytic activity. In bimetallic catalyst design, enhanced dispersion of the phases is beneficial in interfacial sites formation and their tuning. On the other hand, a less active component that can act as structural promoter could be utilised to achieve site isolation and suppress formation of large metal ensembles.

In fact, the surface and bulk composition of catalysts can be easily modified by CO_2, during PDH. This will be leading to changes in the redox, adsorption and electronic properties of the catalysts. These adjustments can affect the activity and selectivity for propane dehydrogenation during the reaction.[70] More detailed discussion about these factors in catalyst design and development will be in Chapter 3.

1.4 Thesis Objective and Research Summary

The global warming and carbon emission have attracted a huge amount of attention from the public and from the research community. Many efforts have been made and

many techniques and processes have been developed and investigated for reducing carbon emissions. Carbon utilisation seems have more advantages in the reuse and recycling of CO_2 compared with CO_2 storage. Furthermore, the high demand of propylene in the chemical industry requires new efficient propylene production process. Therefore, to satisfy both the scientific and industrial aspects of both these needs, catalytic propane dehydrogenation with CO_2 would be a good pathway.

My DPhil research work centers on a catalyst design for high propylene production and selectivity by CO_2 - PDH process. An innovative catalytic system prepared by one-pot synthesis is proposed and described in Chapters 4 and 5, and compared with more conventionally made catalysts (Chapter 3). There are some challenges for this newly developed catalytic system. The first is to examine the differences in the catalyst materials prepared by new method with the conventional impregnation method and how they performed differently during the catalytic process. The second challenge is the improvement of catalytic system. As well as factors in catalyst design that affect catalytic performance, the reaction conditions such as the composition and flow rate of propane and CO_2, reaction temperature and so on are important. The last challenge is about the how to make the process “greener” and more sustainable, especially in views of catalysts. Therefore, this work will move on to the improvement of their catalytic performance and how to rejuvenate spent catalysts to reduce any environmental effects from catalysts disposal and to save cost and energy during catalyst preparation. Based on this work, there is one paper published.[103]

I believe that during my DPhil study and research, a new scientific and technological catalyst preparation method for CO_2-PDH could help to improve the practical CO_2-PDH process towards to the industrial and commercial scale. In addition, with the attendant CO_2 emissions, we can utilise them to produce propylene with high yield and selectivity. this will also help to reach the world propylene demand.

References

1 Z. Jiang, T. Xiao, V. L. Kuznetsov and P. P. Edwards, *Philos. Trans. R. Soc. A Math. Phys. Eng. Sci.*, 2010, **368**, 3343–3364.

2 IPCC, 2014: Climate Change 2014: Mitigation of Climate Change. Contribution of Working Group III to the Fifth Assessment Report of the Intergovernmental Panel on Climate Change [Edenhofer, O., R. Pichs-Madruga, Y. Sokona, E. Farahani, S. Kadner, K. Seyboth, A. Adler, I. Baum, S. Brunner, P. Eickemeier, B. Kriemann, J. Savolainen, S. Schlömer, C. von Stechow, T. Zwickel and J.C. Minx (eds.)]. Cambridge University Press, Cambridge, United Kingdom and New York, NY, USA.

3 C.-H. Huang and C.-S. Tan, *Aerosol Air Qual. Res.*, 2014, **14**, 480–499.

4 G. Centi and S. Perathoner, *Catal. Today*, 2009, **148**, 191–205.

5 Q. Liu, L. Wu, R. Jackstell and M. Beller, *Nat. Commun.*, 2015, **6**, 1–15.

6 R. M. Cuéllar-Franca and A. Azapagic, *J. CO2 Util.*, 2015, **9**, 82–102.

7 M. N. Anwar, A. Fayyaz, N. F. Sohail, M. F. Khokhar, M. Baqar, A. Yasar, K. Rasool, A. Nazir, M. U. F. Raja, M. Rehan, M. Aghbashlo, M. Tabatabaei and A. S. Nizami, *J. Environ. Manage.*, 2020, **260**, 110059.

8 I. Tieso, Historic average carbon dioxide (CO_2) levels in the atmosphere worldwide from 1959 to 2021 (in parts per million)*, https://www.statista.com/statistics/1091926/atmospheric-concentration-of-co2-historic/, (accessed 30 August 2022).

9 I. Tieso, Annual CO_2 emissions worldwide, https://www.statista.com/statistics/264699/worldwide-co2-emissions/,

(accessed 30 August 2022).

10 Rhein, M., S.R. Rintoul, S. Aoki, E. Campos, D. Chambers, R.A. Feely, S. Gulev, G.C. Johnson, S.A. Josey, A. Kostianoy, C. Mauritzen, D. Roemmich, L.D. Talley and F. Wang, 2013: Observations: Ocean. In: Climate Change 2013: The Physical Science Basis. Contribution of Working Group I to the Fifth Assessment Report of the Intergovernmental Panel on Climate Change [Stocker, T.F., D. Qin, G.-K. Plattner, M. Tignor, S.K. Allen, J. Boschung, A. Nauels, Y. Xia, V. Bex and P.M. Midgley (eds.)]. Cambridge University Press, Cambridge, United Kingdom and New York, NY, USA.

11 S. C. Doney, V. J. Fabry, R. A. Feely and J. A. Kleypas, *Ann. Rev. Mar. Sci.*, 2009, **1**, 169–192.

12 P. M. Haugan and H. Drange, *Energy Convers. Manag.*, 1996, **37**, 1019–1022.

13 S. Muraleedharan, All You Need to Know About Ocean Acidification and its Impacts, https://www.ecomena.org/consequences-of-ocean-acidification/, (accessed 15 September 2022).

14 A. Al-Mamoori, A. Krishnamurthy, A. A. Rownaghi and F. Rezaei, *Energy Technol.*, 2017, **5**, 834–849.

15 International Energy Agency (IEA), Global Energy and Carbon emission 2020, *Global Energy Review 2020*, https://www.iea.org/reports/global-energy-review-2020, (accessed 15 September 2022)

16 G. W. Crabtree, M. S. Dresselhaus and M. V Buchanan, *Phys. Today*, 2004, **57**, 39–44.

17 B. Yao, T. Xiao, X. Jie, S. Gonzalez-Cortes and P. P. Edwards, *Catal. Today*, 2018, **317**, 43–49.

18 J. M. Spurgeon and B. Kumar, *Energy Environ. Sci.*, 2018, **11**, 1536–1551.

19 J. J. Eberhart, in *8th Diesel Engine Emissions Reduction Conference - 2002 Department of Energy*, San Diego, 2022.

20 E. S. Rubin, H. Mantripragada, A. Marks, P. Versteeg and J. Kitchin, *Prog. Energy Combust. Sci.*, 2012, **38**, 630–671.

21 G. A. Olah, *Angew. Chemie - Int. Ed.*, 2005, **44**, 2636–2639.

22 Chapter 8 Costs and economic potential, IPCC, 2005: IPCC Special Report on Carbon Dioxide Capture and Storage. Prepared by Working Group III of the Intergovernmental Panel on Climate Change [Metz, B.,O. Davidson, H. C. de Coninck, M. Loos, and L. A. Meyer (eds.)]. Cambridge University Press, Cambridge, United Kingdom and New York, NY, USA, 442 pp.

23 M. Bui, C. S. Adjiman, A. Bardow, E. J. Anthony, A. Boston, S. Brown, P. S. Fennell, S. Fuss, A. Galindo, L. A. Hackett, J. P. Hallett, H. J. Herzog, G. Jackson, J. Kemper, S. Krevor, G. C. Maitland, M. Matuszewski, I. S. Metcalfe, C. Petit, G. Puxty, J. Reimer, D. M. Reiner, E. S. Rubin, S. A. Scott, N. Shah, B. Smit, J. P. M. M. Trusler, P. Webley, J. Wilcox, N. Mac Dowell and N. Mac Dowell, *Energy Environ. Sci.*, 2018, **11**, 1062–1176.

24 J. Gibbins and H. Chalmers, *Energy Policy*, 2008, **36**, 4317–4322.

25 D. Y. C. Leung, G. Caramanna and M. M. Maroto-Valer, *Renew. Sustain. Energy Rev.*, 2014, **39**, 426–443.

26 P. Markewitz, W. Kuckshinrichs, W. Leitner, J. Linssen, P. Zapp, R. Bongartz, A. Schreiber and T. E. Müller, *Energy Environ. Sci.*, 2012, **5**, 7281–7305.

27 M. I. Stewart, in *Surface Production Operations*, Elsevier, Virginia, USA, 3rd Editio., 2014, pp. 433–539.

28 Y. Kong, X. Shen, M. Fan, M. Yang and S. Cui, *Chem. Eng. J.*, 2016, **283**, 1059–1068.

29 B. Arstad, H. Fjellvåg, K. O. Kongshaug, O. Swang and R. Blom, *Adsorption*, 2008, **14**, 755–762.

30 S. Builes, P. López-Aranguren, J. Fraile, L. F. Vega and C. Domingo, *Energy and Fuels*, 2015, **29**, 3855–3862.

31 A. Goeppert, M. Czaun, R. B. May, G. K. S. Prakash, G. A. Olah and S. R. Narayanan, *J. Am. Chem. Soc.*, 2011, **133**, 20164–20167.

32 M. Ding, R. W. Flaig, H. L. Jiang and O. M. Yaghi, *Chem. Soc. Rev.*, 2019, **48**, 2783–2828.

33 X. Wang and C. Song, *Front. Energy Res.*, 2020, **8**, 560849.

34 P. Madejski, K. Chmiel, N. Subramanian and T. Kus, *Energies*, 2022, **15**, 887.

35 C. Font-Palma, D. Cann and C. Udemu, *J. Carbon Res.*, 2021, **7**, 58.

36 A. Vinca, J. Emmerling and M. Tavoni, *Front. Energy Res.*, 2018, **6**, 40.

37 M. Pehnt and J. Henkel, *Int. J. Greenh. Gas Control*, 2009, **3**, 49–66.

38 B. Singh, A. H. Strømman and E. G. Hertwich, *Int. J. Greenh. Gas Control*, 2011, **5**, 911–921.

39 F. M. Baena-Moreno, M. Rodríguez-Galán, F. Vega, B. Alonso-Fariñas, L. F. Vilches Arenas and B. Navarrete, *Energy Sources, Part A Recover. Util. Environ. Eff.*, 2019, **41**, 1403–1433.

40 C. Hepburn, E. Adlen, J. Beddington, E. A. Carter, S. Fuss, N. Mac Dowell, J. C. Minx, P. Smith and C. K. Williams, *Nature*, 2019, **575**, 87–97.

41 R. Marriott, P. Jessop and M. Barnes, in *Carbon Dioxide Utilisation: Closing the Carbon Cycle: First Edition*, Elsevier Inc., 2015, pp. 73–96.

42 J. Wang, H. Zhang, Y. Miao, L. Qiao, X. Wang and F. Wang, *Green Chem.*, 2016, **18**, 524–530.

43 C. Boyère, C. Jérôme and A. Debuigne, *Eur. Polym. J.*, 2014, **61**, 45–63.

44 A. Rafiee, K. Rajab Khalilpour, D. Milani and M. Panahi, *J. Environ. Chem. Eng.*, 2018, **6**, 5771–5794.

45 K. M. K. Yu, I. Curcic, J. Gabriel and S. C. E. Tsang, *ChemSusChem*, 2008, **1**, 893–899.

46 L. Li, N. Zhao, W. Wei and Y. Sun, in *Fuel*, Elsevier Ltd, 2013, vol. 108, pp. 112–130.

47 John Gale, Global status of CCS, in *Policy and Regulation Framworks for CCS WFES 2010*, Tsinghua University, Beijing, China

48 A. D. N. Kamkeng, M. Wang, J. Hu, W. Du and F. Qian, *Chem. Eng. J.*, 2021, **409**, 128138.

49 B. Abdullah, N. A. Abd Ghani and D. V. N. Vo, *J. Clean. Prod.*, 2017, **162**, 170–185.

50 W. Li, H. Wang, X. Jiang, J. Zhu, Z. Liu, X. Guo and C. Song, *RSC Adv.*, 2018, **8**, 7651–7669.

51 P. Styring, D. Jansen, H. de Coninck, H. Reith and K. Armstrong, *Carbon Capture and Utilisation in the green economy*, Report no. 501, The Centre for Low Carbon Futures 2011 and CO2Chem, 2011.

52 L. Brennan and P. Owende, *Renew. Sustain. Energy Rev.*, 2010, **14**, 557–577.

53 N. Von Der Assen, J. Jung and A. Bardow, *Energy Environ. Sci.*, 2013, **6**, 2721–2734.

54 G. Wilson, P. Styring, N. MacDowell, J. Gibbins, S. Brandani, T. Hills, P. Fennell, A. Azapagic, G. Dowson, R. Bell, P. Liang, C. Scholes, B. Smit, M. Mazzotti, R. Graham, R. Ocone, D. Sutter, M. Gazzani, P. Clough, L. Joss, J. Stolaroff, G. Maitland, S. Lyth, M. Dunstan, M. Mota-Martinez, J. Kemper, J.-S. M. Lee, C. Petit, R. Anantharaman, R. Cuellar-Franca, J. Yao and G. Rochelle, *Faraday Discuss.*, 2016, **192**, 303–335.

55 C. R. Jones, B. Olfe-Kräutlein, H. Naims and K. Armstrong, *Front. Energy Res.*, 2017, **5**, 1–13.

56 A. I. Osman, M. Hefny, M. I. A. Abdel Maksoud, A. M. Elgarahy and D. W. Rooney, *Environ. Chem. Lett.*, 2021, **19**, 797–849.

57 R. Zhang, H. Wang, S. Tang, C. Liu, F. Dong, H. Yue and B. Liang, *ACS Catal.*, 2018, **8**, 9280–9286.

58 I. Kainthla, G. V. R. Babu, J. T. Bhanushali, K. S. R. Rao and B. M. Nagaraja, *J. CO2 Util.*, 2017, **18**, 309–317.

59 A. V. Lavrenov, L. F. Saifulina, E. A. Buluchevskii and E. N. Bogdanets, *Catal. Ind.*, 2015, **7**, 175–187.

60 T. Wu, Z.-J. Zhao, G. Sun, L. Zeng, C. Xiong, J. Gong and R. Mu, *Angew. Chemie Int. Ed.*, 2018, **57**, 6791–6795.

61 S. Chen, X. Chang, G. Sun, T. Zhang, Y. Xu, Y. Wang, C. Pei and J. Gong, *Chem. Soc. Rev.*, 2021, **50**, 3315–3354.

62 A. Akah, J. Williams and M. Ghrami, *Catal. Surv. from Asia*, 2019, **23**, 265–276.

63 H. A. Maddah, *Am. Sci. Res. J. Eng. Technol. Sci.*, 2018, **45**, 49–63.

64 J. H. Carter, T. Bere, J. R. Pitchers, D. G. Hewes, B. D. Vandegehuchte, C. J. Kiely, S. H. Taylor and G. J. Hutchings, *Green Chem.*, 2021, **23**, 9747–9799.

65 Z. Y. Wang, Z. H. He, Y. Xia, L. Zhang, K. Wang, W. Wang, Y. Yang, J. G. Chen and Z. T. Liu, *Ind. Eng. Chem. Res.*, 2021, **60**, 2807–2817.

66 R. Bulánek, B. Wichterlová, K. Novoveská and V. Kreibich, *Appl. Catal. A Gen.*, 2004, **264**, 13–22.

67 K. Nowińska, A. Wącław and A. Izbińska, *Appl. Catal. A Gen.*, 2003, **243**, 225–236.

68 E. V. Kondratenko, M. Cherian, M. Baerns, D. Su, R. Schlögl, X. Wang and I. E. Wachs, *J. Catal.*, 2005, **234**, 131–142.

69 S. Sugiyama, T. Osaka, Y. Hirata and K. I. Sotowa, *Appl. Catal. A Gen.*, 2006, **312**, 52–58.

70 G. Li, C. Liu, X. Cui, Y. Yang and F. Shi, *Green Chem.*, 2021, **23**, 689–707.

71 Q. X. Luo, X. K. Zhang, B. L. Hou, J. G. Chen, C. Zhu, Z. W. Z. T. Liu, Z. W. Z. T. Liu and J. Lu, *Catal. Sci. Technol.*, 2018, **8**, 4864–4876.

72 J. J. H. B. Sattler, J. Ruiz-Martinez, E. Santillan-Jimenez and B. M. Weckhuysen, *Chem. Rev.*, 2014, **114**, 10613–10653.

73 A. Kumar, T. M. Bhatti and A. S. Goldman, *Chem. Rev.*, 2017, **117**, 12357–12384.

74 J. T. Grant, J. M. Venegas, W. P. Mcdermott and I. Hermans, *Chem. Rev.*, 2018, **118**, 2769–2815.

75 M. A. Atanga, F. Rezaei, A. Jawad, M. Fitch and A. A. Rownaghi, *Appl. Catal. B Environ.*, 2018, **220**, 429–445.

76 E. Gomez, S. Kattel, B. Yan, S. Yao, P. Liu and J. G. Chen, *Nat. Commun.*, 2018, **9**, 1–6.

77 D. B. Fox, E. H. Lee and M. H. Rei, *Ind. Eng. Chem. Prod. Res. Dev.*, 1972, **11**, 444–446.

78 F. Yang, J. Zhang, Z. Shi, J. Chen, G. Wang, J. He, J. Zhao, R. Zhuo and R. Wang, *Nanoscale*, 2022, **14**, 9963.

79 M. A. Chaar, D. Patel, M. C. Kung and H. H. Kung, *J. Catal.*, 1987, **105**, 483–498.

80 B. M. Weckhuysen and D. E. Keller, *Catal. Today*, 2003, **78**, 25–46.

81 C. T. Shao, W. Z. Lang, X. Yan and Y. J. Guo, *RSC Adv.*, 2017, **7**, 4710–4723.

82 M. W. Schreiber, C. P. Plaisance, M. Baumgärtl, K. Reuter, A. Jentys, R. Bermejo-Deval and J. A. Lercher, *J. Am. Chem. Soc.*, 2018, **140**, 4849–4859.

83 B. Zheng, W. Hua, Y. Yue and Z. Gao, *J. Catal.*, 2005, **232**, 143–151.

84 B. Frank, J. Zhang, R. Blume, R. Schlögl and D. S. Su, *Angew. Chemie - Int. Ed.*, 2009, **48**, 6913–6917.

85 L. Shi, Y. Wang, B. Yan, W. Song, D. Shao and A. H. Lu, *Chem. Commun.*, 2018, **54**, 10936–10946.

86 Z. Li, A. W. Peters, V. Bernales, M. A. Ortuño, N. M. Schweitzer, M. R. Destefano, L. C. Gallington, A. E. Platero-Prats, K. W. Chapman, C. J. Cramer, L. Gagliardi, J. T. Hupp and O. K. Farha, *ACS Cent. Sci.*, 2017, **3**, 31–38.

87 L. Zhang, Z. Wu, N. C. Nelson, A. D. Sadow, I. I. Slowing and S. H. Overbury, *ACS Catal.*, 2015, **5**, 6426–6435.

88 I. Takahara, W. C. Chang, N. Mimura and M. Saito, *Catal. Today*, 1998, **45**, 55–

59.

89 J. Zhu, S. Qin, S. Ren, X. Peng, D. Tong and C. Hu, *Catal. Today*, 2009, **148**, 310–315.

90 Y. N. Sun, Y. N. Gao, Y. Wu, H. Shan, G. Wang and C. Li, *Catal. Commun.*, 2015, **60**, 42–45.

91 I. Ascoop, V. V. Galvita, K. Alexopoulos, M. F. Reyniers, P. Van Der Voort, V. Bliznuk and G. B. Marin, *J. Catal.*, 2016, **335**, 1–10.

92 F. Rahmani, M. Haghighi and M. Amini, *J. Ind. Eng. Chem.*, 2015, **31**, 142–155.

93 X. Du, D.Phil thesis, University of Oxford, 2016.

94 P. Michorczyk, P. Pietrzyk and J. Ogonowski, *Microporous Mesoporous Mater.*, 2012, **161**, 56–66.

95 E. Asghari, M. Haghighi and F. Rahmani, *J. Mol. Catal. A Chem.*, 2016, **418**–**419**, 115–124.

96 P. Michorczyk, J. Ogonowski and K. Zeńczak, *J. Mol. Catal. A Chem.*, 2011, **349**, 1–12.

97 A. Samanta, X. Bai, B. Robinson, H. Chen and J. Hu, *Ind. Eng. Chem. Res.*, 2017, **56**, 11006–11012.

98 Y. Gambo, S. Adamu, A. A. Abdulrasheed, R. A. Lucky, M. S. Ba-Shammakh and M. M. Hossain, *Appl. Catal. A Gen.*, 2021, **609**, 117914.

99 X. Jiang, L. Sharma, V. Fung, S. J. Park, C. W. Jones, B. G. Sumpter, J. Baltrusaitis and Z. Wu, *ACS Catal.*, 2021, **11**, 2182–2234.

100 S. Chen, C. Pei, G. Sun, Z. J. Zhao and J. Gong, *Accounts Mater. Res.*, 2020, **1**, 30–40.

101 A. Abdulrasheed, A. A. Jalil, Y. Gambo, M. Ibrahim, H. U. Hambali and M. Y. Shahul Hamid, *Renew. Sustain. Energy Rev.*, 2019, **108**, 175–193.

102 Y. Gambo, S. Adamu, G. Tanimu, I. M. Abdullahi, R. A. Lucky, M. S. Ba-Shammakh and M. M. Hossain, *Appl. Catal. A Gen.*, 2021, **623**, 118273.

103 Y. Gao, X. Jie, C. Wang, R. M. J. Jacobs, W. Li, B. Yao, J. R. Dilworth, T. Xiao and P. P. Edwards, *Ind. Eng. Chem. Res.*, 2020, **59**, 12645–12656.

Chapter 2

Experimental Methods

This chapter summarises the experimental techniques and procedures applied in this thesis. The preparation of catalysts and the evaluation of catalytic performance are described. Moreover, the variety of physical characterisation techniques used in this work are also introduced.

2.1 Preparation of Catalysts

In the oxidative propane dehydrogenation (PDH) reactions, the activation of the C–H bond of propane is acknowledged as the rate-determining step which determines the catalyst activity. Propylene is formed initially during the reaction and then can more easily undergo complex side reactions, such as further dehydrogenation and cracking. The unsaturated filling of d orbitals over transition metals and Lewis acid M–O sites of metal oxides determine their PDH reactivity. During the development of heterogeneous catalysts, metal-oxide-based catalysts have been exploited for direct PDH reaction due to their affinity for paraffinic C–H bonds and low activity to C–C cleavage, and have exhibited high performance in the reaction. In Chapter 1 and Chapter 3, there is more information and background about catalyst development for PDH. In addition, the ‘support effect’ is also very important in this catalytic system for PDH. Different types of support not only influence the dispersion of the metallic catalysts but also determine the adsorption of reactants at its own acidic and basic sites. Lewis acidic sites on the catalyst surface are well known to be an important adsorption centre, first capturing and then activating propane. The surface basicity enhances CO_2 chemisorption, which

may give merits to the utilisation of CO_2 in the catalysis process. More detailed discussion about the choice of metal oxides, supports and promoter effects is presented in Chapter 3 and Chapter 4.

In this part, the methods for incorporating metal oxides onto the surface of the support by two different preparation methods will be discussed. These methods are the traditional impregnation method and the new so-called 'One-pot Synthesis'.

2.1.1 Impregnation method

A metal oxide is the most common substance that has been doped onto the surface of various supports. The oxides themselves can transfer electrons during the catalytic reaction processes. In addition, the metal oxide may also be the precursor for the formation of dispersed elemental metal on the catalyst surface through reduction. To achieve dispersed metal oxides loaded onto a suitable support, the impregnation method is used and the process is as follows:

(1), Mix granded ZrO_2 [Catalyst support, 99%, Alfa Aesar] powder with a solution of precursor salts (typically, metal nitrates dissolved in a suitable amount (approx. 50 ml) of deionised water) which contains the required elements to be loaded onto the support;

(2), Stir for at least 5 hours to achieve uniform suspension;

(3), Dehydrate the mixture in a beaker to paste with stirring at around 120 °C;

(4), Then continue to dehydrate the paste until it is fully dried to a powder in the oven at 80 °C;

(5), Calcine the solids in air, at 600 °C for 6 hours with ramping 10 °C/min (the temperature is usually higher than the operation temperature of the following catalytic tests) to remove nitrate ions and form metal oxides.

(6), Grind the calcined solid into small particles (that will pass through a 125 μm sieve) and store them in sample vials in air.

2.1.2 One-pot synthesis

One-pot synthesis is a newly developed preparation method for preparing metal oxide catalysts. In this method, no pre-existing solid support is used and the support is itself prepared during the process. The preparation steps are:

(1), Prepare a solution with precursor salts (usually metal nitrates) and zirconium (IV) oxynitrate hydrate (Aldrich, ≥ 99%) dissolved in 350 ml of deionised water which contains the required elements at room temperature;

(2), Add NaOH solution (2 M) dropwise at 60 °C until the pH reaches 11.0;

(3), Age the mixture in a water bath for 2 hours at 60 °C;

(4), Filter out the precipitate and wash three times with deionised water;

(5), Transfer the solid into a 500 ml round-bottom flask with 300 ml deionised water and reflux for 48 hours;

(6), Filter out the solid and dry in the oven at 80°C for more than 12 hours;

(7), Calcine the solid at 600 °C in air for 5 hours with the heating rate 2 °C/min;

(8), Grind the calcined solid into small particles (less than 125 μm) and store them in sample vials.

More details on the preparation of the various catalyst samples will be described in Chapters 3 and 4.

2.2 Catalysts Analysis

2.2.1 Reaction system

The performances of the catalysts for propane dehydrogenation with CO_2 were examined in a fixed-bed micro reactor (M-R-10A, Kun-Lun Yong-Tai Company, China, Figure 2.3) operating at atmospheric pressure. The schematic diagram is shown in Figure 2.1. The feeding gases flow from top of the reactor tube for fully contact with catalyst.

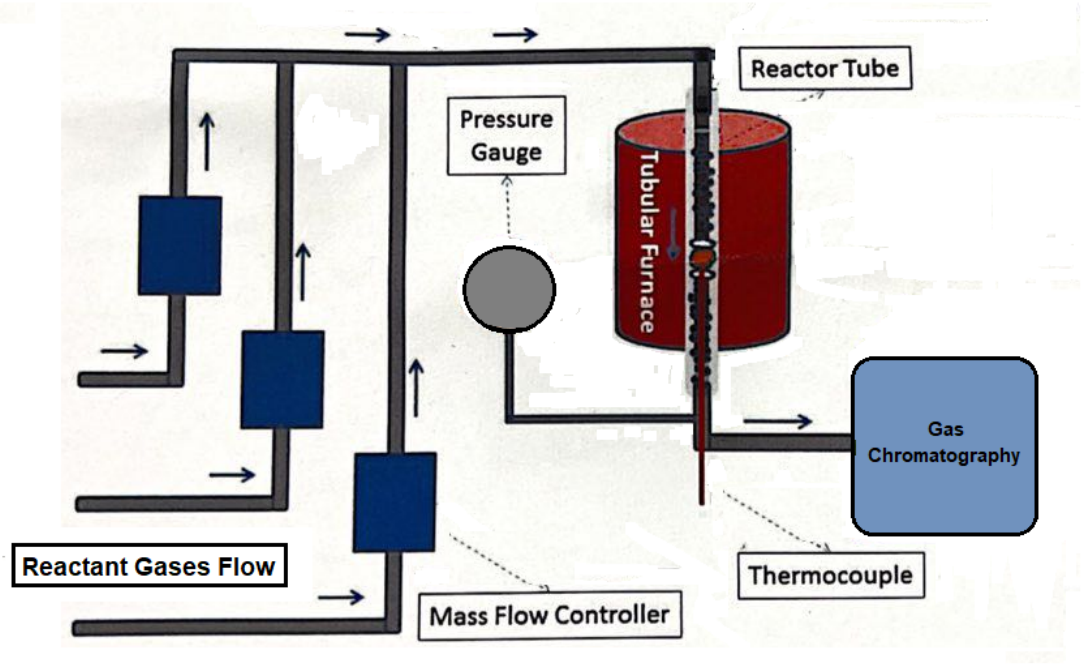


Figure 2.1. Schematic diagram of the micro reactor and online GC.

In the reactor tube, about 300 mg of catalyst power was placed at the middle of the tube where a thermocouple is attached (Figure 2.2). This is to control the reaction temperature and make sure the temperature of the catalyst bed is accurately measured. The calibrated amount of reactant gases (propane and CO_2) were supplied using the mass-flow controllers with the balance being nitrogen gas. The total flow rate used was

25 mL/min. In propane dehydrogenation proposed in this thesis, N_2 is not only used as dilution gas but also acts as an internal standard as it is not involved in the reaction process. The amount of N_2 will be the same before and after the reaction. Therefore, the internal standard, N_2, can be used for calibration by plotting the ratio of the analyte gas signal to the internal standard signal as a function of the analyte gases concentration of the standards. This can enable interpreting the data read directly from the GC detector to obtain quantities such as propane conversion and propylene selectivity. The emerging outlet gas was cooled to room temperature and analysed through a direct link to an on-line gas chromatograph (GC, Perkin Elmer, Clarus 580) with a flame ionization detector (FID) and a thermal conductivity detector (TCD).

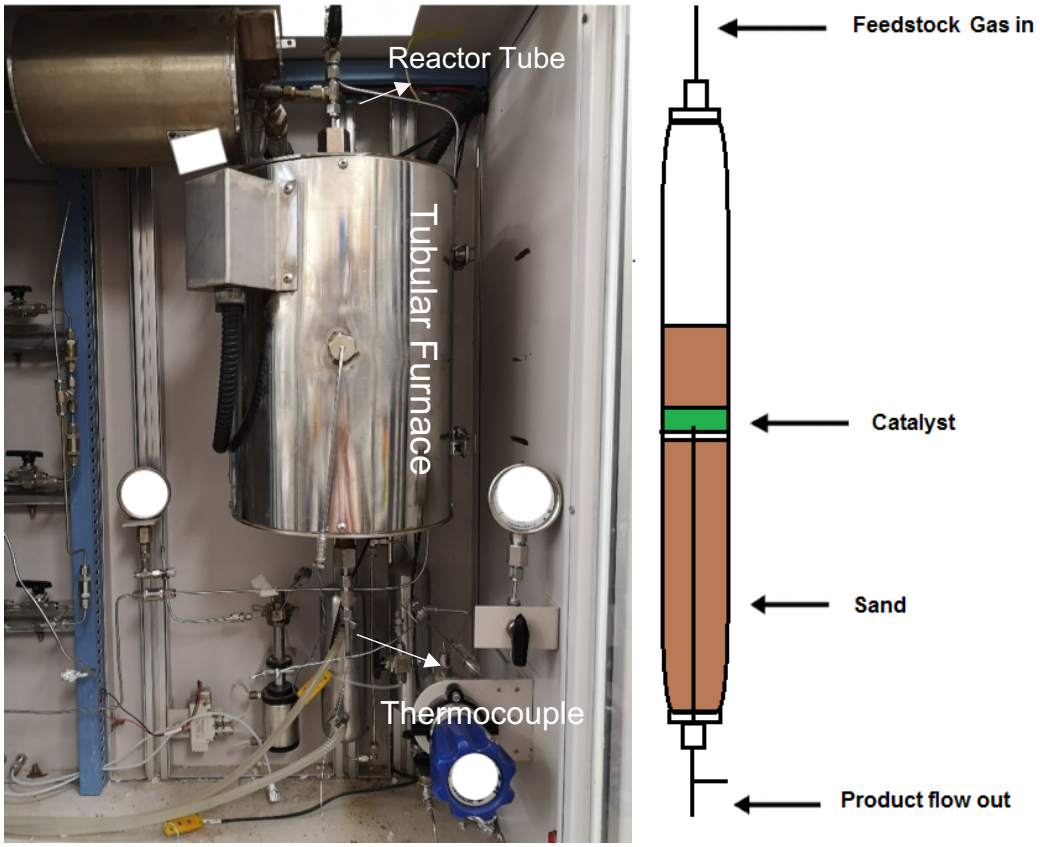


Figure 2.2. Picture of the fixed-bed reactor and diagram of the catalysts loading in reactor tube for activity test.

In addition, the reaction gas flow rate was double-checked accurately using a gas flow meter (Figure 2.3). Usually, under the same setting number on a mass flow controller, gas mixtures with different compositions will achieve different gas flow rates by their volume as the mixtures of gases have different viscosities. In this case, the digital flowmeter is used for checking the flow rate during the reaction process. With the flow rate meter reading, it is easy to mix different gases together with certain quantitative proportions. There exists a roughly proportional relationship between the volume proportion of gas and their responsive intensities on the GC detectors (integrated peak area). In the following chapters, the raw data can be routinely converted to the volume percentages of gas in a mixture and used for the calculation of propane conversion and propylene selectivity.

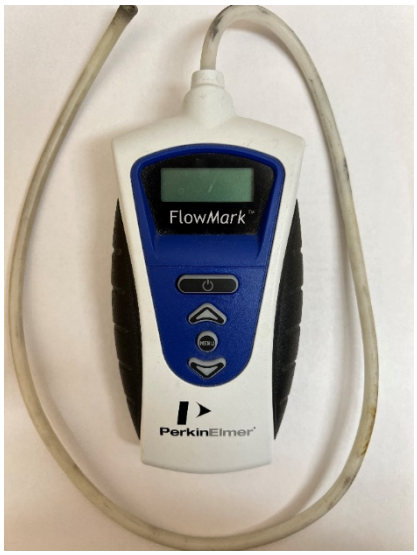


Figure 2.3. Picture of the flow meter used for flow rate check.

2.2.2 Gas Chromatography (GC)

Chromatography is an effective route to separate mixtures especially for gases and liquids. Gas Chromatography (GC) is a commonly-used analytical technique for

separation and identification of compounds in a gas mixture. The technique allows for the detection of each particular compound in a gas mixture – both qualitatively and also quantitatively. It also has high sensitivity to enable quantitative detection of a compound even at very low proportions.

The separation process by gas chromatography is routinely achieved by forcing the mixture to move through both an immobile and immiscible stationary phase. This is based on the distinct migration rates of the components caused by the different adsorption ability on the stationary phase. A component which is adsorbed by the stationary phase easily will have longer retention time than a component which is not adsorbed by the stationary phase. The retention time of a compound is dictated by the time that it takes to pass through the column also known as the retention time in the stationary phase, and each compound therefore has a specific or characteristic retention time. With a successful separation process of a gas mixture through a GC, each component is detected and qualitatively and quantitatively analysed by detectors at the end of the separation column. Peaks are produced for each component at different times in a chromatogram depending upon their absorption characteristics. Consequently, it is important to choose an appropriate stationary phase for detecting the different components of a multi-component/phase mixture. The column dimensions and operating parameters are the key parameters to achieve the maximum of the differences in migration rates of the components. In this thesis, a Perkin-Elmer, Clarus 580 GC is used. The mobile phase is the outlet gas mixture produced from the micro reactor while the stationary phase is a 50 m long GC column with 320 μm in diameter. The stationary phase is mainly silica in the column. After the separation, components will be quantified in the form of peaks one by one at their own retention time. The retention time is the time between sample injection and compound reaching a detector at the end of the column. This is used to identify the compound. The operating

temperature of the oven in this GC system is 200 °C with a heating rate of 25 °C /min from 80 °C to 200 °C.

The GC is equipped with two types of detectors, a flame ionization detector (FID) and a thermal conductivity detector (TCD). FID is widely used in detecting hydrocarbons such as methane, ethane, ethylene and so on. The working of FID is based on the detection of ions formed by combusting the organic compounds. The organic compounds and carrier gas from the column pass through a hydrogen-air flame and the burning of carbon compounds produces detectable product ions. When these ions pass between electrodes placed near the flame they are collected, and a current is produced which is proportional to the amount of compound being burned. This current is then sensed by an electrometer and gives a recordable digital signal on FID.[1,2] In this system, the flow rates of H_2 and air are set to be 45 mL/min and 450 mL/min, respectively and the running temperature is 250 °C for FID.

Hydrocarbons have a particular molar response factor in FID. It is the ratio between the concentration of a hydrocarbon being analysed and the response of the detector to that compound. A chromatogram will show a response from a detector as a peak and the peaks are equal to the carbon number in the compounds. However, the oxygenates such as carbon monoxide (CO) and carbon dioxide (CO_2) and other non-hydrocarbon compounds have lower response factors. Therefore, another detector, the TCD, is used to detect hydrogen, carbon monoxide, carbon dioxide, nitrogen, air, inorganic gases and other compounds. This detector is based on the principle of comparing the thermal conductivities between column effluent flow (sample components in carrier gas) and the reference flow of carrier gas. The carrier gas used for TCD is helium with a flow rate set as 40 mL/min, and the operating temperature is 200 °C. The difference in thermal conductivity between reference flow and effluent flow is generated because the power requirement for keeping the filament temperature constant changes due to the different thermal conductivities of different compositions

of gases. This difference produces a voltage signal which is proportional to the concentration of the sample components, and this allows the composition to be determined.[2] The calibration of the GC is done by using the standard reference gaseous sample which contains a mixture of different hydrocarbons (contains C1-C12). The instrument has systematic error about ± 0.01-0.1%.



Figure 2.4. Picture of GC (Perkin Elmer, Clarus 580).

2.2.3 Techniques used for characterisation of catalysts

The catalysts were carefully characterised both before and after the test experiments by a range of physical techniques. Powder X-ray diffraction (XRD, Bruker D8 ADVANCE Eco diffractometer), scanning electron microscope (SEM, Jeol 840F), Energy-dispersive X-ray spectroscopy (EDS, Zeiss Merlin), thermogravimetric analysis (TGA, TA Instrument, SDT Q-600), X-ray photoelectron spectroscopy (XPS, Thermo Fisher Scientific Nexsa spectrometer), Brunauer–Emmett–Teller (BET, Micromeritics

3flex surface characterisation system) and ammonia-TPD (NH_3-TPD, Micromeritics 2920 surface characterisation system).

2.2.3.1 X-ray Diffraction (XRD)

X-ray Diffraction is the most common characterisation method in solid state chemistry used to identify of a crystalline material and provide information on unit cell dimensions. The fundamental principle of the XRD is based on Bragg's Law (Figure 2.5). When an X-ray beam strikes the atoms in a crystalline solid, the scattering of X-rays from the atoms produces constructive interference at specific angles, thereby producing a diffraction pattern which contains information about the atomic arrangement within the solid.[3] Bragg's Law (Eq. 2.1) is used to determine constructive interference from X-rays scattered by parallel planes of atoms and relates the scattering angle (2θ) (the position of the diffraction peaks) to the distance, d, between parallel planes of atoms.

$$n\lambda = 2d \sin \theta \qquad (2.1)$$

where the variable d is the distance between diffracting planes, and θ is the Bragg angle, the angle of incidence of the X-ray beam with the planes. λ is the wavelength of the incident X-ray and n in the equation is an integer.

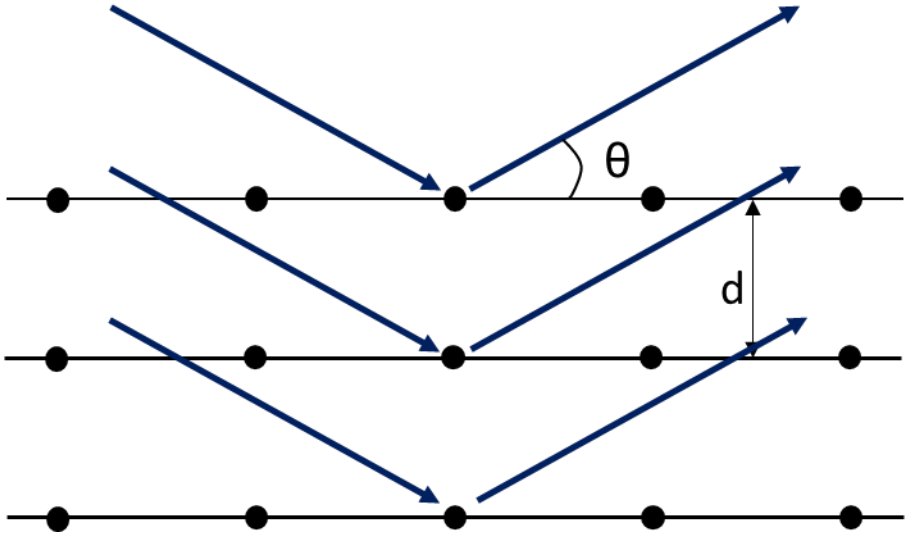


Figure 2.5. Schematic diagram of Bragg's law.

The values of 2θ at which there is constructive interference, and hence a peak in the diffraction pattern is determined by the periodicity of the crystal structure. The intensities of these peaks are determined by the relative arrangement of atoms in the structure and the degree to which the atoms scatter X-rays (which is proportional to atomic number). Different crystal structures have unique diffraction patterns. Hence, the phases present in a certain sample can be identified by comparing with the standard XRD patterns. In addition, the size of particles can be estimated through the Scherrer Equation (Eq. 2.2) by measuring the full-width-at-half-maximum (FWHM) of the diffraction peaks in XRD patterns.[3]

$$\tau = \frac{K\lambda}{\beta Cos\theta} \qquad (2.2)$$

In this equation (Eq. 2.2), τ is the mean size of the ordered (crystalline) domains with units in micro to nanometer scale. λ is the wavelength of the incident X-ray (nm) and K is a dimensionless shape factor with a value close to unity and typically has a value of ca. 0.9, but varies with the actual shape of the crystallite. β is the width at half the

maximum intensity (FWHM) and the θ is the angle of incidence. If the crystalline domains are very small, the long-range periodicity is lost and only very broad features appear in the diffraction pattern. In such cases other short-range probes of the structure are required.

In this thesis, the catalysts were characterised by powder X-ray diffraction (XRD) using a Cu Kα X-ray source (45 kV, 40 mA) on a Bruker D8 Advanced Eco diffractometer. In this study, the pattern was measured by scanning in a range (in 2θ) of 20° to 70° in about 30 min per sample.

2.2.3.2 Scanning Electron Microscopy and Energy-dispersive X-ray spectroscopy (SEM-EDS)

Scanning electron microscopy (SEM) is a powerful analytical technique that has been applied widely in many scientific applications for the examination of solid material structures.

A scanning electron microscope normally consists of electron gun, condenser lenses, apertures, a scanning system and a specimen chamber (Figure 2.6).[4] The electron gun is located at the top of the electron column and generates the electron beam under high vacuum. The free electrons will be generated by thermionic emission at about 2500-3000K using a tungsten filament. The electron beam will be accelerated toward an anode through an adjustable high voltage from 200V to 30 kV, and pass through magnetic lenses. Then the sample will scatter the electrons to produce an image. X-rays emitted by electronic excitations are detected by a suitable detector to identify the elements present in the sample, which gives the elemental analysis data.[4] This will be described in detail below. The images are finally formed by the beam scanning the surface of the material where electrons are emitted from the material by the action of the scanning beam and collected by a detector.[5]

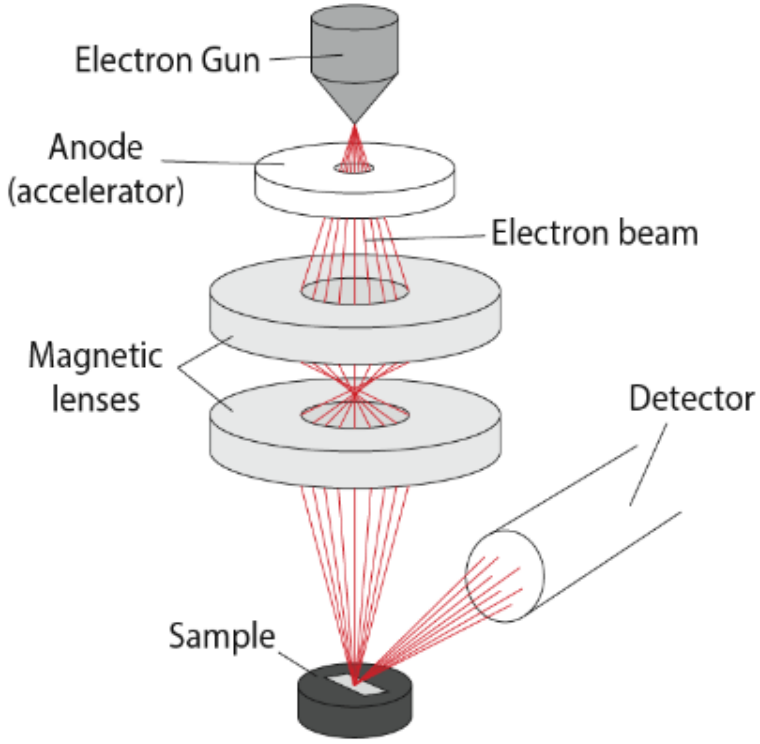


Figure 2.6. Scanning electron microscope column.[4]

There is an X-ray detector mounted on the column to receive the X-ray signal. The sample material is irradiated with electrons resulting in the emission of X-rays characteristic of the elements present. The energy emissions are translated into spectral peaks of varying intensity, and this allows for quantitative determination of elemental composition of the specimen through energy dispersive X-ray spectroscopy (EDS) analysis.

EDS analysis can in principle detect all elements from atomic number 4 (Be) to 92 (U). Quantitative analysis is also possible to determine the concentration of the elements in the specimen sample surface. In the detector, X-ray photons cause ionisation, thereby producing an electrical charge which is then amplified by a sensitive preamplifier.

In this thesis, the scanning electron microscope (SEM-EDS, JEOL 840F) is in general used to characterise the surface morphology of the catalysts before and after the reactions, and the surface elemental analysis was carried out with energy-dispersive X-ray spectroscopy. Another scanning electron microscope (SEM-EDS, Zeiss Merlin) was also employed for some characterisation. All the images were taken by Dr. Xiangyu Jie, and were performed in the Department of Materials, University of Oxford.

2.2.3.3 Thermogravimetric Analysis (TGA)

Thermogravimetric Analysis (TGA) is a characterisation method to determine the thermal properties of materials and to estimate the composition of materials. The technique can measure the weight change and the rate of weight change as a function of temperature under diluent atmospheres. The weight changes of a sample have various reasons. These could include sublimation, decomposition, chemical reactions or desorption and adsorption. The TGA curve produced by the measurement can give information on the thermal stability and oxidative stability of materials. From this it may be possible to deduce the composition of multi-component systems, the decomposition kinetics of materials, the moisture and volatile content of materials and the effect of reactive or corrosive atmospheres on materials. As well as simply measuring the mass, there is also derivative weight-to-temperature plots, known as D-TGA or DTA. These plots (shown in TGA profiles in Chapter 3 and 4) are quantised using the instrumental software, showing the positive and/or negative peaks which relate to the weight losses and/or gains. This helps to identify the weight change even when it is very small and hard to quantify in the TGA curves.

In this thesis, a TA Instrument, SDT Q-600 was employed for TGA measurement. The technique is mainly used to characterise the coke formation on the spent catalysts and to determine the amount of carbon deposition by burning off the deposited carbon in a

stream of flowing air. In the TGA experiment the spent catalysts are heated under air with a heating rate of 10 °C/min to 1000 °C.

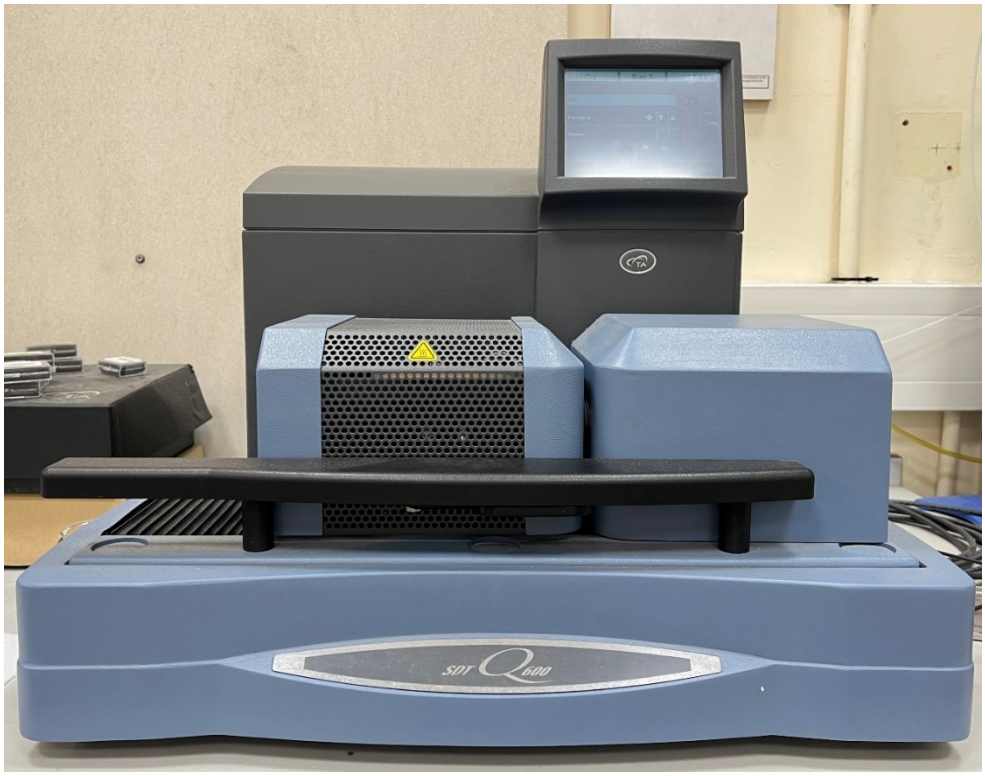


Figure 2.7. Picture of the TA Instrument, SDT Q-600.

2.2.3.4 X-ray Photoelectron Spectroscopy (XPS)

X-ray photoelectron spectroscopy (XPS) is a near surface sensitive analytical technique, in which X-rays bombard a material and the kinetic energy of the emitted electrons is measured. The two major characteristics of this technique that make it powerful as an analytical method are its surface sensitivity (although this is sometimes a disadvantage) and its ability to reveal chemical state information from the elements in the sample.[6] XPS is routinely used to analyse inorganic compounds including metal alloys, semiconductors, catalysts and many others. In the laboratory X-ray sources, XPS easily detects all elements except hydrogen and helium.[6] XPS is a powerful

measurement technique because it can show what elements are present. The technique can be used in profiling of the elemental composition across the surface.

XPS is based on the photoelectric effect arising when high energy photons (usually in the keV range) hit a material with the consequent emission of electrons (photoelectrons). The photoelectron kinetic energy, KE, which is the measured quantity in the experiment, is given by Einstein's law:

$$KE=hv-BE \tag{2.3}$$

where hv is the energy of the incident radiation and BE the binding energy of the electron in a particular level. If the incident photons have enough energy, the sample may be ionised with ejection of photoelectrons from different electronic energy levels and thus a spectrum is produced displaying all accessible energy levels as a distribution of photoelectrons with kinetic energies governed by equation 2.3. In XPS, the sample is irradiated with soft X-rays (energies lower than ~6 keV) and the kinetic energy of the emitted electrons is analysed (Figure. 2.6).[6] Photoelectron peaks are labelled by the element and orbital from which they were ejected. For example, "Na 1s" describes electrons emitted from the 1s orbital of a sodium atom. Any electron with a binding energy less than the X-ray source energy should be emitted from the sample and observed with the XPS technique. All the element have their specificity of the binding energies and the relation between the intensity of the photoelectron peaks and the element concentration.[7] Atoms of a higher positive oxidation state exhibit a higher binding energy due to the extra coulombic interaction between the photoemitted electron and the nucleus. Therefore, chemical information about the different elements present, especially the oxidation state, can be identified using XPS.

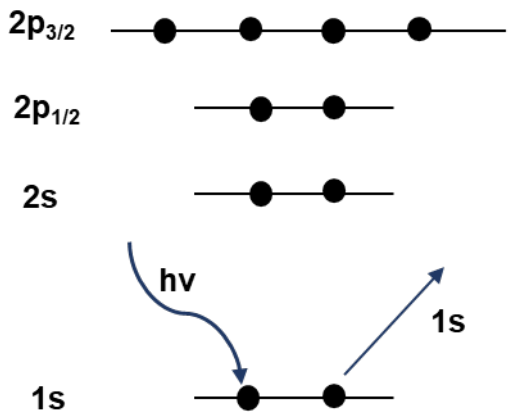


Figure.2.8. X-ray strike of a electron and emission of a photoelectron.[6]

In this thesis, the XPS of samples was performed using a Thermo Fisher Scientific Nexsa spectrometer. Samples were analysed using a micro-focused monochromatic Al X-ray source (72 W, 1.487 keV) over an area of ~400 × 200 μm^2. The materials were analysed at pass energies of 150 eV for survey scans and 40 eV or high-resolution scans with 1 and 0.1 eV step sizes respectively and the data were recorded. Charge neutralisation was achieved using a combination of low energy electrons and argon ions. This is to avoid charging of samples with poor conductivity during the experiment. The resulting spectra were analysed using Casa XPS peak fitting software and details are described in Chapter 3. The XPS analysis tests were done under help with Dr. Shaoliang Guan at the Harwell XPS centre.

2.2.3.5 Temperature-Programme Desorption of Ammonia (NH_3-TPD)

Temperature-Programmed Desorption of Ammonia (NH_3-TPD) is one of the most common and convenient methods to characterise the acidity of a catalyst. Its theoretical basis centres on the relationship between heat and adsorption/desorption

of sorbent gases. According to the different modes of binding between ammonia and adsorbents, it can be divided into physical adsorption and chemical adsorption. In physical adsorption, the ammonia gas interacts with adsorbents by simple physisorption (weak interaction force); and chemisorption, as the name implies, refers to the chemical interaction between ammonia and the adsorbent to form a chemical bond (a stronger interaction force). Most of physical adsorption and chemical adsorption are considered as exothermic processes. Therefore, the reverse process of adsorption, desorption, can occur by some supply of energy to release ammonia. In the NH_3-TPD test, this energy is supplied in the form of thermal energy, that is, the adsorbent that has adsorbed the NH_3 is desorbed by heating in an electric furnace. And the amount of the desorbed ammonia gas will be detected by a TCD detector.

NH_3 molecules adsorbed by chemisorption typically have high binding energies, (as one might expect) therefore significant increases in temperature are necessary to fully desorb the ammonia from these adsorbates. Experiments are typically performed under identical experimental conditions (e.g. heating rates and sample size) so that a qualitative comparison can be made between samples. The different temperatures for the desorption process show the different absorption type between NH_3 and absorbent. Thus during a NH_3-TPD experiment, the amount of desorbed NH_3 is often monitored by mass spectrometry and the surface interactions are explored with infrared spectroscopy.[8]

In this thesis, the catalysts' surface acidity was tested by ammonia-TPD (Micrometrics 2920 surface characterisation system). The catalysts were pre-heated in flowing helium gas for 1h at 450 °C to remove any adsorbed species and cooled down to room temperature, they were then then exposed to ammonia gas at standard temperature and pressure for 1 hour, and then purged with helium and heated linearly at 10 °C/min to 450 °C in 50 ml/min flow rate. The amount of ammonia in the effluent was recorded continuously as a function of temperature. The tests and analysis were done with the

help of Dr. Robert Jacobs at the Surface Analysis Facility (SAF), Chemistry Research Laboratory, Department of Chemistry, University of Oxford.

2.2.3.6 Brunauer, Emmett and Teller (BET) surface analysis

Brunauer, Emmett and Teller (BET) surface analysis is a method to measure the surface area of a solid material. The concept of the BET method is an extension of the Langmuir theory. The Langmuir theory relates the monolayer adsorption of gas molecules, also called adsorbates, onto a solid surface to the gas pressure of a medium above the solid surface at a fixed temperature. There are assumptions be applied for Langmuir theory: (a) all surface sites have the same adsorption energy for the adsorbate. The surface site is defined as the area on the sample where one molecule can adsorb onto; (b) adsorption of a gas molecule at one site occurs independently of adsorption at neighbouring sites; (c) activity of adsorbate is directly proportional to its concentration; (d) adsorbates form a monolayer; (e) each active site can be occupied only by one particle.

The BET theory extends the Langmuir theory to multilayer adsorption with three additional assumptions: (a) gas molecules will physically adsorb on a solid in layers infinitely; (b) The different adsorption layers do not interact; (c) the theory can be applied to each layer. The equation 2.4 is used to determine the monolayer absorbed gas volume (v_m) based on Langmuir theory.

$$\frac{1}{v\left[\left(\frac{p_0}{p}\right)-1\right]} = \frac{c-1}{v_m c}\left(\frac{p}{p_0}\right) + \frac{1}{v_m c} \qquad (2.4)$$

where v is absorbed gas quantity, c is referred to as the BET C-constant, p_0 is the saturated pressure of the adsorbate, p is the equilibrium pressure of adsorbate.

Based on the BET theory, using equation 2.4 can plot a linear graph to determine monolayer adsorbed gas quantity and the BET constant. Take numerical values for slope and intercept to solve for v_m and c. From the monolayer absorbed gas volume (v_m), we can determine total and specific surface area surface area of a solid material is determined by the physical adsorption of a gas (typically nitrogen, krypton, or argon) onto the surface of the sample at cryogenic temperatures (typically liquid nitrogen or liquid argon temperatures). The choice of gas to be used is dependent on the expected surface area and the properties of the sample. In BET surface area analysis, nitrogen is usually used because of its availability in high purity and its strong interaction with most solids. However, the interaction between gaseous and solid phases is usually weak, the surface is cooled using liquid N_2 to obtain detectable amounts of adsorption. The amount of gas adsorbed depends on the exposed surface area but also on the temperature, gas pressure and strength of interaction between the gas and solid. Known amounts of nitrogen gas are then released stepwise into the sample cell. After the saturation pressure, no more adsorption occurs regardless of any further increase in pressure. Highly precise and accurate pressure transducers monitor the pressure changes due to the adsorption process. After the adsorption layers are formed, the sample is removed from the nitrogen atmosphere and heated to cause the desorption of nitrogen from the material and quantify the amount of desorbed N_2.

Once the amount of N_2 has been measured (either by a volumetric or continuous flow technique), calculations of the known gas has been adsorbed are applied.[9] The data collected is displayed in the form of a BET isotherm, which plots the amount of gas adsorbed as a function of the relative pressure (p/p_0). BET surface area analysis must be done in the linear region of the BET plot, which could be systematically evaluated using the Rouquerol transform which is a commonly analysis rule used to fitting and optimising BET results.[10]

In this thesis, the BET surface analysis was applied using the micrometeritics 3flex surface characterisation system, at the Surface Analysis Facility (SAF), Chemistry Research Laboratory, Department of Chemistry, University of Oxford. All the analysis tests were carried out with the help of Dr. Robert Jacobs.

References

1 T. Holm, *J. Chromatogr. A*, 1999, **842**, 221–227.

2 V. G. Berezkin, V. R. Alishoyev and I. b. Nemirovskaya, *gas chromatography of polymers*, Elsevier Science Publishersing Company, Amsterdam, 1977.

3 M. M. Woolfson, *An introduction to X-ray crystallography*, Cambridge University Press, illustrate., 1970.

4 The Scanning Electron Microscope (SEM), https://www.eng-atoms.msm.cam.ac.uk/RoyalSocDemos/SEM, (accessed 15 June 2022).

5 SciMed, A Brief Introduction to SEM (Scanning Electron Microscopy), https://www.scimed.co.uk/education/sem-scanning-electron-microscopy/.

6 F. A. Stevie and C. L. Donley, *J. Vac. Sci. Technol. A*, 2020, **38**, 063204.

7 A. M. Venezia, *Catal. Today*, 2003, **77**, 359–370.

8 The basic background of CO_2/NH_3-TPD, https://wenku.baidu.com/view/401210601ed9ad51f01df22f?aggId=a478073d866fb84ae45c8d3d, (accessed 22 June 2022).

9 BET Specific Surface Area, https://www.particletechlabs.com/analytical-testing/gas-adsorption-and-porosimetry/bet-specific-surface-area, (accessed 19 June 2022).

10 J. Rouquerol, P. Llewellyn and F. Rouquerol, *Stud. Surf. Sci. Catal.*, 2007, **160**, 49–56.

Chapter 3

The Dehydrogenation of Propane by CO_2 Over ZrO_2-Supported Catalysts Prepared by the Impregnation Method

3.1 Introduction

As an important raw material for a variety of polymers and chemical intermediates, propylene is recognised as one of the ubiquitous and important commodities in the international chemical industry. The global propylene demand is growing at a rate of about 5% annually and will be up to approximately 165 million tons by 2030.[1] Therefore, to meet the huge demand in future, highly efficient propylene synthesis is vitally important. Steam Cracking (SC), Fluid Catalytic Cracking (FCC) and Oxidative Propane Dehydrogenation (OPDH) are the primary and conventional methods to obtain this important feedstock chemical. However, the low propylene selectivity under high-temperature operating conditions and the large cost for the raw materials make the current methods ineffective.[2,3] The first two processes, SC and FCC are accompanied by vast quantities of emitted CO_2 which means they must be considered as non-sustainable processes under a recent global environment evaluation.[4]

Oxidative propane dehydrogenation (OPDH) presents an alternative green and promising catalytic technology utilised for the conversion of propane into propylene which is involved in many petrochemical applications.[5]

$$\text{Dehydrogenation: } C_3H_8 \rightarrow C_3H_6 + H_2 \qquad (3.1)$$

$$\Delta H^0_{296} = +124 \text{ kJ/mol } [1]$$

As mentioned in Chapter 1, it is an economical route to produce propylene, and it has been successfully implemented in the industrial process by UOP-licensed Oleflex™ and KBR-licensed Superflex™ technologies.[6] In general, commercial catalysts used for direct dehydrogenation are based on Pt and CrO_x. The endothermic reaction in the PDH process (3.1) requires a high operating temperature to achieve a satisfactorily high yield of propylene. This leads to serious thermal cracking of any reacting (and product) hydrocarbons to generate small alkanes and the ever-present carbon deposit, which is the main reason of the rapid deactivation of the catalysts, thus sacrificing both the propylene selectivity and catalysts' lifetime.[5]

In this case, O_2 becomes a commonly used strong oxidant for PDH as the overall reaction becomes exothermic and thermodynamically unrestricted at lower temperatures (3.2).[6] Hence, the PDH with oxidant is called the oxidative propane dehydrogenation (OPDH). The O_2-PDH is facilitated by various transition metal oxides, supported on various main group and transition metal oxide supports.

$$O_2\text{-PDH: } C_3H_8 + ½\ O_2 \rightarrow C_3H_6 + H_2O \qquad (3.2)$$

$$\Delta H^0_{296} = -118 \text{ kJ/mol } [1]$$

Thus far, of the catalysts reported for the O_2-PDH reaction, vanadium oxide (VO_x), molybdenum oxide (MoO_x), chromium oxide (CrO_x), and gallium oxide (GaO_x) which is less redox active than others, supported on a metal oxide such as SiO_2, ZrO_2, Al_2O_3 and TiO_2, have been extensively investigated.[6–9] In addition, heteroatom-doped nano-carbon materials, for example B-doped nano-carbons and nitrogen-containing carbon matrix, have been explored as metal-free catalysts. Boron nitride, and zeolites and other porous materials such as H-ZSM5, SBA1 and MCM41 have also been introduced into the realm of oxidative propane dehydrogenation process.[3,10–12] Although great

progress and development have been achieved, overcoming the combustion of light alkanes is still a challenge for the higher oxidative capacity catalysts with O_2.[13]

Therefore, we adopt the approach of using CO_2 as a milder oxidising agent to replace O_2, and the route is denoted as CO_2-PDH (3.3). CO_2 is a waste and greenhouse gas and its utilisation has attracted much attention in recent years.[13–16]

$$CO_2\text{-PDH: } C_3H_8 + CO_2 \leftrightarrow C_3H_6 + CO + H_2O \quad (3.3)$$

$$\Delta H^0_{296} = +164 \text{ kJ/mol } [1]$$

In 1972, Fox et al. started using CO_2 as an alternative to O_2 and started the study in OPDH using CO_2.[17] In this CO_2-PDH process, CO_2 acts as a non-traditional, unusual mild oxidant, and oxygen transfer agent to combine with the simple dehydrogenation reaction (reaction 3.1), and also with a reverse water gas shift (RWGS) reaction (3.4). In addition, CO_2 can also reduce the coking effect on the catalyst by the reverse Boudouard reaction (3.5).[18,19]

$$\text{RWGS: } CO_2 + H_2 \leftrightarrow CO + H_2O \quad (3.4)$$

$$\Delta H^0_{296} = +40 \text{ kJ/mol } [20]$$

$$\text{Boudouard: } 2CO \leftrightarrow CO_2 + C \quad (3.5)$$

$$\Delta H^0_{296} = -131 \text{ kJ/mol } [20]$$

3.1.1 Proposed redox cycle of CO_2-PDH

Oxidative propane dehydrogenation is recognised to involve a parallel-series reaction network.[21] This reaction network can be considered to account for the propane conversion to propylene (k_1), the undesired formation of CO_2 from propane (k_2), and the secondary combustion of propylene to CO_2 (k_3). In these cases, the only source of oxygen is the catalyst lattice oxygen.

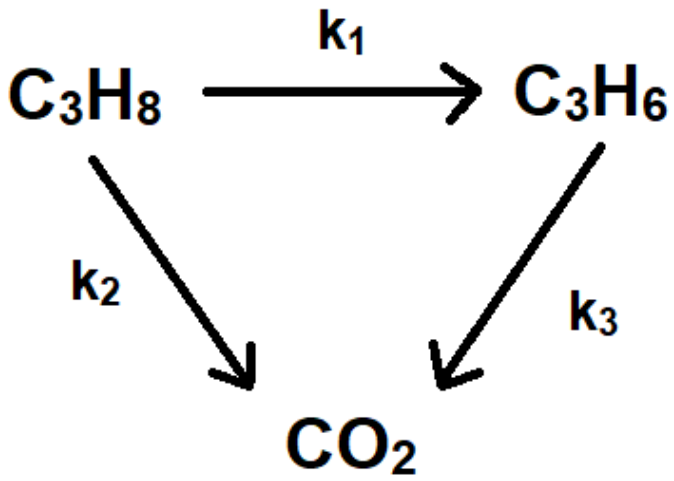


Figure 3.1. Proposed simplified reaction network for propane oxidative dehydrogenation.[21]

The proposed reaction network (Figure 3.1) assumes that propane reacts with the catalyst lattice oxygen producing both propylene and CO_2 as "primary" reactions, while the propane to CO_2 conversion is a "secondary" reaction.[21]

The mechanism for the dehydrogenation of propane with CO_2 has not been thoroughly rationalised, although different pathways have been proposed. It has been reported that the redox and acid−base properties of the catalysts can determine which of two pathways the reaction takes and hence explain the promoting effect of CO_2.[2] One of the routes is considered to occur through the participation of lattice oxygen ions as the selective oxidation species and oxygen vacancies as the adsorption sites. The alternative route is the direct propane dehydrogenation (3.1) coupled with the RWGS reaction (3.4). However, the competitive adsorption among propane, CO_2 and water vapour are the main reasons for potentially lowering the initial propane conversion. This competitive adsorption also can also result in less coking effect and higher stabilities of catalysts in a CO_2 atmosphere.[19,20] The reaction pathway depends on the nature of the catalyst used and the reaction conditions. Further research and

development works are necessary to develop more efficient catalysts to realize this environmentally favourable process.

The CO_2 involved in propane dehydrogenation (PDH) acts a mild oxidant. In this case, the CO_2 can either re-oxidise the reduced metal oxides on the catalyst surface as part of the MvK reaction mechanism or it can consume the hydrogen released by direct dehydrogenation through the RWGS reaction. Previous work by Shishido et al. proposed a chemical mechanism in an attempt to understand how the CO_2 would be involved in PDH over CrO_x-based catalysts and concluded the catalytic cycle mechanism (Figure 3.2) as a redox cycle between Cr(III) and Cr(VI).[19]

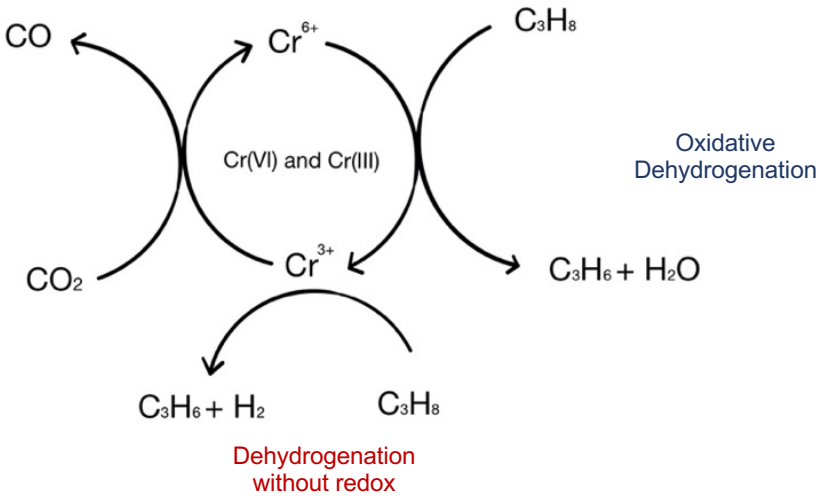


Figure 3.2. Proposed reaction mechanism of dehydrogenation of C_3H_8 in the presence of CO_2.[19]

Redox oxides involve the transfer of electron between species by different oxidation states. Production of H_2 could be an indication of the non-redox pathway. Therefore, the Cr(VI) species provides an oxidative dehydrogenation process and is reduced to a Cr(III) species. Then CO_2 then acts as an mild oxidant to regenerate the Cr(VI) species from Cr(III) thus providing a continuous redox cycle for propane dehydrogenation.[19] The continuous redox cycle will keep catalyst activities, hence increase the catalytic efficiency and enhance the propane conversion and propylene selectivity. Therefore,

the oxidised Cr(VI) and reduced Cr(III) sites are therefore implicated as the major active sites responsible for propane dehydrogenation.

3.1.2 Catalyst design for CO_2-PDH

However, it is important to note that any chemical reactions (conversions) are driven by differences in the Gibbs Free Energy (ΔG^0) between reactants and products of a chemical reaction (under certain conditions). Figure 3.3 shows that the Gibbs free energies are not favourable in converting CO_2, as the most thermodynamically stable form of carbon, to other molecules. The activation of any reaction with CO_2 is therefore very difficult.[22,23]

Progress in the use of CO_2 as a useful reactant will only emerge through judicious use of novel catalytic chemistry.[24] It is highly desirable to develop an efficient catalyst to catalyse CO_2-PDH to form propylene. In catalysis, the active component, promoter, and support are the basic components that usually constitute a catalyst for a particular application.[25] The active sites are the main catalytic centres assembled within the active component, where the propane would interact with the catalysts during reactions to produce propylene.[26] The active sites for OPDH are different for different catalysts. These active sites are widely considered to be reactive oxygen species present in different structural forms on the surfaces of the catalysts. Currently, metal-oxide-based catalysts are the most explored in oxidative propane dehydrogenation (OPDH), and their active sites are mainly lattice oxygen species. The active sites mostly facilitate the OPDH reaction via the Mars-Van Krevelen (MvK) mechanism, involving sequences of oxidation-reduction steps on the metal oxide surface.

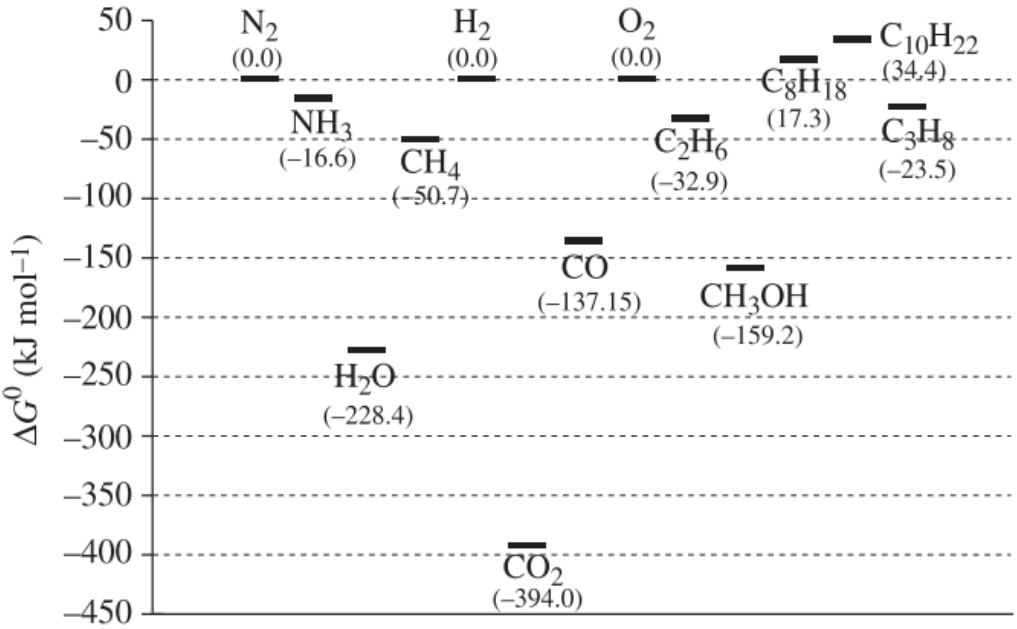


Figure 3.3. Gibbs free energy of formation for selected chemicals (data compiled and calculated from NIST data base, Http://webbook.nidt.gov/chemistry/name-ser.html) Here, ΔG^0 for the constituent elements is taken as the reference point. [24]

Unfortunately, depending on the reaction conditions, many undesired side reactions can occur including dry reforming of propane to syngas (3.7) and propane decomposition, which bring about coke formation through Boudouard reaction (3.6) and carbon monoxide reduction by hydrogen (3.8).

$$C_3H_8 + 3CO_2 \leftrightarrow 6CO + 4H_2 \qquad (3.7)$$

$$\Delta H^{\varnothing} = +620 \text{ kJ/mol} \ [20]$$

$$CO + H_2 \leftrightarrow C + H_2O \qquad (3.8)$$

$$\Delta H^{\varnothing} = -131 \text{ kJ/mol} \ [20]$$

Any combination of reactions 3.3 to 3.7 could be favoured according to the catalyst properties and process conditions. Therefore, different sets of equilibria could be approached and a suitable catalyst should favour only the desirable reaction(s).

The thermodynamic analysis of CO_2-PDH is an important step in the design of suitable catalyst for the process. It provides a basis for experimental and computational studies, as well as understanding the thermodynamic limitations of the process and provide information for catalyst development. The detailed thermodynamics of CO_2-PDH incorporating the effect of different co-feeds and the effect of individual side reactions is required. Zangeneh et al. has showed a detailed computational study of the chemical equilibria that apply to the reactions during CO_2-PDH. The thermodynamic results showed that the equilibrium conversions of propane in the presence of CO_2 are higher than in the presence of an inert gas or hydrogen.[20] However, compared with experimental results, propane conversion for CO_2-PDH are much lower than those predicted by equilibrium due to the catalyst deactivation.[20]

On the other hand, the competitive side reactions also affect the chemical equilibrium of CO_2-PDH. Zangeneh et al. also summarised the comparison results as shown in the figures below.

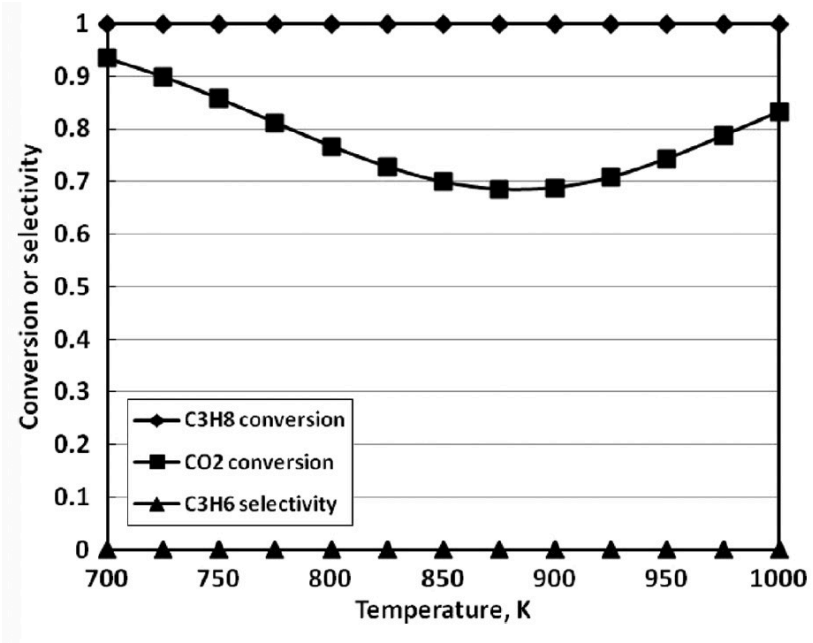


Figure 3.4. The effect of temperature on equilibrium conversion of propane and carbon dioxide and selectivity of propylene in the presence of propane reforming reaction. (C_3H_8/CO_2=1, P=1 bar)[20]

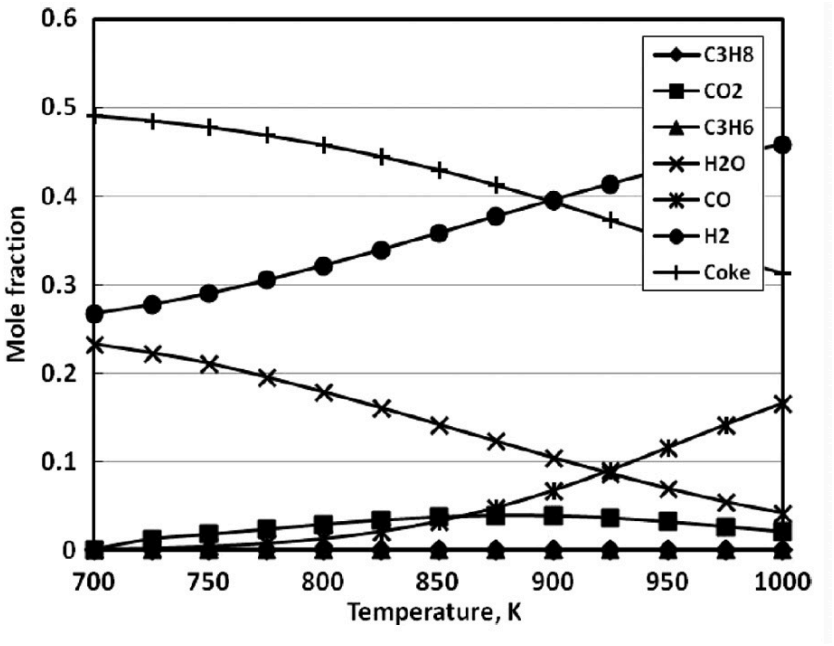


Figure 3.5. The effect of temperature on equilibrium product composition in the presence of propane reforming reaction. (C_3H_8/CO_2=1, P=1 bar)[20]

The thermodynamic simulation between CO_2-PDH and side reactions in Figures 3.4 and 3.5 show a greatly increases propane conversion, but the selectivity propylene is lower. This illustrated the side reactions, such as propane dry reforming and coke formation, are thermodynamically more favourable than the main reaction. Therefore, the thermodynamics of all possible reactions during CO_2-PDH are important for developing the suitable catalysts. Hence to avoid the competitive side reactions and increase propylene selectivity.

3.1.2.1 Promoter effects by mixed metal-oxides catalysts on catalytic performance

In the propane dehydrogenation (PDH) reactions, the activation of the first C–H bond of propane is acknowledged as the rate-determining step which determines the

catalyst activity. The propylene that is formed is more active and can more easily undergo complex side reactions, such as further dehydrogenation and cracking to form methane (CH_4), ethane (C_2H_6) and ethylene (C_2H_4).

Currently, transition metal oxide-based catalysts are the most explored in propane dehydrogenation due to the valence d-orbitals which make them amenable to having various accessible oxidation states. The low-lying empty d orbitals in transition metals such as manganese, iron and chromium in high oxidation states are able to accept electrons and act as Lewis acids. Lewis acid Metal–O sites of metal oxides determine their PDH reactivity. For propane dehydrogenation, the Lewis acid M–O sites in metal oxides can effectively activate the propane C–H bonds.[12,27,28] As reported in Chapter 1, there has been extensive research and development on different types of catalysts for propane dehydrogenation with promising results and these are relatively close to commercialisation.[13]

Various transition metal oxide-based catalysts, including Pt, Cr, Pd, V and Ce, and the main group metal Ga have been reported to have promising PDH catalytic performance,[26] yet suffer from the loss of oxygen under reaction conditions, and rapid deactivation. Over the course of a catalytic cycle, due to the coke deposition, frequent regeneration operations (removal of coke by combustion) are needed.[12] In a recent review, the catalytic performances of different metal-oxide based catalysts have been compared with each other. It has been pointed out that the activity and the propylene selectivity both need to be further improved, along with the catalyst stability during the dehydrogenation. To improve the catalytic behaviour during the PDH with CO_2, mixed metal oxides with optimum metal ratios have also been studied. Elemental Pt-based catalysts are active for propane dehydrogenation due to their affinity for paraffinic C–H bonds. However, the main problems of using Pt particles are C–C cleavage and deep dehydrogenation leading to coke formation, high temperatures during the dehydrogenation and the high cost of Pt. Therefore, to lower the Pt content, modified

Pt-based metal catalysts using a promoter (e.g. metals or metal oxides) have received much recent attention in the research area. It has been reported that the Sn^0 species added into the Pt-based catalysts as promoter increase the propane conversion rate for PDH.[29] For heterogeneous catalysts, adding other metals or metal oxides can help to increase the concentration of oxygen vacancies (more electron accepters) which can help the C–H cleavage during the PDH.[26] After the C–H activation, a reduced site is formed and should be regenerated for the next catalytic cycle. In Chapter 1, we have introduced some investigations on mixed metal catalysts for dehydrogenation process such as $NaWO_4$ mixed with metal Mn on an SiO_2 and WO_x-VO_x-SiO_2.[30–32] Nowadays, more and more metals and metal mixtures are studied for propane dehydrogenation with CO_2, such as Ni, Fe, Mn, and Mo.[4,24,33–35]

By mixing the different metal oxides on supports as new catalytic systems for PDH, the nature of the catalytic surface will be affected and may enhance the catalytic stability and activity. This will, in principle, increase the catalytic efficiency and lower the cost and energy utilisation of catalyst preparation.

3.1.2.2 The effect of the support on catalytic performance

In addition to promoters, good supports for propane dehydrogenation need to be thermally stable, especially under dehydrogenation conditions. Their textural properties such as specific surface area, and their chemical properties such as acid–base properties, and thermal stability have been demonstrated to have significant influences on the catalytic performance.[12] Different supports can also modify various properties of catalysts, improving the dispersion of activated sites or changing the surface electronic properties due to the interaction with the catalyst. The support materials include main group and fully oxidised early transition metal oxides (such as alumina, silica, titania, ceria, zirconia, and magnesium oxide), zeolites, and carbon-

derived materials such as activated carbon and carbon nanofibers.[12] Besides, metal oxide clusters supported on metal-organic frameworks have shown good prospects for low-temperature PDH performance. Because of the competitive adsorption between CO_2 and propane, the acidity and basicity of the catalysts' surface is very important. During the reaction, CO_2 was adsorbed by basic sites on the catalyst surface and this inhibits the competitive propane adsorption. So, this competition reduces the propane conversion to propylene during propane dehydrogenation.

CrO_x-based catalysts generally have good performance in propane dehydrogenation, but it is strongly influenced by the nature of the support.[36] In early work led by Ge *et al.*, the prominent activity of Cr_2O_3/SiO_2 has been confirmed via screening tests on Cr_2O_3, Cr_2O_3/SiO_2, $Cr_2O_3/\gamma\text{-}Al_2O_3$, Cr_2O_3/ZrO_2, Cr_2O_3/TiO_2, and Cr_2O_3/MCM-41.[37] In the presence of CO_2, the partially oxidised Cr_2O_3 surface and the boundaries of Cr_2O_3 and SiO_2, are responsible for the improved C_3H_6 yield.[38] Although high CO_2 conversion can be achieved on the ZrO_2-supported counterpart, its strong basicity leads to lower C_3H_6 selectivity but higher selectivity toward CO and CH_4.[14,37,39,40] Competitive adsorption between CO_2 and C_3H_8 occurs on supports with amphoteric properties, such as γ-Al_2O_3, leading to decreased catalytic performance, especially at higher CO_2 partial pressures.[19,41] MCM-41-supported Cr catalysts exhibit comparable activity to the SiO_2-supported counterpart, which is associated with its ordered mesoporous structure with large surface area and pore volume.[42] Such prominence is also evident on zeolites SBA-15 and SBA-1.[39,43] The ordered mesoporous structure and large surface area not only helps to improve Cr surface density but also the dispersion of the Cr^{6+} species, thereby benefiting C_3H_6 formation. Nonetheless, the structural stability these porous materials is still an unsolved problem, which is fatal for industrial applications. The propylene selectivity of zeolite-supported catalysts is also not high enough because of their strong acid sites. The support plays a decisive role in determining surface metal oxide structures and the surface reducibility by affecting the dispersion of the metal

species as the active phase. Irrespective of metal-support interaction, the surface area of support affects the metal dispersion. Furthermore, zeolite synthesis is complicated, time-consuming and costly. The Al/Si ratio also affects the support properties during the PDH as it could change their structures and surface acidity.[36] Nowinska et al. reported that there are some tendency of increase in selectivity towards propene and decrease in propane conversion with the increase in Si/Al ratio.[44]

Different kinds of support can improve the dispersion of active surfaces and also change the catalysts surface property due to the interaction between the dopant and the support surface.[45] In the work of Bugrova et al. XPS results showed the different ratio between Cr(V) and Cr(VI). The chromium had a better dispersion over the ZrO_2 surface, about 66% of Cr(VI) in CrO_x/ZrO_2 sample (total Cr content). In comparison, on γ-Al_2O_3, Cr(VI) was about 35% of the total Cr content.[46]

3.2 Chapter Overview

For the propane dehydrogenation process, the role of CO_2 and the mechanism of the reaction are fundamental to our understanding of how these heterogeneous catalysts operate. These are highly dependent on both the metal oxides at active sites and the support material used. In addition, the propane dehydrogenation and the RWGS reaction are competitive and will result in different catalytic performances with different catalysts. Moreover, the catalyst deactivation by catalyst sintering and carbon deposition represent additional, ever-present challenges, as catalyst aggregation and carbon deposition increase at higher reaction temperatures and lower H_2 partial pressures, respectively. Redox catalyst deactivation is also caused by the reduction of metal oxides during the dehydrogenation, in which case CO_2 becomes a viable means of reactivating those catalysts.

In the body of research centred on transition metal oxides, CrO_x-based catalysts appeared to exhibit excellent activity in the dehydrogenation reaction.[36,47] It also has been reported that a great increase in product yield occurs using CrO_x-based catalysts.[48] However, the toxicity of the chromium and the deactivation of the catalysts are still the main challenges in this area. In this chapter, the research will be based on the CrO_x catalysts supported on ZrO_2. The work will study the promoter effect on CrO_x-based catalysts by adding different promoter metal oxides including V, Mn, Zn and Ca. V has been widely reported as a dopant for metal oxides for oxidative propane dehydrogenation.[20,49,50] Mn is chosen as it has various oxidation states so could show a good redox ability during the reaction. Zn is one of the well-researched metals used for light alkane dehydrogenation.[51–53] Ca as an alkaline earth metal, has a basic oxide, and the basic properties could affect the catalyst surface basicity. The investigations of the various catalyst systems will focus on their catalytic performance, propylene selectivity and their stability, and the CrO_x-only catalysts and the promoted CrO_x

catalysts will be compared. The characterisation will be applied to these catalysts both before and after reactions.

3.3 Experimental Methods

3.3.1 Preparation of catalysts

In this chapter, CrO_x-based catalysts were chosen for development and adding other metal oxides as promoters was explored. 2 mmol (about 8-10wt%) of Cr precursors [Chromium (III) Nitrate Nonahydrate, Acros Organics, ≥ 99%] were supported on 10 mmol of ZrO_2 [Alfa Aesar] using the method shown in Figure 3.6 which is described as an impregnation method. The process for the preparation of the catalysts is described in detail in Chapter 2. All fresh catalysts were ground thoroughly and passed through a 125 μm mesh sieve. The following Table 3.1 lists the designed catalysts and the precursors of added promoting oxides. All the catalysts, except the one with no promoter, have the molar ratio Cr : promoter : Zr of 1:1:5.

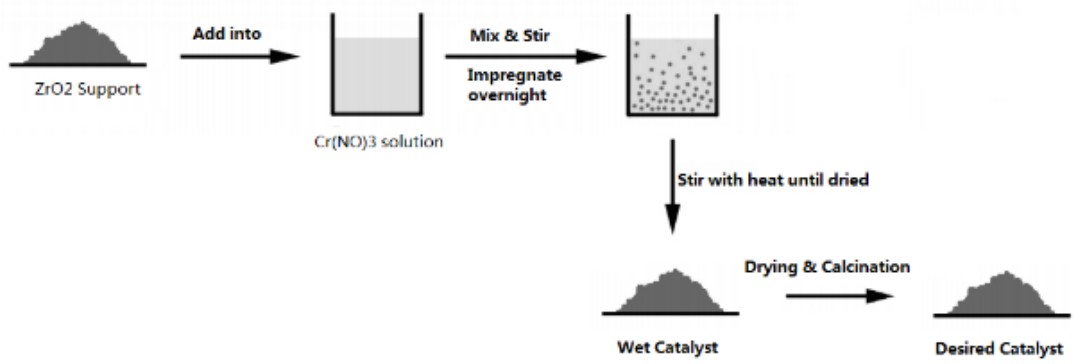


Figure 3.6. Catalyst preparation procedure of the widely-used impregnation method.

Table 3.1. Summary of the designed CrO_x-based catalysts supported on 10 mmol ZrO_2.

Catalysts	Precursors	Amount of Precursors
2Cr-ZrO_2	$Cr(NO_3)_3$	2 mmol
2Cr/Mn-ZrO_2	$Cr(NO_3)_3$, $Mn(NO_3)_2$	2 mmol; 2mmol
2Cr/Zn-ZrO_2	$Cr(NO_3)_3$, $Zn(NO_3)_2$	2 mmol; 2mmol
2Cr/V-ZrO_2	$Cr(NO_3)_3$, $VO(NO_3)_3$	2 mmol; 2mmol
2Cr/Ca-ZrO_2	$Cr(NO_3)_3$, $Ca(NO_3)_2$	2 mmol; 2mmol

3.3.2 Catalyst characterisation

In this chapter, the samples were characterised before and after reactions by a range of physical techniques, encompassing thermogravimetric analysis (TGA, TA Instrument, SDT Q-600), powder X-ray diffraction (XRD, Bruker D8 Advance Eco) and X-ray photoelectron spectroscopy (XPS). The catalysts' surface acidity was tested by NH_3-TPD (Micromeritics 2920 surface characterisation system). The details of these characterisation methods are outlined in Chapter 2.

3.3.3 Catalytic activity tests

3.3.3.1 Thermodynamic study of 2Cr-ZrO_2 for CO_2-PDH

The catalytic activity can be affected by various conditions, such as the reaction temperature and the ratio of feed gases (C_3H_8/CO_2). The 2Cr-ZrO_2 catalyst without any promoter was tested under different conditions to find the suitable conditions for the catalysts and to explore the effects of the conditions on the catalytic results. All the tests were operated in an M-R-10A fixed-bed micro reactor (Kun-Lun Yong-Tai Company, China) for 5 hours.

The following conditions were varied:

a. Temperature. The thermal test conditions were all the same apart from the reaction temperature which ranged from 350-600 °C. Based on the previous research, the temperature range of dehydrogenation of C2–C4 alkanes with CO_2 were calculated in the temperature range of about 300–500 °C.[54] The feedstock gases are the mixture of $C_3H_8/CO_2/N_2$ with mole ratio of C_3H_8: CO_2: N_2 = 10%: 30%: 60%.

b. Ratio between C_3H_8/CO_2. Because of the competitive adsorption on the catalysts surface, the ratio of the feedstock gases could be one of the conditions that could affect the catalytic performance. In this case, the activity tests were carried out with different C_3H_8/CO_2 ratios, from 1:1 to 1:5. For this test the total flow rate wasn't changed and a reaction temperature of 550 °C was used in all cases.

3.3.3.2 Catalytic performance for CO_2-PDH

The catalytic performances of the all the CrO_x-based catalysts as prepared above for CO_2-PDH were operated in an M-R-10A fixed-bed micro reactor (Kun-Lun Yong-Tai Company, China). The catalyst was pre-treated in N_2 from room temperature to 500 °C at 15 °C/min and kept for 10 min to reach a stable state. Then heating was continued up to 550 °C at 5 °C/min and was kept for 10 min to be steady. For PDH reaction, the feedstock gases were a mixture of $C_3H_8/CO_2/N_2$ with mole ratio of C_3H_8: CO_2: N_2 = 10%: 30%: 60%. All tests were carried under atmospheric pressure and at 550 °C for 10 hours. Due to the design of the reactor, the flow rate of the reaction required manual adjustment, which inevitably increases the experimental error for the tests. In addition, N_2 as the balance gas for control of the total flow rate, is used from the in-house gas tank which serves the whole building. The flow rate is difficult to stabilise during the reaction and therefore the minimum stable gas flow rate for the instrument which can be controlled reliably is 25 mL/min after several flow rate tests. The emerging reaction products were analysed through a direct link to an on-line gas chromatograph (GC,

Perkin Elmer, Clarus 580) with a flame ionisation detector (FID) and a thermal conductivity detector (TCD). The propane conversion, propylene selectivity and yields obtained in this work are calculated using equations 3.6 to 3.8 below. The experimental deviations over three separate identical experiments were less than ± 5% showing reasonable reproducibility. The estimation of the error is calculated based on the method shown in the appendix. The n is the number of moles of the chemicals into or out of the reaction flow.

$$\text{Yield of Propylene} = \text{Selectivity} \times \text{Conversion } \% \tag{3.6}$$

$$\text{Conversion of propane} = \frac{n_{C_3H_8\ in} - n_{C_3H_8\ out}}{n_{C_3H_8\ in}} \times 100\ \% \tag{3.7}$$

$$\text{Selectivity of propylene} = \frac{n_{C_3H_6}}{3 \times n_{CH_4} + 2 \times n_{C_2H_4} + n_{C_3H_6}} \times 100\ \% \tag{3.8}$$

3.4 Results and Discussion

3.4.1 Catalytic performance of 2Cr-ZrO_2

Chemical processes aimed at the utilisation and conversion of CO_2 are driven in a thermodynamic sense by the difference in Gibbs Free Energy (ΔG^0) between the resulting final chemical products, and CO_2 and the targeted reactants at the relevant experimental conditions. However, as mentioned before in this chapter, CO_2 being a highly stable molecule will require a substantial amount of energy, effective catalysts and optimised reaction conditions for any chemical conversion process of CO_2 into the target of fuels or high-value chemical products. Hence, the motivation to overcome this thermodynamic boundary is to find out the suitable temperature which allows the 2Cr-ZrO_2-catalysed propane dehydrogenation with CO_2 to be favourable. Enhancing the catalyst performance (i.e. maximising the propylene selectivity and reactants conversion) by changing the reaction conditions is possible in a real-world process, but identifying a relatively robust and effective chemical system to act as the catalyst is a precondition of further improvement by modifying conditions.

3.4.1.1 Characterisations of 2Cr-ZrO_2

Firstly, the general surface structural information was checked by X-ray diffraction for comparison with pure commercial ZrO_2 and Cr-oxide species. The catalyst contains different oxidation states of Cr. The XRD could, in principle, identify the Cr_2O_3 and Cr metal easily (if they are sufficiently abundant and with high enough crystallinity) but not, for example, Cr(VI) compounds present in a non-crystalline form.[40] The diffraction peaks at 2Θ=24.6, 28.3, 31.7, 34.0, 40.9 and 50.4 suggested the presence of the Cr_2O_3 rhombohedral phase (α-Cr_2O_3)[55,56].As expected, no metallic Cr (at 2θ = 24.2, 28.2, 31.4, 34.3, 41.5, 50.0, 53.0, 55.5, and 60.0°; JCPDS 37-1484) was found.[40] In addition, the

diffraction patterns of the commercial ZrO_2 support showed peaks characteristic of the monoclinic form. It is a little bit unfortunate that there are many overlaps between the Cr_2O_3 and ZrO_2 patterns. The XRD pattern is dominated by ZrO_2 which is present in 5-fold excess (Cr : Zr ratio of 1 : 5) compared with Cr compound and Zr is a much stronger scatter of X-rays than Cr, which makes it difficult to quantify the Cr_2O_3 phase. The surface information of catalyst can be confirmed by more characterisation techniques.

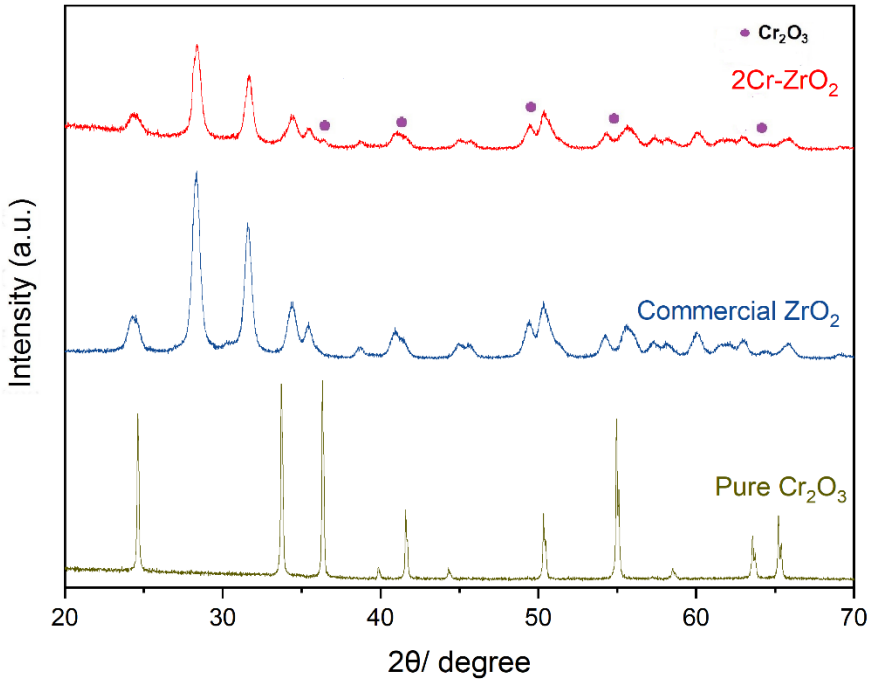


Figure 3.7. XRD pattern of 2Cr-ZrO_2 (red), the pure Cr_2O_3 (green) and ZrO_2 (commercial). The 2Cr-ZrO_2 pattern is dominated by the ZrO_2 support material.

In addition, the diffraction patterns suggest that the Cr species and ZrO_2 have slightly smaller crystallite sizes as compared to the pure materials. The slight broadening of the ZrO_2 peaks and the lack of readily identifiable Cr species identification suggests that they are present in the form of very small crystallites or lack bulk crystallinity.

The TGA data (Figure 3.8) of shows the weight loss of 2Cr-ZrO_2 during heating in air. The initial decrease with weight loss of about 1-2%, completed by around 100-150 °C is due to the moisture evaporation from the catalyst.[57] In general, the catalyst is thermally stable between at 400-800 °C (the range of our catalytic reaction temperatures).

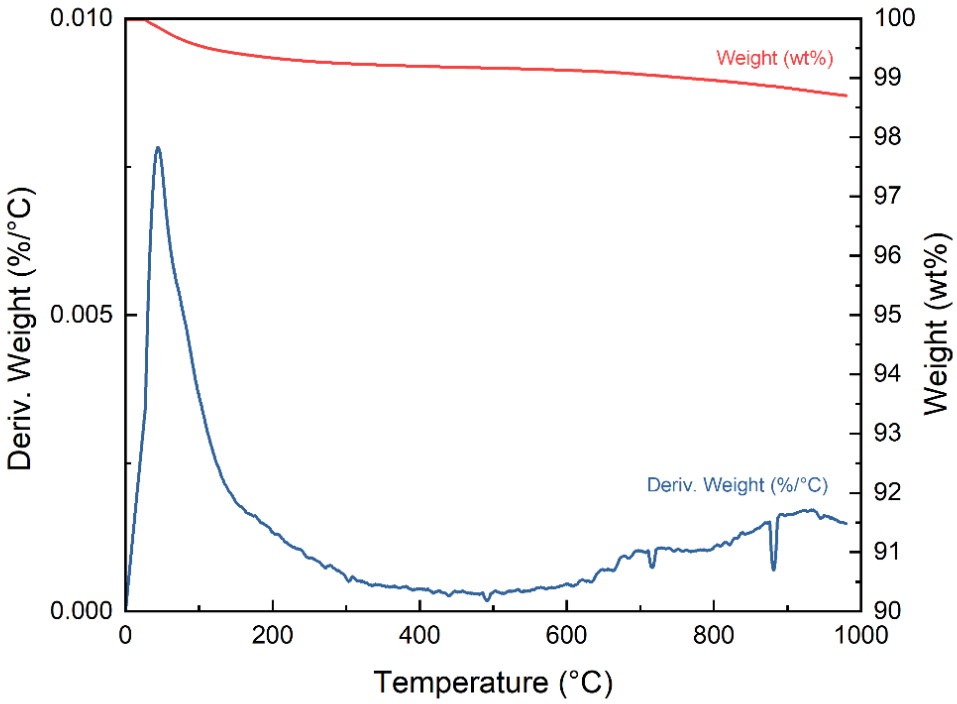
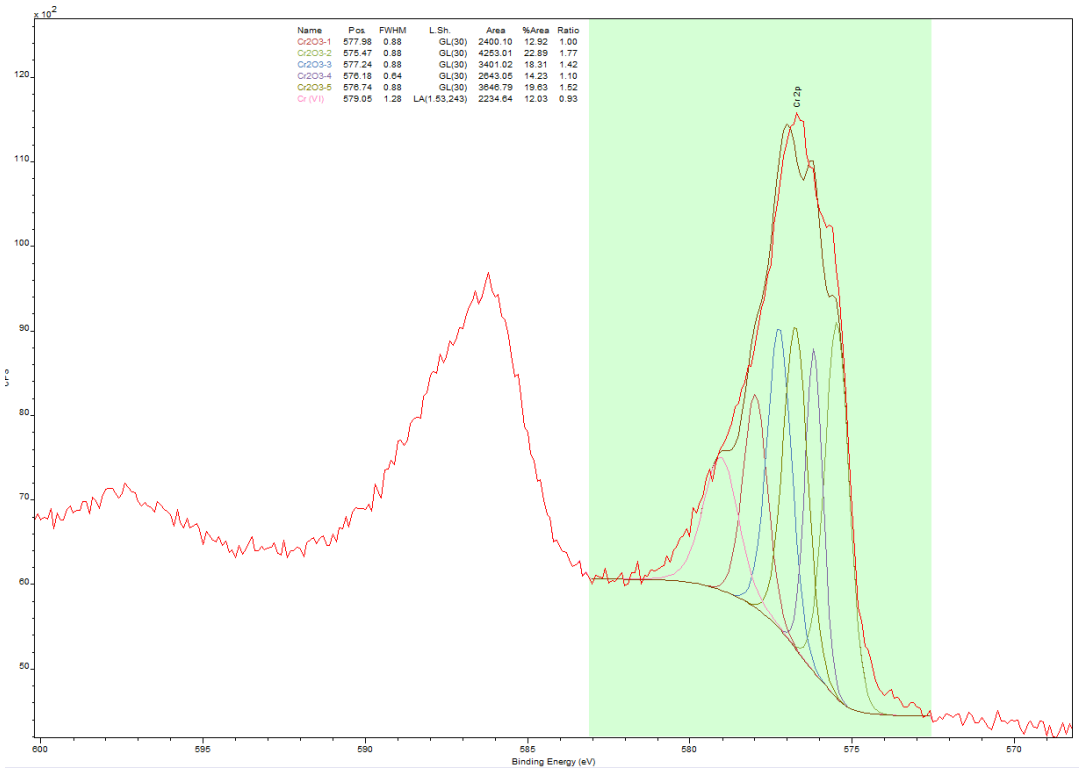


Figure 3.8. TGA data and derivative plots of temperature programmed oxidation (TPO) of the 2Cr-ZrO_2.

The oxidation states of Cr species obviously control the redox reactions taking place throughout the dehydrogenation process as shown in Figure 3.2. The oxidised Cr(VI) and reduced Cr(III) sites are proposed as the major catalytically-active sites responsible for propane dehydrogenation. However, the X-ray diffraction method, relies on the phases being crystalline and the Bragg peaks being non-overlapping for the different phases present and according to Figure 3.7 the Cr^{3+} species cannot be

reliably identified. We therefore employed XPS to probe the actual oxidation state of Cr species on the top surface layers of the catalyst.



Name	Pos.	FWHM	L.Sh.	Area	%Area	Ratio
Cr2O3-1	577.98	0.88	GL(30)	2400.10	12.92	1.00
Cr2O3-2	575.47	0.88	GL(30)	4253.01	22.89	1.77
Cr2O3-3	577.24	0.88	GL(30)	3401.02	18.31	1.42
Cr2O3-4	576.18	0.64	GL(30)	2643.05	14.23	1.10
Cr2O3-5	576.74	0.88	GL(30)	3646.79	19.63	1.52
Cr (VI)	579.05	1.28	LA(1.53,243)	2234.64	12.03	0.93

Figure 3.9. XPS peak fitting of Cr species of 2Cr-ZrO_2.

The fitting parameters for chromium $2p_{3/2}$ spectra are based on spectra taken from a series of well-characterised standard compounds by Biesinger.[58,59] In this thesis, this fitting can determine the presence, and amount, of Cr(III) and Cr(VI) in the various materials. The asymmetry in the metal peak is defined by CasaXPS software and is based on spectra from an argon ion sputter-cleaned pure metal surface.[58] As shown in references 58 and 59, the Cr(III) oxide species will consist of five individual multiplet peaks. This is because on photoionisation from the 2p core level the

angular momenta will couple with the unpaired 3d electrons.[60] This results in a range of transition energies and therefore, in Figure 3.9, the peak for Cr_2O_3 is fitted by five peaks. Cr(VI) species, where there are no 3d electrons, give rise to a single feature in the 2p XPS spectrum. The quantification of the Cr(VI) species (single peak at 579.5 eV from average of literature data)[61] is limited by the overlap with the multiplet splitting of the Cr(III) species. Based on the sample CasaXPS fitting graph of Cr species example in the study by Biesinger in 2004,[58] the Cr(III) species are dominant in the samples with the sharp peaks centred at 576.7 ev about 88%. The Cr(VI) is around 579.64 eV, with a concentration of 12%.

3.4.1.2 Catalyst activity under different conditions

As mentioned previously, the catalytic activity can be affected by various experimental conditions, such as the reaction temperature, the feed gas flow rate and the ratio between C_3H_8 and CO_2. At this stage, 2Cr-ZrO_2 was tested at different temperatures to identify the conditions for the propane dehydrogenation process giving rise to the optimal degree of propane conversion and propylene selectivity. It has been proved that using CO_2 as oxidant can lower the temperature in propane dehydrogenation. The temperature range to be targeted in thermodynamic calculations has been localised in the range 300 - 500 °C which can be easily achieved under experimental conditions.[54] The catalytic dehydrogenation process was attempted below 400 °C, but the results showed that the reaction wasn't successful and occurred only to a small extent (propane conversion less than 5%), so subsequent experiments focused on higher reaction temperatures.

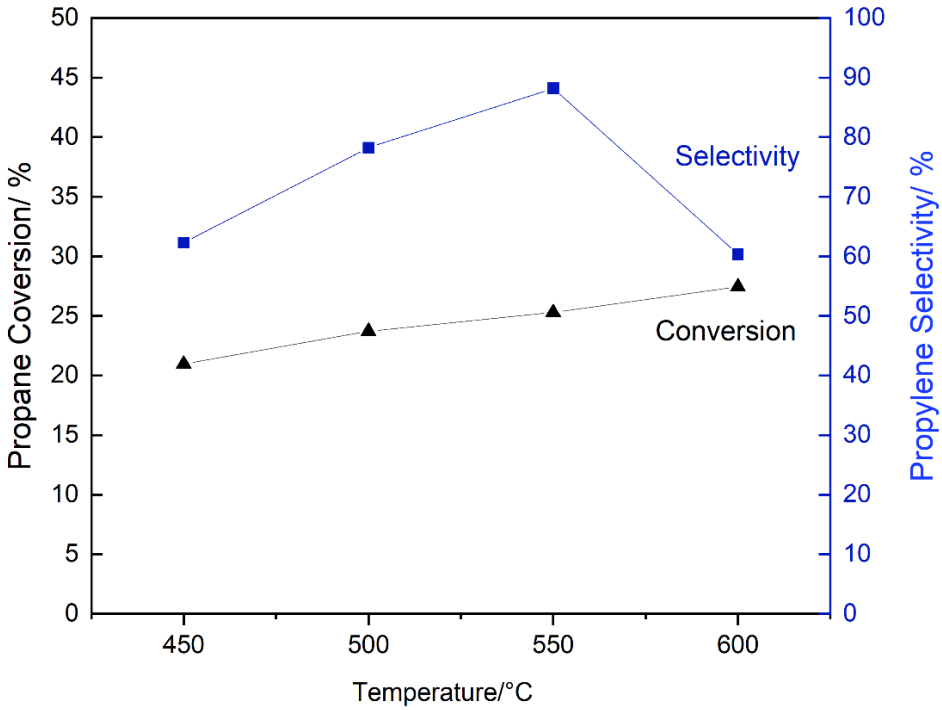


Figure 3.10. Propane conversion and propylene selectivity over 2Cr-ZrO_2 at various temperatures. (% Errors: conversion: ± 0.3-1.2%, selectivity, ± 2.2-3.4%)

The percentage conversion of propane increases slightly as the reaction temperature increases (Figure 3.10). However, in contrast, the propylene selectivity has a maximum of 90% at 550 °C which indicates that this is the optimal temperature for a higher propylene selectivity. The tests were also performed at the higher temperatures of 650 °C and 700 °C. These tests consistently showed a very low selectivity for propylene, below 50%, but an increase in the production of methane. This means that the reaction now involves cracking to form methane (CH_4), hydrogen and carbon, also possible propane dry reforming. The dehydrogenation of C_3H_8 in the presence of CO_2 can be significantly affected by various competing side reactions which are deleterious to the targeted C_3H_6 yield, selectivity and indeed to the stability of the operating catalyst. These also include the cracking (formation of CH_4 and C_2H_4) and coke formation as side reactions which are the main deactivation processes for the catalysts.[20,45,62,63]

When the standard Gibbs free energy of reaction ΔG_r^0 for the dehydrogenation of light alkanes with CO_2 is low, the higher is the possibility of cracking for a family of hydrocarbons and dry reforming.[20,54] C_3H_6 will be further cracked to smaller hydrocarbons and even carbon, so the selectivity will be reduced. Importantly, the ubiquitous deposition of carbon on the catalysts' surface will also reduce their lifetime.[24,54]

From our results outlined above, for this kind of CrO_x-based catalyst, it can be stated that at 550 °C, the balance between the propane conversion and propylene selectivity reached a maximum for these catalysts. At higher temperature, the cracking process and other side reaction overtake the dehydrogenation process. Propylene selectivity is reduced and the catalyst lifetime is decreased. However, a temperature below 400 °C, is not enough to activate the propane dehydrogenation process at all.

One of the roles of CO_2 is to shift the equilibrium of the oxidative propane dehydrogenation reaction to the product side by consuming produced H_2 via the RWGS (3.4), thereby resulting in enhanced C_3H_8 conversion.[15] The CO_2 adsorbed strongly on the chromium oxide sites that were active and selective for the dehydrogenation of propane, enhancing the effects of the support on secondary reactions.[40] The presence of CO_2 in the reactant mixture can cause strong suppression of catalyst activity, selectivity, and yield towards propylene. In relation to the effect of C_3H_8/CO_2 ratios, a high CO_2 partial pressure leads to higher C_3H_8 conversion yet presents a detrimental impact on C_3H_6 production as shown in the diagram in Figure 3.11 and in the commentary below.

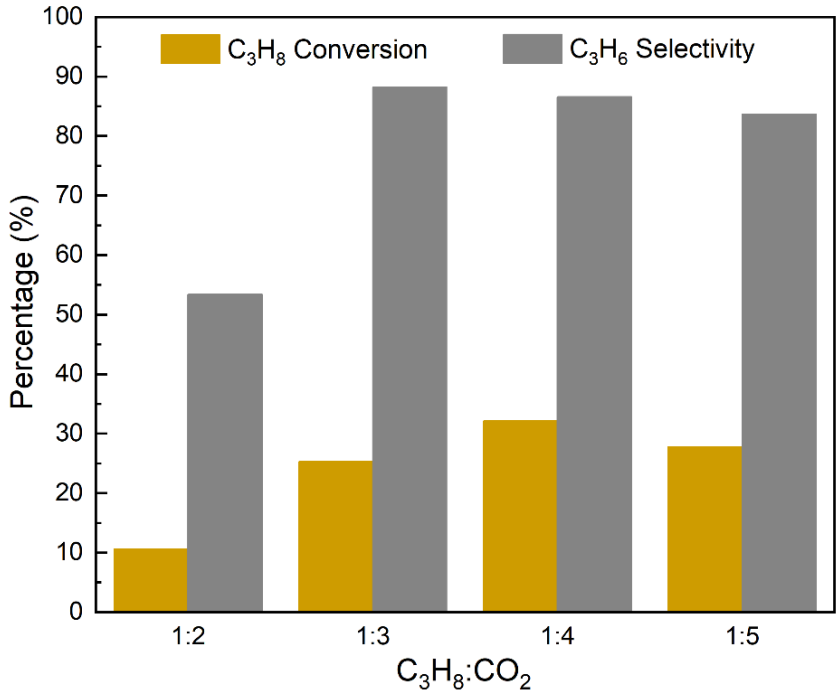


Figure 3.11. Propane conversion and propylene selectivity over 2Cr-ZrO_2 with different ratios of C_3H_8/CO_2. (% Errors: conversion: ± 0.7-3.1%, selectivity: ± 1.8-4.2%)

The propane conversion and propylene selectivity under different reactant stream compositions are shown in Figure 3.11. The comparative analysis revealed that increasing the CO_2:C_3H_8 ratio has a generally positive effect on propylene formation and propane conversion. The result with CO_2:C_3H_8 ratio 1:1 resulted in negligible propane conversion and would have large errors (more than 5%) so it is not included in this case. Furthermore, the test results also showed that the production of H_2 and CO decreased (about 5-10% decrease) with an increase of CO_2 as the molar ratio of C_3H_8:CO_2 was changed from 1:2 to 1:4. This is due to the fact that dry reforming of propane to produce syngas (CO and H_2) competes with the oxidative dehydrogenation of propane to propene using CO_2 at the chosen operating temperature.[63,64] Therefore, it is desirable to kinetically limit the occurrence of dry reforming of propane and promote oxidative dehydrogenation of propane by increasing the CO_2 content of the gas stream. In addition, the gas flow rate could also affect the reaction results. However, due to the

instrument limitations as mentioned before, the experimental error increases when low gas flow rates are used which reduces the reliability of the results. Thus, it was not possible to study the effects on PDH of changing the flow rate. The thermodynamic simulated calculation done by Du showed that an increase in the total flow rate tended to decrease the C_3H_8 conversion as competitive adsorption occurred due to the different side reactions.[45]

It has been reported that with higher temperatures and CO_2/C_3H_8 ratios can reduce coke formation tendency and propylene yield as well, except for catalysts controlling undesired side reactions kinetically.[20] From the results shown above, 2Cr-ZrO_2 has optimal performance at a reaction temperature of 550 °C with the C_3H_8: CO_2 ratio of 1:3. A higher CO_2 concentration can enhance the percentage conversion of C_3H_8 but it reduces the propylene yield. In addition, the rapid coke formation and the competitive dry reforming reaction are the main deactivation routes of the catalysts under higher CO_2 feeding.

3.4.2 Reactions over ZrO_2-supported CrO_x-based catalysts with different metal oxides as promoters

The recent development of catalysts has involved more attention being paid to the use of bimetal oxides or even mixtures of more metals. The reasons are, firstly, to reduce the use of Cr as it is toxic, and obviously harmful to humans and the environment, and hard to dispose of after the catalyst lifetime. In addition, adding other metals can also affect the chemistry of the catalysts' surfaces. As mentioned before, the surface acidity and basicity play a very important role in CO_2-PDH, and these properties may be controlled by substituting Cr by other metals.

In Figure 3.10. (A) and (B) we show the evolved propane conversion and the propylene selectivity with time on stream (min) for the oxidative dehydrogenation of propane with carbon dioxide using ZrO_2 supported CrO_x-based catalysts doped with different promoter metals. All tests were carried out under the same reaction conditions noted in 3.3.3.2. Considering the conversion of propane and selectivity for propylene by using 2Cr-ZrO_2 catalyst, it is apparent that these two aspects respond in various ways to the different metals chosen as promoters.

Samples of 2Cr/Zn-ZrO_2 and 2Cr/Mn-ZrO_2 gave a relatively higher activity for propane conversion at the very beginning of the reaction than the pure 2Cr-ZrO_2 system. The conversions reached over 40% in the first hour of the reaction and the maximum propylene yield reached 30% with 80% selectivity using the Mn-promoted catalyst. However, the fast decrease in propane conversion for 2Cr/Zn-ZrO_2 and 2Cr/Mn-ZrO_2 with increasing reaction time shows the uniqueness and short lifetime of these two catalysts. This is attributed to deleterious carbon deposition on the catalysts' surfaces that block/cover the catalytically active sites and consequently deactivated the catalysts.

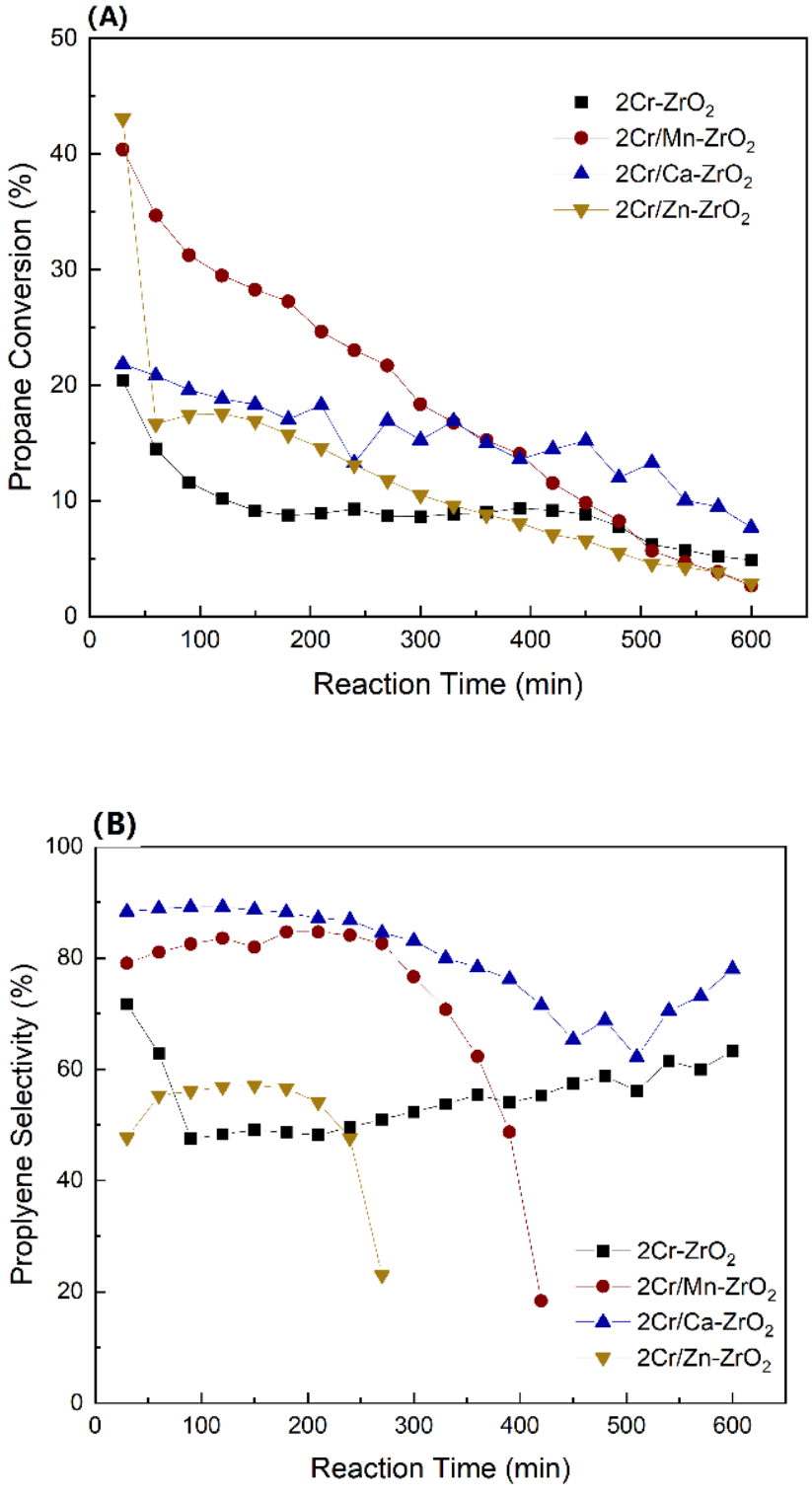


Figure 3.12. (A) The propane conversion (% Errors: pure Cr: ± 0.7-1.3%, Mn: ± 1.5-2.1%, Ca: ± 0.4-1.3%, Zn: ± 1.9-4.3%) and (B) propylene selectivity from the various samples during a 10h reaction. (% Errors: pure Cr: ± 0.7-4.3%, Mn: ± 3.3-4.2%, Ca: ± 1.6-2.8%, Zn: ± 2.5-4.7%)

In addition, both Zn and Mn catalysts also show a quite extraordinary behaviour in propylene selectivity. The Zn catalyst reached about 55% propylene selectivity in a 5-hour-reaction but this suddenly dropped to below 20% in the sixth hour. The decrease of the selectivity can be considered as a consequence of the deactivation of the catalyst. At longer times there was an apparent upturn in the selectivity for propylene, but at these times the yield had dropped to about 5%, so this was not investigated further. The data show the fast deactivation of both catalysts, and the short catalytic lifetime. In this case, these two catalysts, 2Cr/Zn-ZrO_2 and 2Cr/Mn-ZrO_2, are not good enough for CO_2-PDH. However, they did show high initial propane conversion and 2Cr/Mn-ZrO_2 also had over 80% propylene selectivity for a sustained period prior to the sharp drop as the catalyst became deactivated. Further development and alteration could be applied to these catalysts to optimise their advantageous characteristics and potentially increase their catalytic lifetime. Compared with 2Cr/Zn-ZrO_2 and 2Cr/Mn-ZrO_2, the CaO promoted catalysts, 2Cr/Ca-ZrO_2 showed a more stable behaviour. Although the maximum propane conversion was only about 20% and there was a decrease to about 8-9% conversion after 10h reaction, it had the best propylene selectivity of about 90%. As the reaction proceeded, the production of coke on the surface of the catalysts caused the deactivation of the catalysts and while the selectivity for propylene declined with reaction time, it was maintained much better than for 2Cr/Zn-ZrO_2 and 2Cr/Mn-ZrO_2.

The detailed nature of the catalyst active sites obviously plays a significant role in the catalyst performance. For propane dehydrogenation, both acidic and basic sites of a catalyst are critically important to the catalyst performance. In the dehydrogenation of propane over reducible metal oxide catalysts, the metal oxides are electron-deficient, and the more electrophilic the species are, the more reactive and less selective they are likely to be in oxidative reactions with propane.[26] They are the active sites for the C-H cleavage to convert C_3H_8 to C_3H_6; then, CO_2 acts as an oxidising agent which can

re-oxidise the reduced metal oxides as part of the catalytic cycle. These redox mechanisms have been proposed in Figure 3.2.[13]

The balance of the acidity and basicity of the catalysts' surface is very important. Ammonia can be used as a probe molecule to explore the overall acid properties of the catalyst surface using temperature-programmed desorption (TPD). Surface acidity of the catalysts were tested using NH_3-TPD. The catalysts showed strong and weak acid sites with different acid strengths (Figure 3.13). The peak at 150-290 °C could be attributed to the weak physisorption of the NH_3 at a weakly acidic site, whilst the other peak at 300-450 °C could be ascribed to desorption of NH_3 adsorbed at a strongly acidic site.[65,66] Table 3.2 shows the amount of the weak and strong acidic sites. The amounts are calculated by adding the amount of NH_3 adsorbed by the catalysts at different temperature range and divided the amount of catalysts used for NH_3-TPD test.

Table 3.2. Summary of NH_3-TPD data the CrO_x-based catalysts with different promoters.

	Acidic Sites [mmol/g (NH_3)]		
Catalysts	**Weak**	**Strong**	**Total**
2Cr-ZrO_2	0.26	0.15	0.41
2Cr/Mn-ZrO_2	0.82	0.11	0.93
2Cr/Zn-ZrO_2	0.52	0.008	0.528
2Cr/Ca-ZrO_2	0.23	0.008	0.238

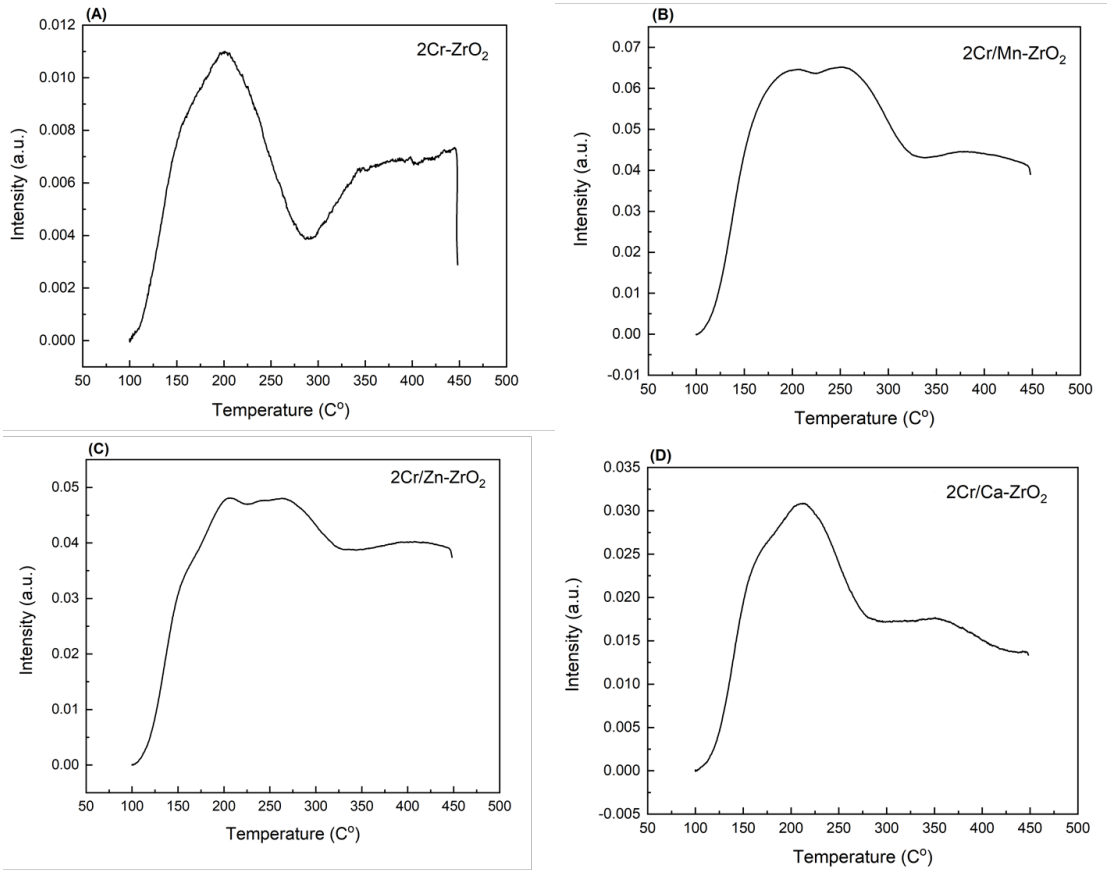


Figure 3.13. NH_3 desorption data vs. temperature by NH_3-TPD of (A) 2Cr-ZrO_2, (B) 2Cr/Mn-ZrO_2, (C) 2Cr/Zn-ZrO_2 and (D) 2Cr/Ca-ZrO_2 prepared by impregnation method.

Ca as a well-known alkaline earth metal with a basic oxide is expected to reduce the surface acidity in this catalytic system. The significant decrease in concentration of acid sites due to addition of a CaO promoter also proves this (Table 3.2). The stronger acidity of Zn(II) and Mn(II) resulted in higher propane conversion and propylene selectivity. But high surface acidity has been found to promote side reactions resulting in carbon formation, which results in the rapid deactivation of the catalysts.[12,25] In this case the CaO promoter played the role of promoting the conversion rate with a more stable catalyst during CO_2-PDH.

CO_2-TPD is a very useful characterisation method for testing the basicity of material surface. Oliveira et al has tested the basicity of Cr-ZrO_2 using CO_2-TPD. It has been

reported that high basicity is not expected in amorphous and tetragonal ZrO_2, the strong basic sites observed could have been formed by the interaction of different species of chromium oxide with ZrO_2.[40]

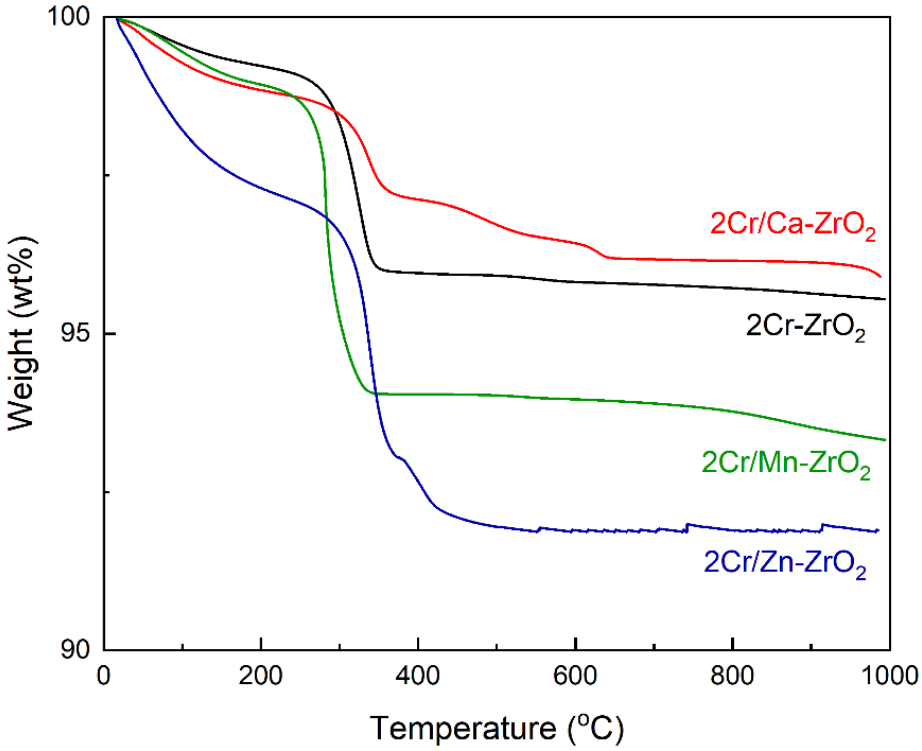


Figure 3.14. TGA diagram of four spent catalysts.

In this case, the “spent” catalysts were characterised further using TGA. It has been observed that the catalyst colour changed from green/yellow to black after the catalytic tests. The TGA of four spent catalysts under air is shown in Figure 3.14. All samples had weight losses at round 350-400 °C, which could indicate the presence of carbon which is burnt-off during the analysis. In fact, the burning temperature of carbon would be affected by its surrounding supporting material and environment. The identification of carbon may need other characterisation method to confirm the carbon contains, such as TGA-MS. Importantly, the catalysts turned back to their original colour from before the PDH process after the TGA runs. Comparing the TGA results (Figure. 3.14)

with the catalytic results (Figure 3.12), it is obvious that the coke formation is the main causes of the deactivation of the catalysts. Both Zn and Mn promoted catalysts showed significant weight loss due to combustion of carbon on the catalyst surface. On the other hand, the use of the alkaline CaO promoter, importantly, reduced the coking effect and showed the least carbon loss in the TGA data. From the TGA data, the amount carbon formed per mmol of ZrO_2 are 0.96 mmol on 2Cr-ZrO_2, 0.57 mmol on 2Cr/Ca-ZrO_2, 1.02 mmol on 2Cr/Mn-ZrO_2 and 1.13 mmol 2Cr/Zn-ZrO_2.

Therefore, basic catalytic sites assist the absorption and consumption of CO_2 whereas acidic sites determine the adsorption and subsequent activation of propane. A strong acidity has been proposed to increase the metal-oxygen bond strength in the redox-active cluster leading to a decrease in the reactivity.[55] The acidity of chromium-based catalytic system serves as one of the crucial factors in determining the catalytic activity in oxidative dehydrogenation reactions. However, a stronger surface acidity also leads to the formation of carbonaceous cracking products, and thus less alkene selectivity is obtained.

The catalytic test was also applied on V-promoted catalysts, but the results showed extremely low conversion of propane, which were hard to quantify. The numbers were smaller than the systematic errors inherent to the reactor used. However, there are many studies of VO_x based catalysts which show their ability in PDH.[12,50,67,68] It might be need further investigation on the reaction conditions, the amount of vanadium oxide and the ratio between two metals.

As a summary of this section, we can see that both acid and base sites determine the adsorption and activation of propane, which an important factor in the catalytic performance. The transition metal oxides as acid sites could improve the cleavage of C–H bond and increase the propane conversion; surface basicity helps to attract and consume CO_2, which not only makes this reaction attractive for possible CCU, but also to diminish the extent of coking to enhance the lifetime of the catalysts. Thus, there is

evidence that both mild acidity and basicity should be controlled and balanced precisely.

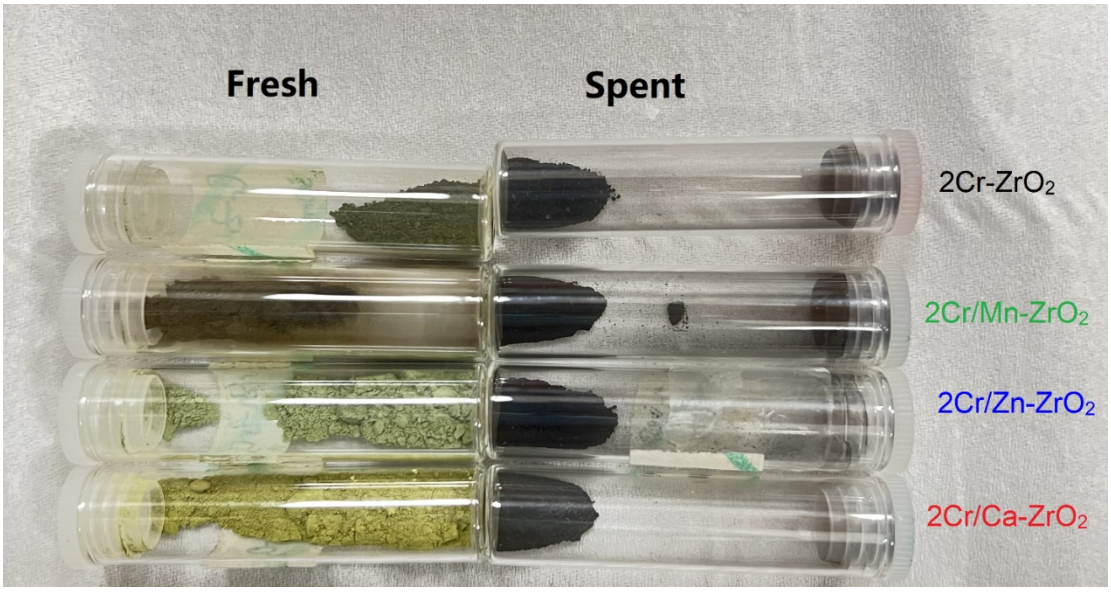


Figure 3.15. Picture of the four catalysts as their fresh and spent forms.

3.5 Conclusion

In this chapter we reported a detailed study of the CrO_x-based catalysts with different promoters prepared by the impregnation method for the dehydrogenation of propane using CO_2. The surface characterisation results provided important surface information of the 2Cr-ZrO_2 system. The XRD analysis revealed that the surface structure of catalyst is dominated by the support, ZrO_2. No crystalline Cr_2O_3 species can be detected unambiguously, perhaps suggesting that it is highly dispersed over the support surface. However, the XPS data proved the presence of both Cr(III) and Cr(VI) species in the catalysts. Kinetic tests were applied to find out the most suitable reaction conditions for the further tests of catalysts with additional metals incorporated. From the results, the Cr-only catalyst has optimum performance at a reaction temperature of 550 °C with the C_3H_8: CO_2 ratio in the incoming gas stream of 1:3 with the minimum usable flow rate of 25 mL/min. It has been reported that raising the proportion of CO_2 was able to increase the C_3H_8 conversion but reduce the propylene yield. It should be noted that the reaction flow rate was kept at 25mL/min for all reactions due to the reactor limitation, so the effect of varying this was not studied in this work.

We have also demonstrated the catalytic properties of four catalysts with different promoters (Ca, Zn, Mn and V) during the propane dehydrogenation process with CO_2 for comparison with the non-promoted catalyst, 2Cr-ZrO_2. Firstly, NH_3-TPD tests on all the catalysts showed the different surface acidity of the catalysts. Ca as an alkaline earth metal, results in the lowest surface acidity. The general activity of catalysts decreases with the time on stream. All catalysts showed the continual decrease in conversion rate, propylene selectivity and yield. The Zn- and Mn-promoted catalysts had the most obvious decrease in propane conversion and propane yield compare with non-promoted Cr catalysts. The deactivation of the catalyst was significant with an extended reaction time, which is due to the carbon coking effect. However, by adding Ca as a promoter, the deactivation effects were significantly reduced. The results from

Figure 3.10 clearly show that both the propane conversion and propylene selectivity are noticeably improved with the addition of the CaO promoter as the Ca-promoted Cr catalysts showed a more stable and gentle decrease. The data also reveal that the Ca promoter has an important role in protecting the catalysts from the time-dependent deactivation through the deposition of carbonaceous material. This was supported by the TGA results of spent catalysts with the CaO promoter which showed a lower carbon content.

The results highlight the effects of the different promoters and the importance of the catalyst's surface environment for CO_2-PDH. The high initial conversion and selectivity of Mn-promoted catalysts showed the potential promise of this kind of catalyst. But due to its a high oxidising ability (very acidic metal species), the deactivation of the catalyst is significant. On the other hand, the inclusion of CaO as a promoter results in a better catalyst selectivity and the propylene yield increases compared with other promoted and non-promoted catalysts. It protects the catalysts against carbon deposition and therefore maintains catalytic activity with a longer lifetime. Thus, the Ca-promoted Cr catalysts would be most suitable for further research and investigation for the dehydrogenation process.

References

1 Z. Y. Wang, Z. H. He, Y. Xia, L. Zhang, K. Wang, W. Wang, Y. Yang, J. G. Chen and Z. T. Liu, *Ind. Eng. Chem. Res.*, 2021, **60**, 2807–2817.

2 E. Nowicka, C. Reece, S. M. Althahban, K. M. H. Mohammed, S. A. Kondrat, D. J. Morgan, Q. He, D. J. Willock, S. Golunski, C. J. Kiely and G. J. Hutchings, *ACS Catal.*, 2018, **8**, 3454–3468.

3 J. M. Venegas, W. P. McDermott and I. Hermans, *Acc. Chem. Res.*, 2018, **51**, 2556–2564.

4 I. Kainthla, G. V. R. Babu, J. T. Bhanushali, K. S. R. Rao and B. M. Nagaraja, *J. CO2 Util.*, 2017, **18**, 309–317.

5 H. A. Maddah, *Am. Sci. Res. J. Eng. Technol. Sci.*, 2018, **45**, 49–63.

6 Q. X. Luo, X. K. Zhang, B. L. Hou, J. G. Chen, C. Zhu, Z. W. Z. T. Liu, Z. W. Z. T. Liu and J. Lu, *Catal. Sci. Technol.*, 2018, **8**, 4864–4876.

7 B. XU, B. ZHENG, W. HUA, Y. YUE and Z. GAO, *J. Catal.*, 2006, **239**, 470–477.

8 B. Frank, J. Zhang, R. Blume, R. Schlögl and D. S. Su, *Angew. Chemie - Int. Ed.*, 2009, **48**, 6913–6917.

9 V. Schwartz, H. Xie, H. M. Meyer, S. H. Overbury and C. Liang, *Carbon*, 2011, **49**, 659–668.

10 C. H. Hendon, A. J. Rieth, M. D. Korzyński and M. Dincă, *ACS Cent. Sci.*, 2017, **3**, 554–563.

11 Z. Li, A. W. Peters, V. Bernales, M. A. Ortuño, N. M. Schweitzer, M. R. Destefano, L. C. Gallington, A. E. Platero-Prats, K. W. Chapman, C. J. Cramer, L. Gagliardi, J. T. Hupp and O. K. Farha, *ACS Cent. Sci.*, 2017, **3**, 31–38.

12 S. Chen, X. Chang, G. Sun, T. Zhang, Y. Xu, Y. Wang, C. Pei and J. Gong, *Chem. Soc. Rev.*, 2021, **50**, 3315–3354.

13 M. A. Atanga, F. Rezaei, A. Jawad, M. Fitch and A. A. Rownaghi, *Appl. Catal. B Environ.*, 2018, **220**, 429–445.

14 Y. Cheng, F. Zhang, Y. Zhang, C. Miao, W. Hua, Y. Yue and Z. Gao, *Cuihua Xuebao/Chinese J. Catal.*, 2015, **36**, 1242–1248.

15 P. Michorczyk, K. Zeńczak-Tomera, B. Michorczyk, A. Węgrzyniak, M. Basta, Y. Millot, L. Valentin and S. Dzwigaj, *J. CO2 Util.*, 2020, **36**, 54–63.

16 Z. H. He, C. S. Jiang, K. Wang, Z. Y. Wang, N. Li, W. T. Wang and Z. T. Liu, *Catal. Today*, 2020, **356**, 579–588.

17 D. B. Fox, E. H. Lee and M. H. Rei, *Ind. Eng. Chem. Prod. Res. Dev.*, 1972, **11**, 444–446.

18 P. Michorczyk, P. Kuśtrowski, A. Kolak and M. Zimowska, *Catal. Commun.*, 2013, **35**, 95–100.

19 T. Shishido, K. Shimamura, K. Teramura and T. Tanaka, *Catal. Today*, 2012, **185**, 151–156.

20 F. T. Zangeneh, A. Taeb, K. Gholivand, and S. Sahebdelfar, *Chem. Eng. Commun.*, 2016, **203**, 557-565.

21 S. Rostom and H. De Lasa, *Ind. Eng. Chem. Res.*, 2018, **57**, 10251–10260.

22 C.-H. Huang and C.-S. Tan, *Aerosol Air Qual. Res.*, 2014, **14**, 480–499.

23 T. Wilberforce, A. Baroutaji, B. Soudan, A. H. Al-Alami and A. G. Olabi, *Sci. Total Environ.*, 2019, **657**, 56–72.

24 Z. Jiang, T. Xiao, V. L. Kuznetsov and P. P. Edwards, *Philos. Trans. R. Soc. A Math. Phys. Eng. Sci.*, 2010, **368**, 3343–3364.

25 A. Abdulrasheed, A. A. Jalil, Y. Gambo, M. Ibrahim, H. U. Hambali and M. Y. Shahul Hamid, *Renew. Sustain. Energy Rev.*, 2019, **108**, 175–193.

26 Y. Gambo, S. Adamu, A. A. Abdulrasheed, R. A. Lucky, M. S. Ba-Shammakh and M. M. Hossain, *Appl. Catal. A Gen.*, 2021, **609**, 117914.

27 J. Zhu, M. L. Yang, Y. Yu, Y. A. Zhu, Z. J. Sui, X. G. Zhou, A. Holmen and D. Chen, *ACS Catal.*, 2015, **5**, 6310–6319.

28 B. Zhu, J. Meng, W. Yuan, X. Zhang, H. Yang, Y. Wang and Y. Gao, *Angew. Chemie - Int. Ed.*, 2020, **59**, 2171–2180.

29 M.-L. Yang, Y.-A. Zhu, X.-G. Zhou, Z.-J. Sui and D. Chen, *ACS Catal.*, 2012, **2**, 1247–1258.

30 J. Zhu, S. Qin, S. Ren, X. Peng, D. Tong and C. Hu, *Catal. Today*, 2009, **148**, 310–315.

31 Y. N. Sun, Y. N. Gao, Y. Wu, H. Shan, G. Wang and C. Li, *Catal. Commun.*, 2015, **60**, 42–45.

32 I. Ascoop, V. V. Galvita, K. Alexopoulos, M. F. Reyniers, P. Van Der Voort, V. Bliznuk and G. B. Marin, *J. Catal.*, 2016, **335**, 1–10.

33 T. Wu, Z.-J. Zhao, G. Sun, L. Zeng, C. Xiong, J. Gong and R. Mu, *Angew. Chemie Int. Ed.*, 2018, **57**, 6791–6795.

34 S. Yusuf, L. Neal, V. Haribal, M. Baldwin, H. H. Lamb and F. Li, *Appl. Catal. B Environ.*, 2018, **232**, 77–85.

35 N. Mimura and M. Saito, *Catal. Today*, 2000, **55**, 173–178.

36 F. Rahmani, M. Haghighi and M. Amini, *J. Ind. Eng. Chem.*, 2015, **31**, 142–155.

37 X. Ge, H. Zou, J. Wang and J. Shen, *React. Kinet. Catal. Lett.*, 2005, **85**, 253–260.

38 I. Takahara, W. C. Chang, N. Mimura and M. Saito, *Catal. Today*, 1998, **45**, 55–59.

39 P. Michorczyk, P. Pietrzyk and J. Ogonowski, *Microporous Mesoporous Mater.*, 2012, **161**, 56–66.

40 J. F. S. de Oliveira, D. P. Volanti, J. M. C. Bueno and A. P. Ferreira, *Appl. Catal. A Gen.*, 2018, **558**, 55–66.

41 M. Kocoń, P. Michorczyk and J. Ogonowski, *Catal. Letters*, 2005, **101**, 53–57.

42 E. Asghari, M. Haghighi and F. Rahmani, *J. Mol. Catal. A Chem.*, 2016, **418**–**419**, 115–124.

43 P. Michorczyk, J. Ogonowski and K. Zeńczak, *J. Mol. Catal. A Chem.*, 2011, **349**, 1–12.

44 K. Nowińska, A. Wącław and A. Izbińska, *Appl. Catal. A Gen.*, 2003, **243**, 225–236.

45 X. Du, D.Phil thesis, University of Oxford, 2016.

46 T. A. Bugrova, V. V. Dutov, V. A. Svetlichnyi, V. Cortés Corberán and G. V. Mamontov, *Catal. Today*, 2019, **333**, 71–80.

47 L. Le, M. Yang, C. Xiao and A. Chen, *Integr. Ferroelectr.*, 2017, **182**, 202–209.

48 R. Zhang, H. Wang, S. Tang, C. Liu, F. Dong, H. Yue and B. Liang, *ACS Catal.*, 2018, **8**, 9280–9286.

49 P. Hu, W. Z. Lang, X. Yan, L. F. Chu and Y. J. Guo, *J. Catal.*, 2018, **358**, 108–117.

50 H. Alasiri, S. Ahmed, F. Rahman, A. Al-Amer and U. B. Majeed, *Can. J. Chem. Eng.*, 2019, **97**, 2340–2346.

51 Y. Zhang, Y. Zhou, L. Huang, S. Zhou, X. Sheng, Q. Wang and C. Zhang, *Chem. Eng. J.*, 2015, **270**, 352–361.

52 C. Yu, Q. Ge, H. Xu and W. Li, *Catal. Letters*, 2006, **112**, 197–201.

53 J. Liu, Z. Zhang, Y. Jiang, X. Jiang, N. He, S. Yan, P. Guo, G. Xiong, J. Su and G. Vilé, *Appl. Catal. B Environ.*, 2022, **304**, 120947.

54 X. Du, B. Yao, S. Gonzalez-Cortes, V. L. Kuznetsov, H. Almegren, T. Xiao and P. P. Edwards, *Faraday Discuss.*, 2015, **183**, 161–176.

55 A. M. El-Toni, A. S. Al-Awadi, A. E. Abasaeed, A. Al-Fatesh, M. Alhoshan, J. P. Labis, A. Khan and S. M. Al-Zahrani, *Ceram. Int.*, 2018, **45**, 1125–1134.

56 F. Rahmani, M. Haghighi and S. Mahboob, *Ultrason. Sonochem.*, 2016, **33**, 150–163.

57 M. Chen, in *Materials Science and Engineering of Carbon*, Tsinghua University Press Limited, 2016, pp. 249–272.

58 M. C. Biesinger, C. Brown, J. R. Mycroft, R. D. Davidson and N. S. McIntyre, *Surf. Interface Anal.*, 2004, **36**, 1550–1563.

59 M. C. Biesinger, B. P. Payne, A. P. Grosvenor, L. W. M. Lau, A. R. Gerson and R. S. C. Smart, *Appl. Surf. Sci.*, 2011, **257**, 2717–2730.

60 R. P. Gupta and S. K. Sen, *Phys. Rev. B*, 1975, **12**, 15–19.

61 M. Biesinger, X-ray Photoelectron Spectroscopy (XPS) Reference Pages, http://www.xpsfitting.com/2008/09/chromium-metal-oxide-and-hydroxide.html, (accessed 20 May 2022).

62 S. Sahebdelfar, M. T. Ravanchi, F. Tahriri Zangeneh, S. Mehrazma and S. Rajabi, *Chem. Eng. Res. Des.*, 2012, **90**, 1090–1097.

63 X. Jiang, L. Sharma, V. Fung, S. J. Park, C. W. Jones, B. G. Sumpter, J.

Baltrusaitis and Z. Wu, *ACS Catal.*, 2021, **11**, 2182–2234.

64 A. S. Sandupatla, K. Ray, P. Thaosen, C. Sivananda and G. Deo, *Catal. Today*, 2020, **354**, 176–182.

65 Y. Weng, S. Qiu, L. Ma, Q. Liu, M. Ding, Q. Zhang, Q. Zhang and T. Wang, *Catalysts*, 2015, **5**, 2147–2160.

66 M. Hamidzadeh, M. Ghassemzadeh, A. Tarlani and S. Far, *Orient. J. Chem.*, 2016, **32**, 481–490.

67 Z. F. Han, X. L. Xue, J. M. Wu, W. Z. Lang and Y. J. Guo, *Cuihua Xuebao/Chinese J. Catal.*, 2018, **39**, 1099–1109.

68 N. Jeon, H. Choe, B. Jeong and Y. Yun, *Catal. Today*, 2020, **352**, 337–344.

Chapter 4

One-Pot Synthesis of CrO_x-based Catalysts for CO_2-PDH

4.1 Introduction

As mentioned in the Chapter 1 and Chapter 3, because of the high ability of CrO_x-based catalyst surfaces to activate C–C and C–H bonds, CrO_x-based catalysts have been a preferred choice in the process of propane dehydrogenation. There has been much reported work and studies (mentioned in Chapter 3) in the literature devoted to the selection of the optimum loading content, promoters, supports and reaction conditions (temperature, flow rate, etc.) of CrO_x-based catalysts for CO_2-PDH. The development of more effective catalytic systems is still the main research and study area for CO_2-PDH.

Apart from the effects of different metal oxides and promoters (see Chapter 3), the structure of the catalyst surface also plays a decisive role in determining the nature of the surface metal oxide catalytic sites. The surface reducibility will be affected by the dispersion of the metal oxide species as the active phase. Irrespective of any metal-support interaction, the surface area of the support material could obviously affect the metal catalyst dispersion. For CO_2-PDH, most catalysts are designed as mesoporous materials due the molecule sizes of CO_2 and propane and the need for them to easily to diffuse onto and adsorb on the solid surface.

In the investigation of different catalytic process, mesoporous inorganic catalysts (e.g. Ni-based catalysts for dry reforming, Fe-based catalysts for recycling of waste plastic) have attracted a lot of scientific interest due to their uniform mesopore sizes, high specific surface areas and ease of surface functionalisation, which are features important in catalytic applications.[1]

There are various synthetic processes or preparation methods for different mesoporous catalysts. Impregnation (or incipient wetness), see Chapter 3, is one the most common and simple methods for catalyst preparation, because it is a simple procedure and has the flexibility to include different catalyst promoters.[1] Usually a certain amount of support is immersed in a precursor solution. The solution will be evaporated first, then the slurry obtained is dried and then calcined at the appropriate temperature. A large number of metal oxide catalysts are prepared by this impregnation method (details in Chapters 2 and 3). The procedure for ion exchange preparation is similar to that of impregnation. The procedure involves the suspension of support powder into a precursor solution and subsequent filtration. (This method is not used in this thesis). In both preparation methods, the procedure consists of the preparation of precursor solutions including a certain amount of solid support material.[2] The sol–gel method is another widely applied approach to mesoporous solid preparation, especially in the case of obtaining various families of siliceous materials such as zeolites (e.g. MCM, SBA). It has been widely used for the synthesis of various zeolites. However, it is generally not suitable for the preparation of non-siliceous materials because the hydrolysis and polymerisation reactions of transition-metal alkoxides are harder to control compared to those of silica alkoxides.[3] The development of the nanocasting technique opened a new way for the synthesis of ordered mesoporous inorganic materials. In this method, a well-ordered mesoporous structure of the matrix, typically siliceous (e.g. SBA-15, KIT-6) or carbonaceous (e.g. CMK-3, OMC) material is filled with a precursor, which is then converted into the

desired inorganic materials by thermal treatment and removal of the hard template. Up to now, many different inorganic materials such as mesoporous boron nitrites, GaN, AlN, and Si_3N_4 have been successfully prepared by nanocasting.[4,5]

In 2013, Wu et al. reported hydrothermal preparation of Cr_2O_3-ZrO_2 for CO_2-PDH and showed higher catalytic activity than the conventional impregnated CrO_x-based catalysts.[6] The key difference in this method is that the support material is not already in the solid phase. They used a mixture of aqueous zirconium oxy-nitrate solution and $Cr(NO_3)_3$ solution as the source of both the supporting zirconia and the catalytically active Cr. Then added ammonia solution to produce a hydroxide suspension. The mixtures were moved to an autoclave and hydrothermally treated under static conditions (i.e. without stirring) for 24 hours at 110, 150 and 180 °C. During Wu *et al.*'s preparation of the material, the co-precipitation method was also applied for producing the hydroxide suspension. The co-precipitation method is another commonly used method to prepare heterogeneous solid materials, especially in the preparation of nanoparticles.[7] This method, also starting from solution, involves dissolving the starting materials in a common solvent and then adding a precipitating agent so as to form a homogeneous inorganic solid. The precipitate can then be decomposed at a high temperature to produce the target mixed-metal oxide material. The starting materials can be simple metal salts that can easily be dissolved in water or other appropriate solvents. It has been noted that co-precipitation helps to get more uniformly mixed material, and it has the advantages of being a simple process, requiring a low calcination temperature for a short time, and with good product performance shown in many catalytic applications.[8]

There is a literature report which described that a Ni-based catalyst for reforming plastic waste prepared by the co-precipitation method[1] achieved higher activity and stability compared with the impregnated catalyst with the same composition owing to the high Ni dispersion, high surface area, and small Ni metal crystallite size.[2] Yao et al.

reported Ni catalysts for steam reforming prepared by different methods and showed that different synthetic methods can enable tuning of the surface acid−base properties, crystalline structure, and textural properties.[1,9] Therefore, catalyst synthesis methods, in particular the method in which the metal is loaded, is a crucial factor to be considered for catalyst activity. The physical and chemical structure of the catalyst, including the porosity, reducibility and stability would be strongly influenced by the preparation process.[1]

By taking inspiration from the co-precipitation, hydrothermal and sol-gel processes, we have developed a new preparation route for CrO_x-based catalysts, named 'One-pot Synthesis'. It can be expected that the different synthetic methods would result in different chromium species on the catalyst surface and the different chromium species may behave differently in CO_2-PDH. This is the subject of this chapter.

4.2 Chapter Overview

So far, the supported CrO_x-based catalysts have been documented as some of the most promising catalysts for CO_2-PDH.[6] And a CaO promoter is able to affect the balance of acidity and basicity on surface, which are important properties for CO_2-PDH. In addition, different preparation methods enable control of the nature of the active sites and their availability, potentially tuning the chemical properties.

Therefore, in this chapter, we report studies of CrO_x-based dehydrogenation catalysts supported on ZrO_2 which have been prepared by a new process which we term a "one-pot synthesis". In this synthetic protocol, all precursors (the catalyst, the support and the promoters) are initially dissolved into a solution mixture, NaOH is then added to increase the pH level of the solution and co-precipitate out the solids as an intimately mixed solid mixture. The precipitate suspension is then heated under reflux conditions for 48 hours to ensure further mixing of all constituents. The preparation steps are shown in Figure 4.1.

Different Cr contents with CaO promoter are studied here in catalytic activity tests together with subsequent catalyst characterisation. The support/promoter effects on the catalyst performance both with and without CaO as promoter were also investigated. This work has been published in the journal, Industrial & Engineering Chemistry Research (I&ECR) in June 2020.[10]

4.3 Experimental Methods

4.3.1 Catalyst preparation

The preparation of the one-pot catalysts has been introduced in Chapter 2. The aqueous solution was prepared by mixing chromium (III) nitrate nonahydrate (Sigma-Aldrich, ≥ 99%) and 10 mmol zirconium (IV) oxynitrate hydrate (Aldrich, ≥ 99%). 1-4 mmol of Cr were used in these reactions. For the catalyst with Ca-oxide promoter, 2 mmol of calcium nitrate tetrahydrate (Sigma-Aldrich, ≥ 99%) was also dissolved in the solution. The solution was stirred vigorously at room temperature and NaOH solution (2 M) was added dropwise at 60 °C until the pH reached 11.0. The mixture was then aged in a water bath for 2 hours at 60 °C. The precipitate was filtered off and washed three times with deionised water. Then 300 ml of deionised water was added to the solid in a 500 ml round-bottom flask and the mixture refluxed for 48 hours. The remaining solids were filtered off and dried in the oven at 80 °C for more than 12 hours and then calcined at 600 °C in air for 5 hours with the temperature reached at a heating rate of 2 °C/min (Figure 4.1). For comparison purposes, the catalysts were prepared with variable contents, xCr/Ca-ZrO_2 and xCr-ZrO_2 (x=1-4, mmol of Cr, Ca= 2 mmol, with 10 mmol ZrO_2) all being made by the one-pot synthesis. All fresh catalysts were ground thoroughly and passed through a 125 μm mesh sieve. In addition, the CrO_x-based catalysts prepared by impregnation method (as described in Chapter 3) were chosen as a reference for comparing structural differences of the catalysts prepared by different methods.

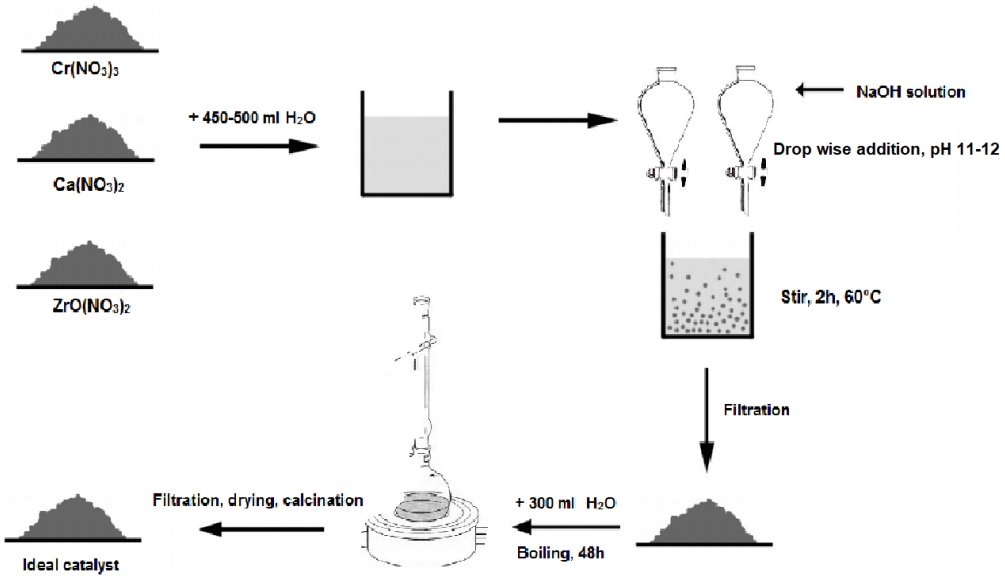


Figure. 4.1. Catalyst preparation procedure using the one-pot synthesis protocol.

Table 4.1. Summarisation of the catalysts used in this chapter.

Catalysts	Precursors	Preparation Method	Molar ratio of metals (Cr:Ca:Zr)
2Cr-ZrO_2 (imp)	$Cr(NO_3)_3$, ZrO_2	Impregnation	2:10 (no Ca)
2Cr-ZrO_2	$Cr(NO_3)_3$, $ZrO(NO_3)_2$	One-pot	2:10 (no Ca)
1Cr/Ca-ZrO_2	$Cr(NO_3)_3$, $ZrO(NO_3)_2$ $Ca(NO_3)_2$		1:2:10
2Cr/Ca-ZrO_2			2:2:10
3Cr/Ca-ZrO_2			3:2:10
4Cr/Ca-ZrO_2			4:2:10

4.3.2 Catalyst characterisation

In this chapter, the samples were characterised before and after reactions by a range of physical techniques and the detailed characterisation methods are outlined in Chapter 2.

The powder X-ray diffraction (XRD) used a Cu Kα X-ray source (45 kV, 40 mA) on a BRUKER D8 ADVANCE Eco diffractometer to check the crystallinity and structural differences between one-pot catalysts and impregnated catalysts. The scanning range (in 2θ) in this study was 20° to 70°. Thermogravimetric analysis (TGA) in air was used to characterise the stability of the catalysts before the reaction and to determine the amount of carbon deposited on the spent samples. The sample was heated from room temperature to 1000 °C at a heating rate of 10 °C/min under air with a flow rate of 10 ml/min. A scanning electron microscope (SEM, ZEISS EVO) was used to characterise the surface morphology of the samples before and after the dehydrogenation process. The surface element concentrations were analysed by Energy-dispersive X-ray spectroscopy (EDS, ZEISS EVO). The catalysts' surface acidity was tested by ammonia-TPD (Micrometrics 2920 surface characterisation system). The catalysts were pre-heated in flowing helium gas for 1h at 450 °C and cooled down to room temperature, they were then then exposed to ammonia for 1 hour, and then purged with helium and heated linearly at 10 °C/min to 450 °C in 50 ml/min argon. The amount of ammonia in the effluent was recorded continuously as a function of temperature. Brunauer, Emmett and Teller (BET) surface analysis was used to measure the materials surface area using the micromeritics 3flex surface characterisation system.

4.3.3 Catalyst activity test

The performances of catalysts for propane dehydrogenation with CO_2 were examined using the same instrument and conditions as described in Chapter 2 and Chapter 3. The results of catalytic performance including the propylene yield and selectivity, propane conversion, CO_2 conversion, CO yield and carbon balance data were calculated using the equations below. The catalytic activity tests are done over three

separate identical experiments with errors less than ± 5% to show the reasonable reproducibility. Errors are calculated by the method shown in Appendix.

$$\text{Yield of Propylene} = \text{Selectivity} \times \text{Conversion} \quad \% \tag{4.1}$$

$$\text{Conversion of propane} = \frac{n_{C_3H_8\ in} - n_{C_3H_8\ out}}{n_{C_3H_8\ in}} \times 100\ \% \tag{4.2}$$

$$\text{Selectivity of propylene} = \frac{3 \times n_{C_3H_6}}{n_{CH_4} + 2 \times n_{C_2H_4} + 3 \times n_{C_3H_6}} \times 100\ \% \tag{4.3}$$

$$\text{Conversion of } CO_2 = \frac{n_{CO_2\ in} - n_{CO_2\ out}}{n_{CO_2\ in}} \times 100\ \% \tag{4.4}$$

$$\text{Yield of CO} = \frac{n_{co}^{out}}{3 \times n_{co_2}^{in}} \times 100\ \% \tag{4.5}$$

$$\text{Carbon Balance} = \frac{3 \times n_{C_3H_6} + 2 \times n_{C_2H_4} + n_{CH_4} + n_{CO}}{3 \times n_{C_3H_8} + n_{CO_2}} \times 100\ \% \tag{4.6}$$

$$\text{Selectivity of ethene} = \frac{2 \times n_{C_2H_4}}{n_{CH_4} + 2 \times n_{C_2H_4} + 3 \times n_{C_3H_6}} \times 100\ \% \tag{4.7}$$

$$\text{Selectivity of methane} = \frac{n_{CH_4}}{n_{CH_4} + 2 \times n_{C_2H_4} + 3 \times n_{C_3H_6}} \times 100\ \% \tag{4.8}$$

4.4 Results and Discussion

4.4.1 Catalyst characterisations of impregnated catalyst and one-pot catalyst

Figure 4.2 shows the XRD patterns of CrO_x-based with ZrO_2 supported catalysts prepared by two different methods; namely our one-pot synthesis (shown as red, 2Cr-ZrO_2 and blue, 2Cr/Ca-ZrO_2) and the conventional impregnation method (green, 2Cr-ZrO_2). As mentioned in Chapter 3, some of the Cr species in catalysts appear as chromia. The same as in Chapter 3, these chromia are hardly to be detected and largely obscured by the stronger peaks from the zirconia phase and the background. The XRD suggested there may be some crystalline Cr_2O_3 (rhombohedral phase (α-Cr_2O_3)[11,12]), but this is not clearly confirmed in the XRD patterns.

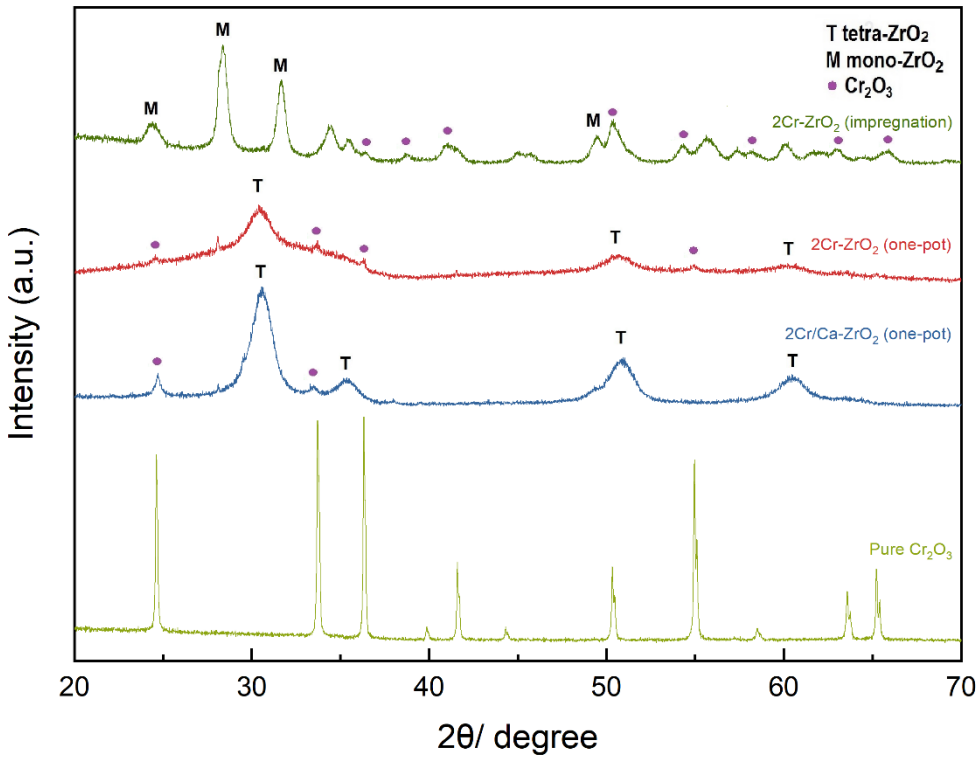


Figure 4.2. XRD pattern of both the impregnation method 2Cr-ZrO_2 (dark green), and the one-pot synthesis 2Cr-ZrO_2 (red) and that with the Ca-oxide promoter, 2Cr/Ca-ZrO_2 (blue). The XRD pattern of pure Cr_2O_3 is shown in light green for reference.

In addition, the diffraction patterns of the commercial ZrO_2 support (used as support for impregnation catalysts) showed peaks characteristic of the monoclinic form, the standard baddeleyite structure, whereas for the samples synthesised via the one-pot reaction method, the tetragonal phase of ZrO_2 was detected. In addition, these data suggest that our one-pot reaction gives a much smaller particle size for the ZrO_2, as evidenced by the larger diffraction peak widths (see below). Figure 4.3 shows the ZrO_2 structure from commercial material, used as a support during the impregnation method and for comparison, ZrO_2 prepared by the one-pot reaction (without addition of other metals). The diffraction peaks at 2θ of 30.3, 35.4, 50.0, and 60.0° were characteristic of the tetragonal fluorite-like ZrO_2 phase (JCPDS 50-1089), while peaks at 2θ of 24.2, 28.2, 31.4, 34.3, 41.5, 50.0, 53.0, 55.5, and 60.0° were characteristic of the monoclinic ZrO_2 phase (JCPDS 37-1484).[13]

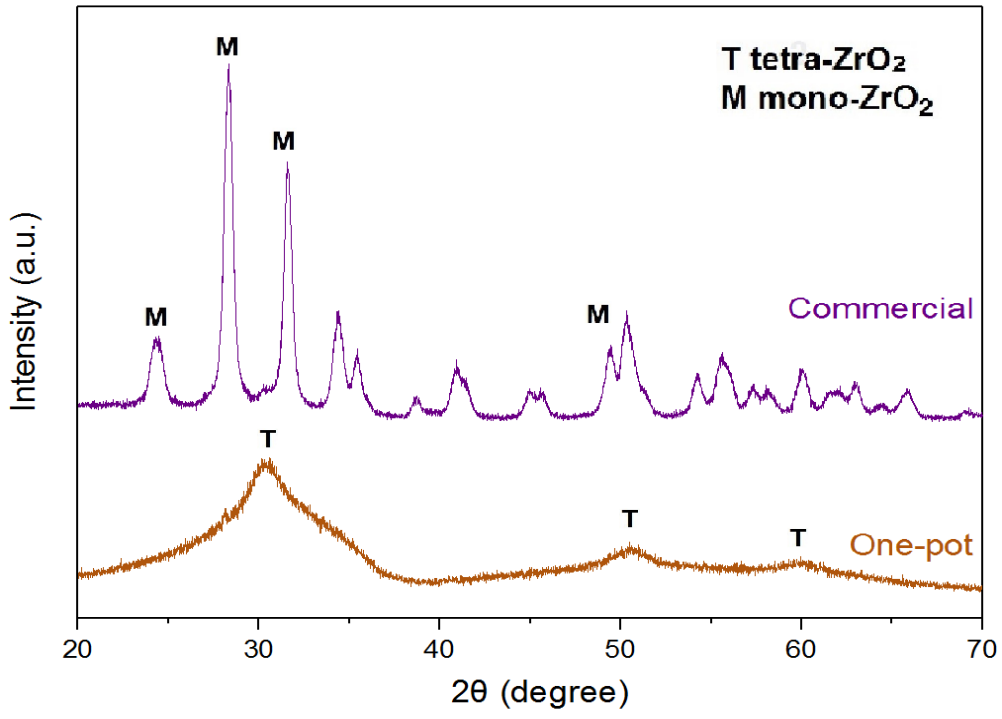


Figure 4.3. XRD pattern of commercial (purple) and one-pot synthesis ZrO_2.

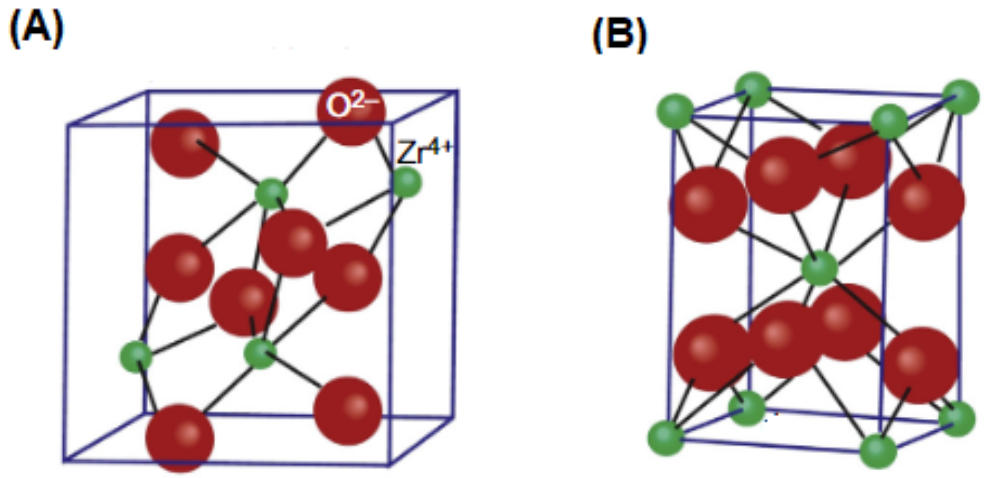


Figure 4.4. The crystal structure of ZrO_2 (A) monoclinic phase and (B) tetragonal phase.[14]

In comparison, the 'one-pot' synthesised Cr catalysts (2Cr-ZrO_2, Figure 4.2. red) showed a totally different XRD diffraction pattern where the Cr_2O_3 was either in the form of very small crystallites or had lost its bulk crystallinity. In these materials there is much more ZrO_2 than Cr species, and Zr is also a much stronger scattered and will always dominate the patterns. The XRD pattern of the Ca-oxide promoted catalyst 2Cr/Ca-ZrO_2 is broadly similar to that from 2Cr-ZrO_2. The only defined ZrO_2 peaks correspond to its the tetragonal phase. That no obvious crystalline peaks of chromia were observed, could suggest that chromia is homogeneously mixed with zirconia.[6] Alternatively the peaks from chromia could be hidden under the background.

Arising from the intimate mixing of all reactants, another possibility is that the one-pot synthesis method produces a solid solution structure where the Cr and Zr are chemically linked by O-bridges in small polymeric surface cluster structures, or indeed incorporated into the host support structure itself. These possibilities appear, therefore, fundamentally different from the conventional metal oxide/support mixtures (Cr/ZrO_2) synthesis routes.[15] The general definition of a solid solution is that of a solid in which a second component is substitutional incorporated into the lattice of another, 'host' solid with or without a significant change of the overall crystal structure of the parent

structure. For the one-pot synthesised catalysts, such a solid solution would involve Cr oxides (and potentially Ca oxide also) substituted into the (host) ZrO_2 support itself. Our proposal is that such substituted species will be located in the top few surface layers with large surface area or porosity (as they are detected in XPS, an acknowledged surface-sensitive technique). This contrasts with the situation where Cr and Ca species are deposited as particle of the oxides on the exterior surface of the support. In addition, the observation that the structure of the ZrO_2 phase is changed may also support the solid solution concept.

The surface of the ZrO_2 catalyst appears far smoother for the one pot reaction (Figure 4.5) possibly arising from the oxides being substituted within the ZrO_2 rather than deposited on the surface. The one-pot synthesis has been used in other areas for preparing nanoparticles where solid solution formation has been invoked.[16,17] For example, Nomura *et al.* showed the presence of a Li-based solid solution in a Li-metal-oxide system ($Li[Ni0.18Li0.20Co0.03Mn0.58]O_2$) using the same synthetic approach.[18]

Further investigation using local structural probes such as X-ray Absorption Spectroscopy such as EXAFS and XANES, would be required to completely identify the possible formation of such cluster species and/or the formation of a solid solution.

To investigate the material distribution, nature and status of the Cr species on the catalyst, SEM-EDS were conducted on the samples prepared by both the one-pot synthesis and impregnation methods. The EDS results identify the elements contained in the catalyst by wt% and how they are distributed on the catalysts. The EDS mapping (Figure 4.6) reveals that the sample prepared by the impregnation method of Chapter 3 has Cr species that are not dispersed uniformly showing the formation of large CrO_x particles compare with catalyst from one-pot synthesis. However, SEM only shows the material surface information, the detailed structure requires TEM. Awadi *et al.* showed low-magnification TEM images of Cr-MCM-41 prepared by the impregnation method.[11]

The image shows that the metal oxides are on the surface of the support. As MCM-41 is a mesoporous material, the CrO_x species are also found on the surface of pores.[19]

The surface morphologies of Cr-ZrO_2 catalysts prepared by the two different methods were also studied by SEM-EDS analysis. As a general observation, catalysts prepared by the one-pot synthesis method have noticeably widely dispersed Cr species (Figure 4.7), which is indeed consistent with our XRD studies. Moreover, the SEM images show that 2Cr-ZrO_2 prepared by this method is more compact with a smoother surface (Figure 4.5(B)).

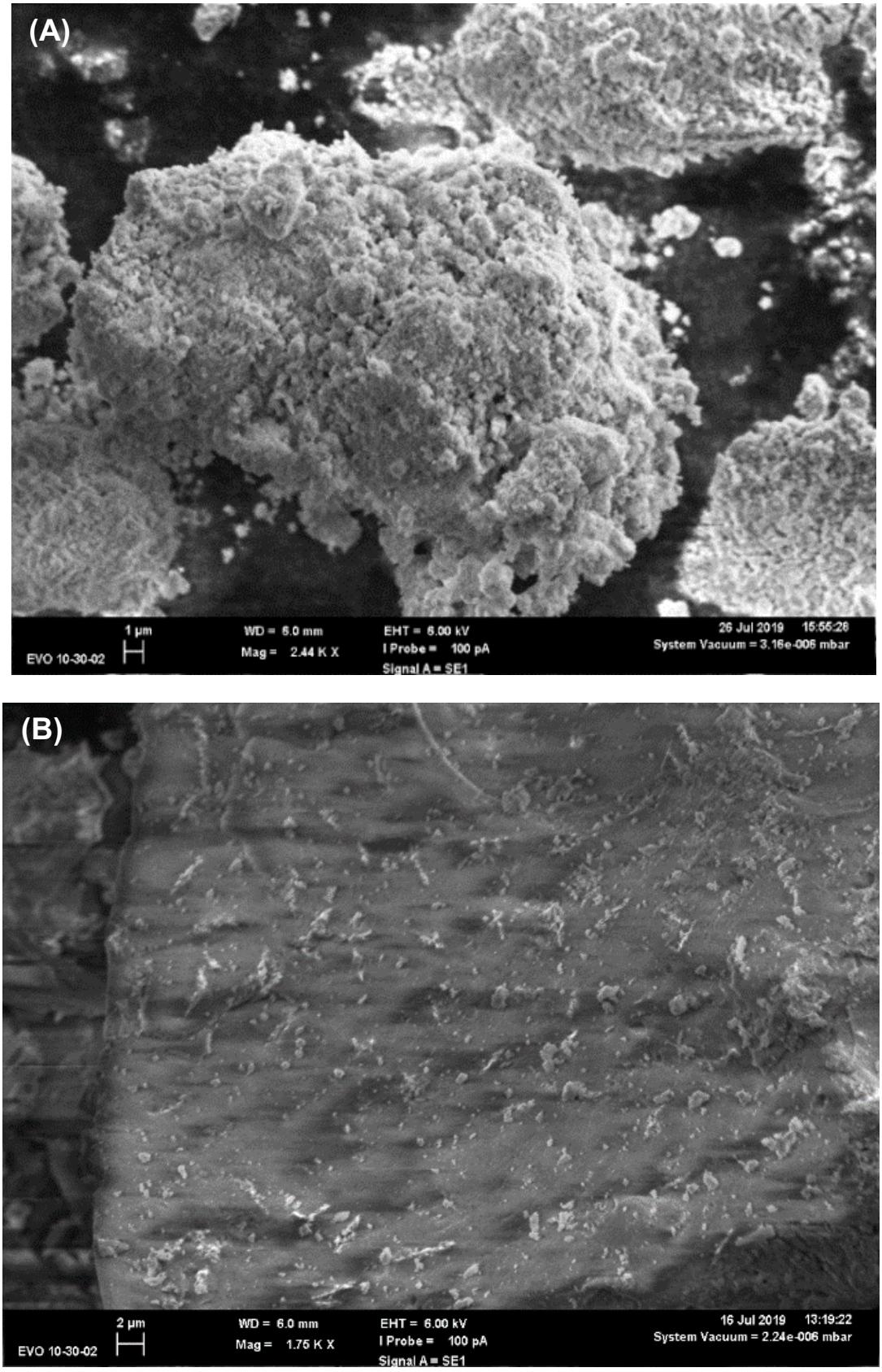


Figure. 4.5. SEM images of (A) 2Cr-ZrO_2 (imp) catalysts prepared using the impregnation method and (B) 2Cr-ZrO_2. catalysts prepared using the one-pot synthesis method.

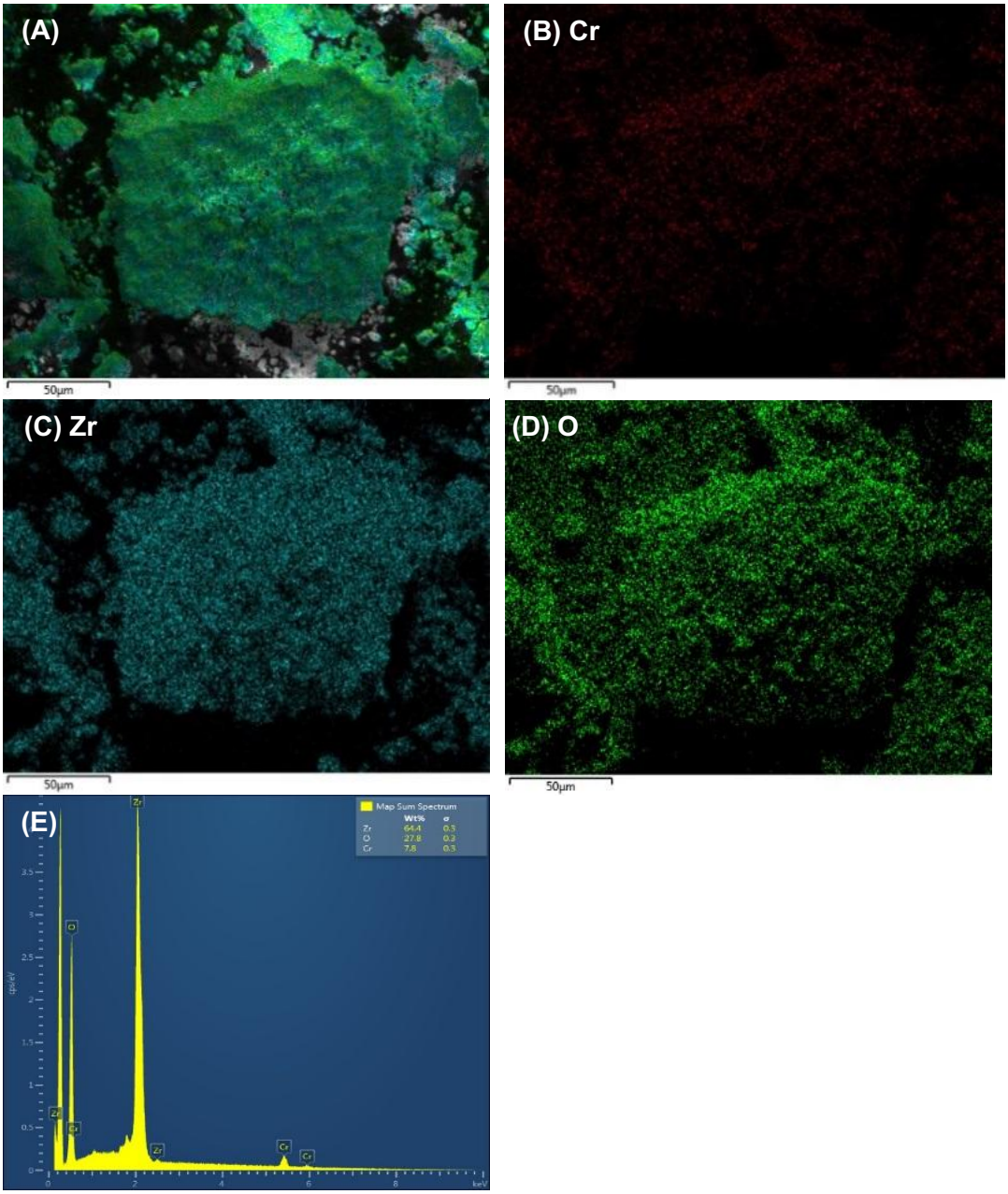


Figure 4.6. SEM images and EDS mapping of the elemental species on the surface of 2Cr-ZrO_2 (imp) samples prepared using impregnation method. (A) SEM (backscattered electron), (B) Cr map, (C) Zr map, (D) O map, and (E) EDS spectrum.

Table 4.2 shows the EDS elemental analysis of the impregnation catalyst sample and the two one-pot synthesised catalysts.

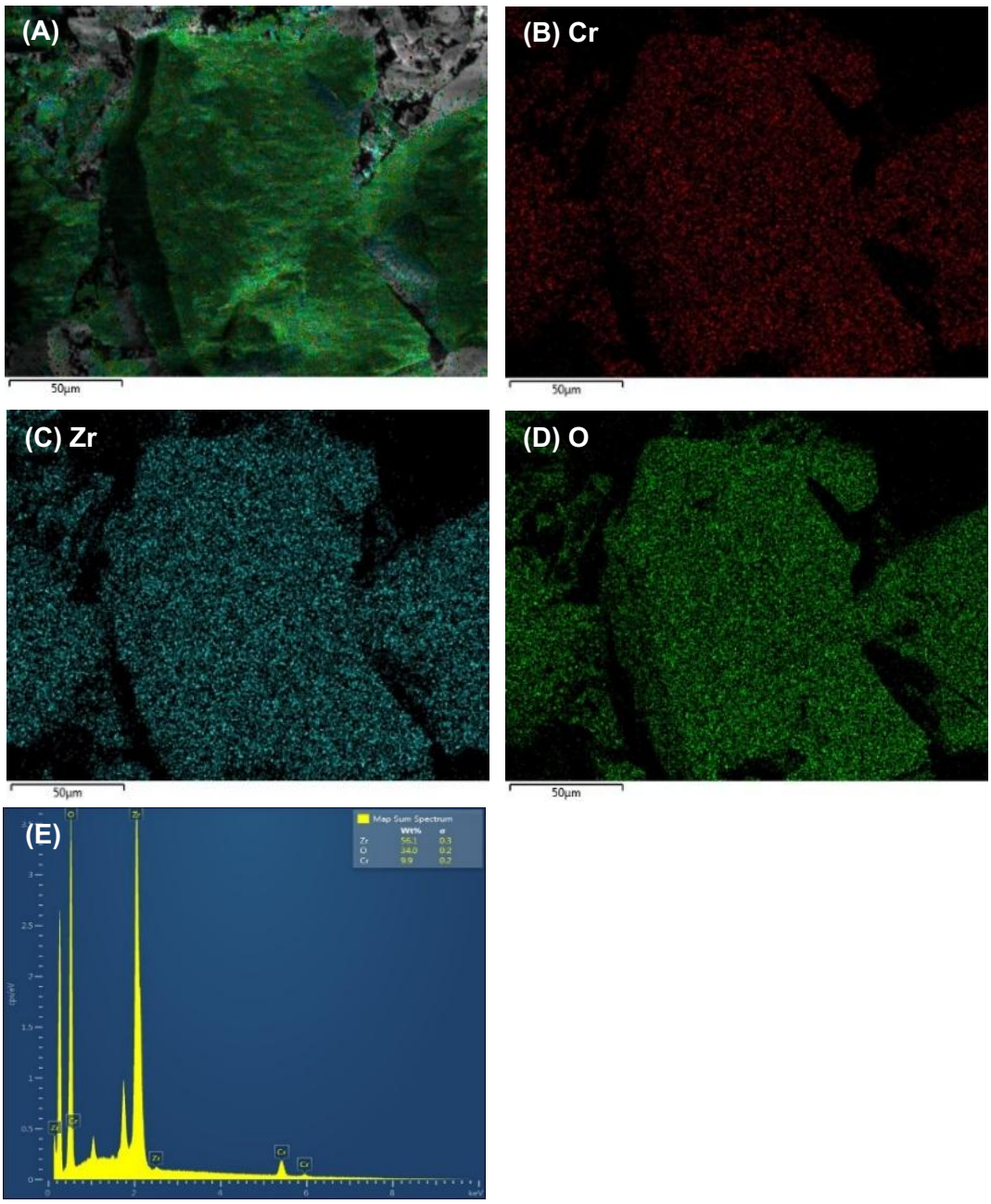


Figure 4.7. SEM images and EDS mapping of the elemental species on the surface of 2Cr-ZrO_2 samples prepared using one-pot synthesis. (A) SEM (backscattered electron), (B) Cr map, (C) Zr map, (D) O map, and (E) EDS spectrum.

Table 4.2. Elemental analysis data of Cr, Zr, Ca and O in catalysts in wt%.

Catalysts	EDS elemental analysis/ wt%			
	Cr	Zr	Ca	O
2Cr-ZrO_2 (imp)	7.8	64.4	/	27.8
2Cr-ZrO_2	9.9	56.1	/	34.0
2Cr/Ca-ZrO_2	8.9	49.3	5.8	36.0

The EDS elemental mapping of both catalysts revealed that for samples prepared by the impregnation method (Figure 4.6), 2Cr-ZrO_2 (imp) catalyst has a Cr content of 7.8 wt%, whereas for the one-pot synthesised 2Cr-ZrO_2 catalyst the Cr content is 9.9 wt%, similar to the stoichiometric value (about 8-10 wt%) used in preparation (Figure 4.7). Because EDS mapping analysis only shows the elemental composition on the surface of the particles and the elements in the bulk are not readily detected by EDS, this suggests that the distribution of Cr is considered as homogeneous. Furthermore, the degree of dispersion on the surface will also affect the data. If the distribution is inhomogeneous there will be Cr-rich and Cr-poor regions on the surface. The one-pot catalysts showed a uniform and better distribution of Cr and in an amount, which corresponded to the stoichiometry of the synthesis. This again points to the solid solution structure as providing a more uniform distribution of Cr species in the catalyst when using one-pot preparation method. Comparing the two different preparation methods, the one-pot synthesis has all precursors in one solution for co-precipitation which one might expect would lead to a better Cr loading than the impregnation method.

Comparing the two preparation methods, the SEM observations shown in Figure 4.6 and 4.7 were helpful in gaining insights into the morphologies of both CrO_x species and the ZrO_2. A good dispersion or distribution of the catalytically active Cr species in the catalysts suggests that there are a large number of well-dispersed active sites. Thus, both the incoming reactants (propane and CO_2 gases) can diffuse more readily to

active sites during CO_2-PDH process and this would result in a good catalytic performance for the PDH.

Furthermore, the surface area measurements of these catalysts showed very different values. Based on BET tests, 2Cr-ZrO_2 (imp) has surface area only about 31.91 m^2/g, whereas, the one-pot catalyst, 2Cr-ZrO_2 has a much larger surface area of 154.53 m^2/g.

The TGA data (Figure 4.8) shows that all samples are thermally stable between at 400-600 °C (the range of our catalytic reaction temperatures). Interestingly, there was weight loss of about 1-2% observed at around 650 °C and 850 °C respectively for the 2Cr-ZrO_2 and 2Cr/Ca-ZrO_2 catalysts prepared by the one-pot method, whereas the 2Cr-ZrO_2 (imp), prepared by the impregnation methods remained approximately the same mass through this temperature range (Figure 4.8 (B)). In this project, we didn't investigate further as the reaction temperatures used is only 550 °C because at higher temperatures a dry reforming process would likely take over. It would be useful to further study the change at higher temperature, including the loss of additional mass (which perhaps is a consequence of reduction of Cr(VI) and O_2 loss), but this is outside the scope of this project.

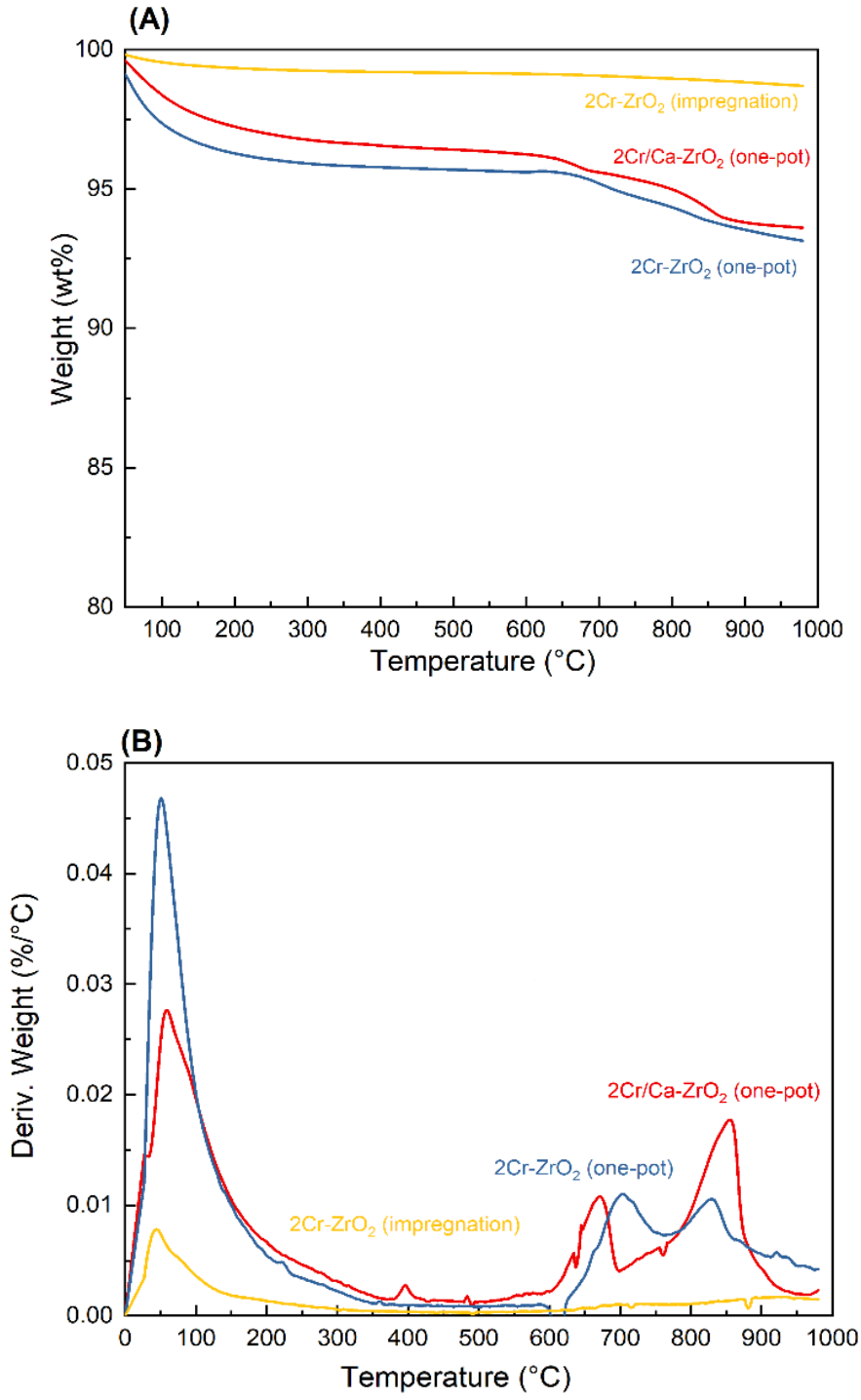
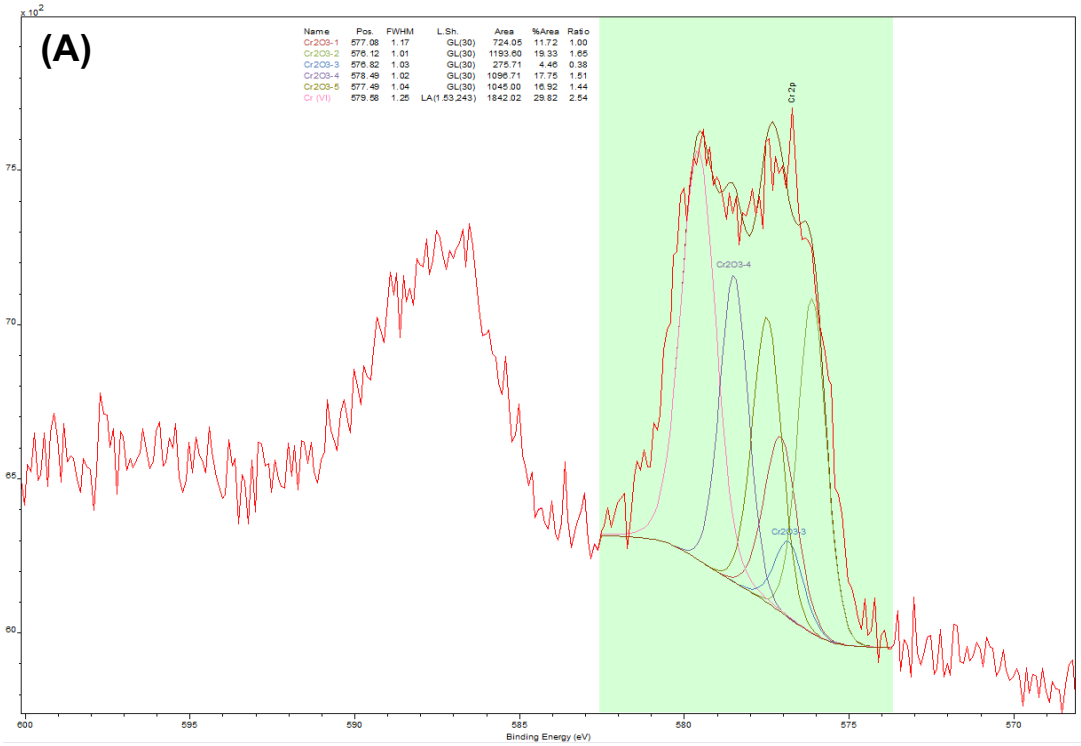


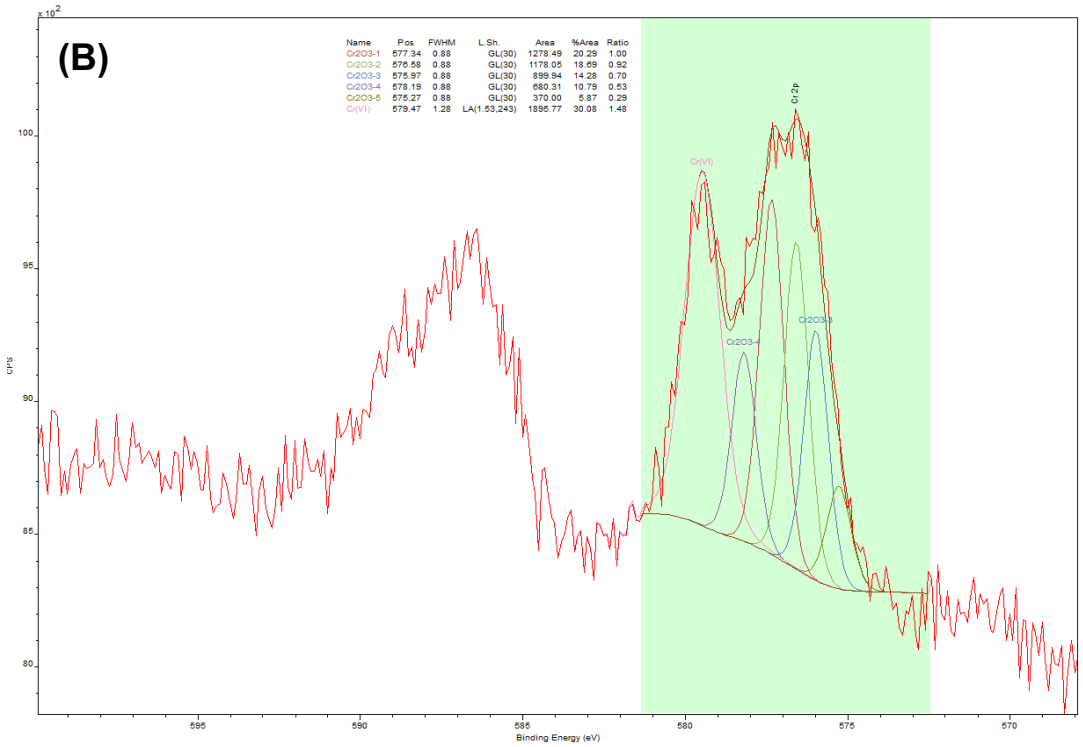
Figure 4.8. (A)TGA data and (B) derivative plots of temperature programmed oxidation (TPO) of two one-pot catalysts (Blue-2Cr-ZrO_2, Red-2Cr/Ca-ZrO_2) and impregnation catalyst (Yellow-2Cr-ZrO_2).

In summary, the catalysts prepared by the one-pot synthesis method showed different morphological structures, crystallinity and catalyst-distribution characteristics as compared with those made by the impregnation method. One assumption could be the catalysts are more likely to form a solid solution throughout the ZrO_2 support, together with a more uniform metal oxide (active sites) dispersion from the one-pot synthesis. We surmise at this stage that the precipitation and calcination processes occurring during the one-pot synthesis could potentially result in chemical bond formation through O–bridge between Cr–O cluster polymeric units and the ZrO_2 whilst the CrO_x is probably simply loaded onto the ZrO_2 surface during the impregnation process. In an attempt to determine the nature of the different catalysts produced by the two synthetic approaches, other characterisation techniques were employed.

X-ray diffraction will only identify the crystalline phases, and the only one that seemed to be visible in small amounts was the Cr(III) oxide which we assume is a side-phase. The ZrO_2-based phase had extremely broad peaks. We therefore employed XPS to probe the actual oxidation state of Cr species on the top surface layers of the catalyst. The XPS results are summarised in Table 4.3. The presence of unpaired d-electrons in Cr (III) has cause the characteristic peak splitting in XPS results (described in Chapter 3).



Name	Pos.	FWHM	L.Sh.	Area	%Area	Ratio
Cr2O3-1	577.08	1.17	GL(30)	724.05	11.72	1.00
Cr2O3-2	576.12	1.01	GL(30)	1193.60	19.33	1.65
Cr2O3-3	576.82	1.03	GL(30)	275.71	4.46	0.38
Cr2O3-4	578.49	1.02	GL(30)	1096.71	17.75	1.51
Cr2O3-5	577.49	1.04	GL(30)	1045.00	16.92	1.44
Cr (VI)	579.58	1.25	LA(1.53,243)	1842.02	29.82	2.54



Name	Pos.	FWHM	L.Sh.	Area	%Area	Ratio
Cr2O3-1	577.34	0.88	GL(30)	1278.49	20.29	1.00
Cr2O3-2	576.58	0.88	GL(30)	1178.05	18.69	0.92
Cr2O3-3	575.97	0.88	GL(30)	899.94	14.28	0.70
Cr2O3-4	578.19	0.88	GL(30)	680.31	10.79	0.53
Cr2O3-5	575.27	0.88	GL(30)	370.00	5.87	0.29
Cr(VI)	579.47	1.28	LA(1.53,243)	1895.77	30.08	1.48

Figure 4.9. XPS peak fitting of Cr species of one-pot synthesis catalyst (A) 2Cr-ZrO_2 and (B) 2Cr/Ca-ZrO_2.

The XPS results (Figure 4.9) also show that unlike the catalysts prepared by the impregnation method there is a much larger amount of Cr(VI) species present (giving an extra peak at higher binding energy than in the Cr(III) case) when the one-pot method is used than in the impregnation route. The oxidation states of Cr species would be expected to control the redox reactions taking place throughout the dehydrogenation process. With that in mind, the percentage of the different oxidation states, Cr(III) and Cr(VI), were determined from integration of the XPS data. As Table 4.3 and the spectra in Figure 4.9 show, the catalysts obtained by the one-pot method

reproducibly show more than twice as much oxidised Cr(VI) species as in the catalysts obtained by the impregnation method. From these data, we can conclude that the proportion of Cr(III) to Cr(VI) species depends on the catalyst preparation methods.

Table 4.3. Binding energies of the various Cr species for both the impregnation catalysts 2Cr-ZrO_2 (imp) and those from the one-pot synthesis 2Cr-ZrO_2 and 2Cr/Ca-ZrO_2.

Catalysts	Cr $2p_{3/2}$ Binding Energy (ev)		Cr(III)/ %	Cr(VI)/ %
	Cr(III)	Cr(VI)		
2Cr-ZrO_2 (imp)	576.7	579.64	87.97	12.03
2Cr-ZrO_2	577.2	579.58	70.18	29.82
2Cr/Ca-ZrO_2	576.7	579.47	69.92	30.08

From the various characterisation results, it is clear that the catalysts' morphological structure, the levels of the two Cr oxidation state species and corresponding surface catalytic properties are noticeably different between the two groups of differently prepared catalyst samples.

The impregnation method appears to physically "load" the metal oxides onto the ZrO_2 support surface to form a conventional metal oxide-on-support catalytic system. In contrast, the one-pot synthesis method, provides a rather different environment which stems perhaps from the fact that all the precursor cationic species are co-precipitated, leading to form more uniform solids. Furthermore, the subsequent treatment of the co-precipitated solids under reflux for 48 hours, might facilitate a change to either a substituted solid (surface layer) phase or indeed bonding entities, such as O-bridged Cr polymeric cluster species bonded to the Zr host. This method also leads to a much larger amount of fully-oxidised Cr(VI) species.

It is well established that ammonia can be used as a probe molecule to explore the overall acid properties of a catalyst surface using the technique of temperature-

programmed desorption (TPD). For the ammonia gas contacting with a solid catalyst, both physical absorption and chemical absorption occurs. Then the ammonia desorbed on the material is detected by temperature programming carried using nitrogen carrier gas. The acidic sites, involving both their strong and weak absorption sites can be calculated from the peak area change during the desorption process.

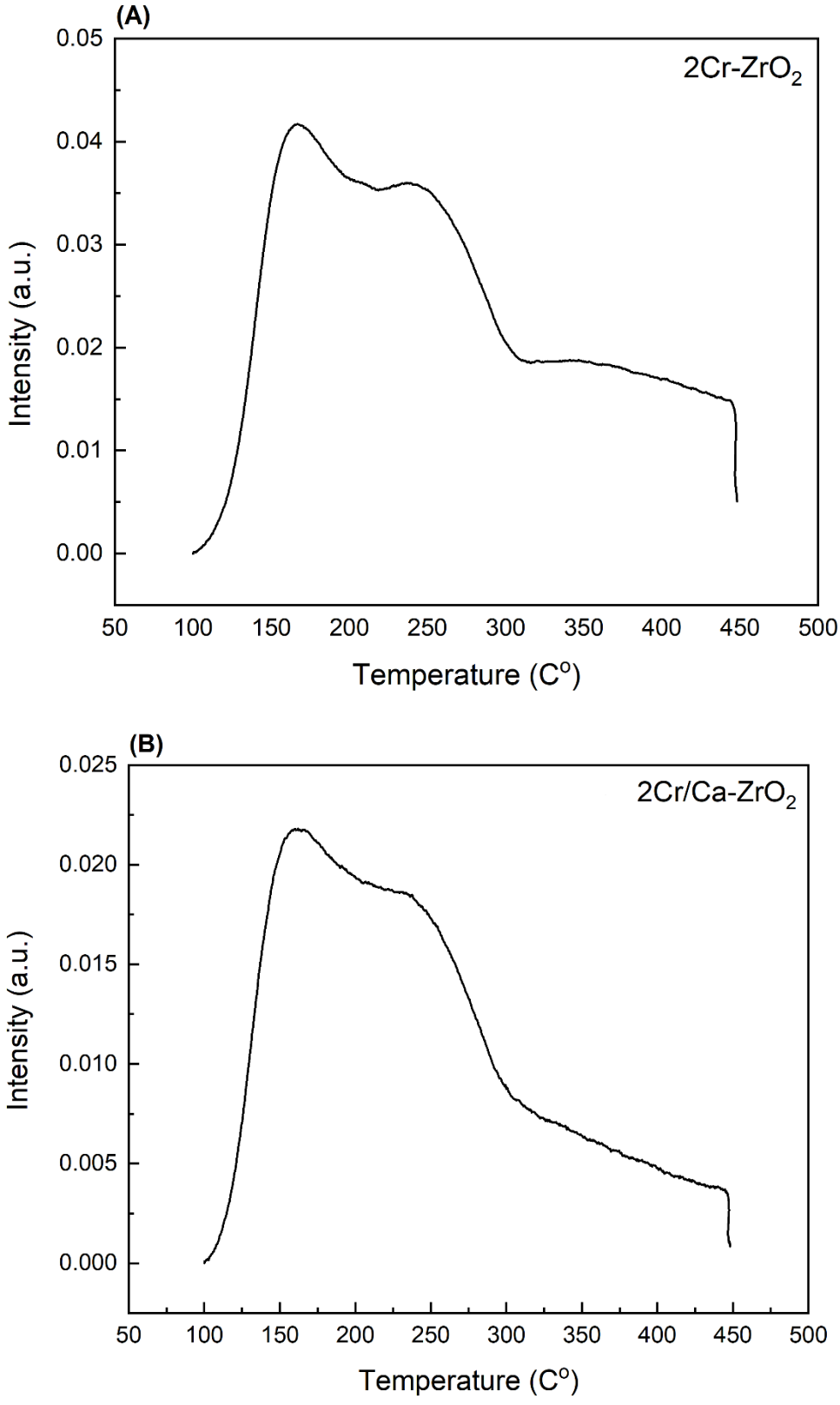


Figure 4.10. NH_3 desorption data vs. temperature by NH_3-TPD of (A) 2Cr-ZrO_2 and (B) 2Cr/Ca-ZrO_2 prepared by one-pot synthesis.

The impregnation-derived catalysts, 2Cr-ZrO_2, showed both strong and weak acid sites as reported in Chapter 3 (Figure 3.11). In Chapter 3, we said that the peaks at 150-290 °C could be attributed to the weak adsorption of the ammonia and peaks at 300-450 °C could be ascribed to strong desorption of ammonia adsorbed and the acidity is 0.15 mmol/g.[20,21] The one-pot synthesised catalysts show a desorption where there are no obvious signs of sites of different acidities. The acidity of 2Cr-ZrO_2 is 0.56 mmol/g and the 2Cr/Ca-ZrO_2 is 0.02 mmol/g. From the results, we found that by changing the preparation method, the acidity of catalysts was not changed very much. However, adding the alkaline Ca as promoter, the acidity of the material decreased, which is consistent with the results showed in figure 3.11 in Chapter 3.

As we can see from the characterisation results of the catalysts from two different preparation methods, the one-pot catalysts showed large differences in the surface properties and structures compared with impregnation catalysts. The XRD patterns showed a different crystallinity and bulk structure of the support between the two kinds of catalysts. The greater dispersion of Cr and the larger surface area of the one-pot catalysts could increase their catalytic activity; the low surface acidity could stabilise the catalysts away from coking effect and result in longer lifetimes. The catalytic tests were applied and the results are shown below.

4.4.2 Catalytic activity tests of one-pot catalysts

The catalytic activities of the 'one-pot'-prepared catalysts were tested in a fixed-bed micro reactor at 550 °C and for 10 hours. The tests were done in the same way as in Chapter 3. The feedstock gases were a mixture of $C_3H_8/CO_2/N_2$ at a total 25 ml/min flow rate, with a mole ratio of C_3H_8: CO_2: N_2 = 10%: 30%: 60%. In Figure 4.11, we show the evolved propane conversion and the propylene selectivity with time on stream (min) for the oxidative dehydrogenation of propane with carbon dioxide using 2Cr-ZrO_2

catalyst. The conversion reached over 20% after 1h reaction, and the propylene yield was around 19% with 90% selectivity. The propylene selectivity remained at a ca. 90% for nearly 200 min whereas the conversion gradually dropped to 7% after a 10h reaction period. This is attributed to deleterious carbon deposition on the catalysts surface that blocks/covers the catalytically active sites and consequently deactivates the catalysts. The conversion of CO_2 shown in Table 4.4, was around 6% after 3h-reaction and the final conversion was 3.2% with 17.8% CO yield. All the data are the average of three separate identical experiments, with percentage errors less than 5%. The detailed calculation method is shown in the Appendix.

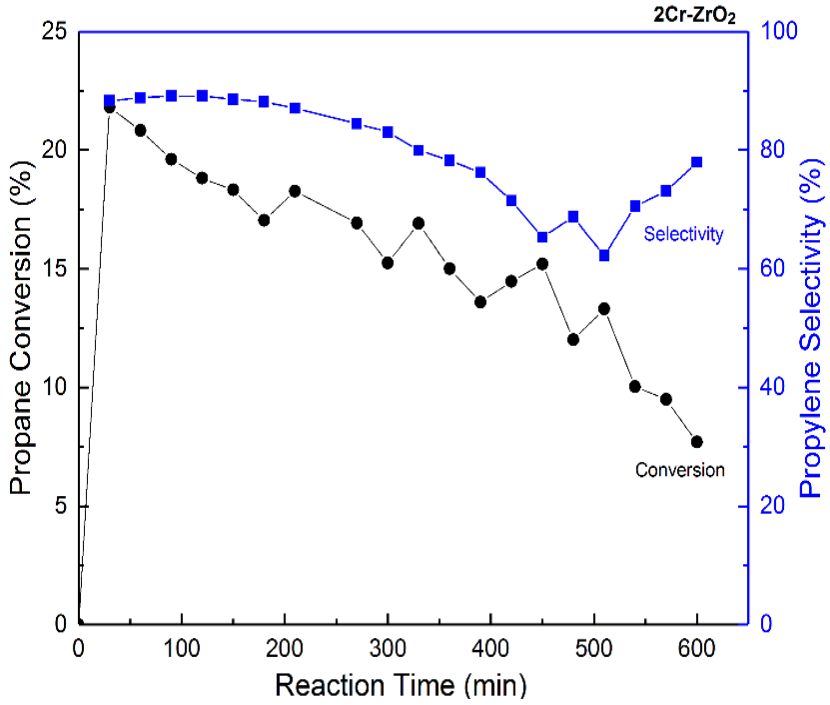


Figure 4.11. The propane conversion and propylene selectivity from the sample using 2Cr-ZrO_2 prepared by one-pot synthesis in a 10h catalytic test reaction. (% Error: conversion: ± 1.3-3.2%, selectivity: ± 2.9-4.4%)

The conversion rates of PDH can be affected significantly by the ratio between propane and CO_2, the flow rate of the gases, the reaction temperature and amount of active

metal oxide content. It has been reported that an increase in the C_3H_8/CO_2 ratio and the Cr content can improve the propane conversion during PDH.[12,22–24] In Chapter 3, the catalytic conditions have been clearly tested using CrO_x-based catalyst. For controlling the variables, in this work on the one-pot catalysts, the test conditions were all the same as the optimal ones in Chapter 3 and Cr/Ca-ZrO_2 catalysts with different Cr-contents were carefully compared. Compared with the results of impregnated catalysts shown in Figure 3.10, the one-pot catalysts, 2Cr-ZrO_2, showed a more gradual decrease in propane conversion and a higher propylene selectivity. The catalytic results were consistent with the expectations based on the characterisation data, the better dispersion of the active catalytic sites and a greater proportion of the Cr(VI) species.

The detailed nature of the catalyst active sites obviously plays a significant role in the catalyst performance which has been discussed in Chapter 3. It has been known that both acidic and basic sites of a catalyst are critically important to the catalyst performance. The dehydrogenation of propane over reducible metal oxide catalysts, such as chromium oxides, in the presence of CO_2 has been proposed to follow a redox mechanism.[22] Previous work by Shishido et al. proposed a chemical mechanism for propane dehydrogenation with CO_2 using CrO_x-based catalysts also shown in Figure 3.2 in Chapter 3. Therefore, we assume our process using one-pot catalyst shares a similar catalytic cycle.[15] Thus, propane is oxidised to propylene with the simultaneous reduction of the chromium (VI) oxide and subsequently the reduced metal oxide catalyst is re-oxidised (Cr(III) oxidised to Cr(VI)) by CO_2.[25]

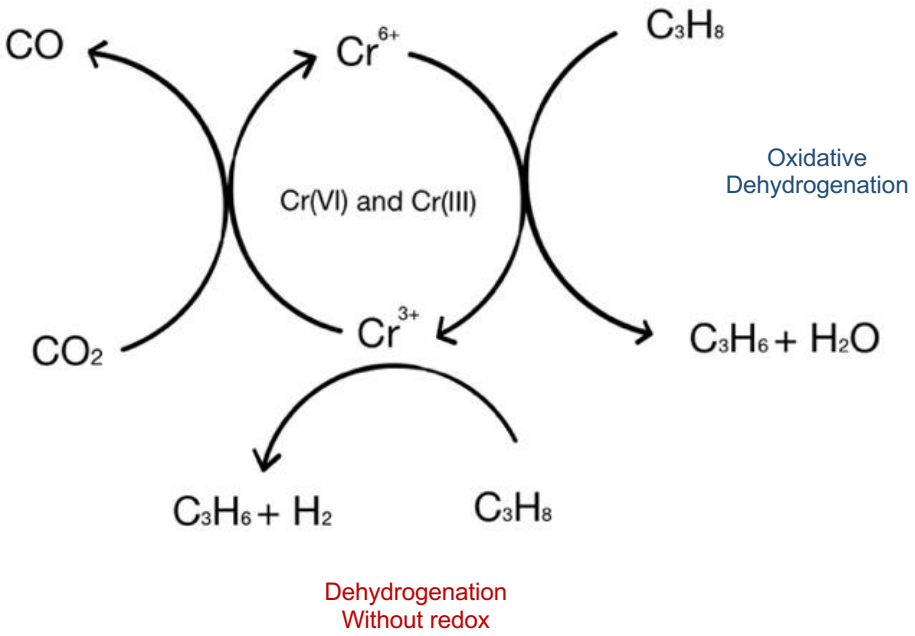


Figure 4.12. Proposed reaction mechanism of dehydrogenation of C_3H_8 in the presence of CO_2.[15]

Basic catalytic sites assist the absorption and consumption of CO_2 whereas acidic sites determine the adsorption and subsequent activation of propane. A stronger acidic site has been proposed to increase the metal-oxygen bond strength in the redox active cluster leading to a decrease in the reactivity.[11] The acidity of chromium-based catalytic system serves as one of the crucial factors in determining the catalytic activity in oxidative dehydrogenation reactions. However, a stronger surface acidity also leads to the formation of carbonaceous cracking products, and thus less alkene selectivity is obtained.

Based on the discussion in Chapter 3, Ca oxide is a good promoter to improve the catalyst performance and is able to help optimise the balance between the acidity and basicity of the catalysts. Therefore, we show the catalytic performances of Ca-promoted 2Cr/Ca-ZrO_2 and 3Cr/Ca-ZrO_2 catalysts prepared through the one-pot

approach for the oxidative dehydrogenation of propane with CO_2 under the same conditions (Figure 4.13).

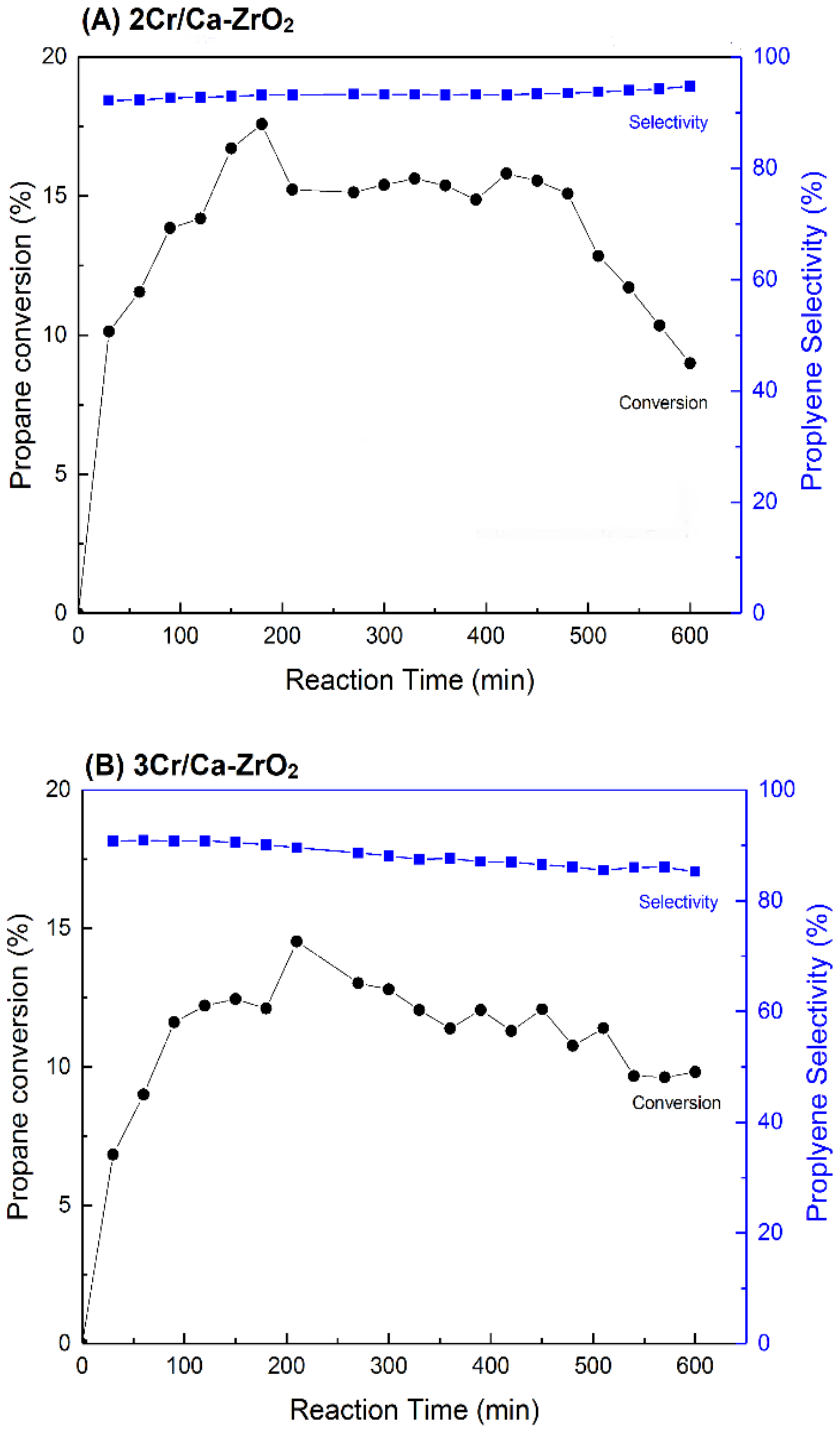


Figure 4.13. The propane conversion and propylene selectivity from the various samples (A) 2Cr/Ca-ZrO_2 and (B) 3Cr/Ca-ZrO_2 from one-pot synthesis during a 10h reaction. (% Error: conversion: ± 0.5-2.4%, selectivity: ± 0.2-0.6%)

We note that the catalyst's stability as well as the propylene selectivity were improved for one-pot catalysts compare with the impregnation catalysts show in Figure 3.10. The Ca oxide promoted system obtained through impregnation is described in Chapter 3 (Figure 3.10). As the activity tests reveal (Figure 4.13.(A)) the propane conversion increased for the first 180 min and reached a value of ca. 20% conversion and at this time the CO_2 conversion is about 5%. Then the propane conversion slightly decreased to about 17% and kept at this quasi-steady state for a period of 500 min. Importantly, over 95% selectivity to propylene formation was achieved. The propylene yield was 20% in first 3 hours and decreased to 15% after a 10-hour reaction.

It should be noted that unlike the 2Cr-ZrO_2 catalysts, a quasi-steady conversion rate between 200 min to 500 min was observed over the Ca promoted 2Cr/Ca-ZrO_2 catalyst. This clearly indicates, importantly, the Ca promoted Cr/Ca-ZrO_2 catalysts have enhanced stability in terms of resisting coke formation which has also been evidenced in our post-reaction characterisation (see below). The temperature programmed oxidation (TPO) analysis of spent samples showed only ca 5 wt.% carbon content in the 2Cr/Ca-ZrO_2 catalyst, whereas the 2Cr-ZrO_2 catalyst contained ca 10 wt.% carbon residues (Figure 4.15). The EDS results in Figure 4.15. (F) and 4.16. (G) also reveals the lower surface carbon percentage in the 2Cr/Ca-ZrO_2 catalyst.

By adding the Ca oxide promoter, therefore, the results show a noticeable increase in the conversion in the initial 3 hours with subsequent slow decrease, thereafter (Table 4.4). Hence the deactivation of the Ca-oxide-promoted catalysts was slower as the decrease of the propane conversion wasn't as rapid as for the non-promoted catalysts, and also gave a higher selectivity. The 2Cr/Ca-ZrO_2 catalyst shows a stable and high propane conversion, and a high propylene selectivity and yield. The maximum conversion reached 20% at 180 min and the conversion stayed constant at around 16-18% between 210-480 min. This constant performance level only occurred with the

2Cr/Ca-ZrO_2 catalyst by one-pot synthesis and was not shown by the impregnation catalysts (Figure 3.10 (A)).

The carbon is a solid material and can't be detected by GC when it presents as coke. Therefore, to know the amount of coking on the catalyst surface, the carbon balance will be introduced to quantitatively determine the coking formation. The carbon balance of a reaction is a percentage of the carbon amount involved during the chemical reaction by calculating the carbon contents before and after the reaction. In this case, the carbon balance of CO_2-PDH with different catalysts process from GC results using equation 4.6. The carbon balance of CO_2-PDH with all one-pot catalysts was calculated and determined to be over 93% after the reaction as shown in Table 4.5. This demonstrates the CO_2 conversion of the 2Cr/Ca-ZrO_2 was 4% at 180 min with CO yield 46.7%. The CO_2 conversion of different one-pot catalysts are calculated using equation (4.4) and summarised in Table 4.5. The carbon balance shows that the Ca-promoted catalysts have a higher carbon balance about 96% than the non-promoted catalyst, about 92%. Thus, by adding the Ca promoter, it is kind of inhibits the carbon coking on the catalysts surface as the carbon balance is higher.

In addition, the Ca promoter clearly affects the surface acidity, as reported in Chapter 3. The acidity is calculated from the NH_3-TPD profile, the 2Cr/Ca-ZrO_2 catalyst has a very low surface acidity compared with 2Cr-ZrO_2. Similar results were reported by Xu et al. showing that this difference is mainly due to the surface basicity.[20] It seems that the low acidity would decrease the propane conversion due to the competitive adsorption effect between propane and CO_2. However, according to Du et al., this could enhance the propylene selectivity in the PDH with CO_2 by inhibiting the further adsorption and cracking of propylene on the catalyst surface.[26]

The Cr content and oxidation state are themselves important parameters that can affect the conversion rates of PDH and this has also been investigated. We prepared a series of Cr/Ca-ZrO_2 catalysts using the one-pot synthesis method, with different Cr

contents. 1, 2, 3 and 4 moles of Cr per 10 moles of Zr were used in the one-pot synthesis to prepare different catalysts, and these were named as Cr/Ca-ZrO_2, 2Cr/Ca-ZrO_2, 3Cr/Ca-ZrO_2 and 4Cr/Ca-ZrO_2, with the amount of added Ca kept constant per mole of Zr as shown in Table 4.4. The propane conversion, propylene yield and selectivity by propane dehydrogenation with CO_2 on these prepared catalysts are summarised in table 4.4. The catalytic results for 4Cr/Ca-ZrO_2 showed an extremely low conversion of propane, to the extent that it was difficult to calculate. The numbers were smaller than systematic errors intrinsic to operating with the reactor. The high Cr content apparently “poisons” the catalysts, accelerating the deactivation of the catalyst and shortens its lifetime during the catalytic cycle.

The propane conversion increased as the Cr content increased from 1 mmol Cr to 2 mmol, the 2Cr/Ca-ZrO_2 catalyst showed the best catalytic performance for both propane conversion and propylene selectivity, reaching maximum values of 20.2% conversion and 94.6% selectivity, respectively. The propylene yield with this catalyst was also the best (about 20.1%). However, a further increase in the Cr loading resulted in a decrease of both propane conversion and propylene yields. This is attributed to the fact that at such high Cr contents the Cr_2O_3 (Cr^{3+}) species for propane dehydrogenation will be more dominant than the active chromate or poly-chromate ones (Cr^{6+}).[11] Further characterisations such as XPS, could be applied to all the fresh and spent 2Cr-ZrO_2 and 2Cr/Ca-ZrO_2 catalysts to explore this further.

Table. 4.4. Summary of catalytic results of four separate 'one-pot' catalysts with 1-3 mmoles of Cr loading.

	Conversion / %		Selectivity / %						Yield / %	
	C_3H_8		C_3H_6		CH_4		C_2H_4		C_3H_6	
Catalyst	3h	10h	3h	10h	3h	10h	3h	10h	3h	10h
1Cr/Ca-ZrO_2	3.6	13.1	87.9	44.7	6.5	27.1	5.5	28.2	3.2	5.9
2Cr/Ca-ZrO_2	20.2	9.5	93.5	94.6	4.0	0.5	2.8	5.0	20.1	14.9
3Cr/Ca-ZrO_2	12.1	9.8	90.1	85.3	7.1	10.0	4.3	12.3	15.0	8.6
2Cr-ZrO_2	17.0	7.7	88.2	78.0	7.5	7.9	3.5	14.1	15.0	6.0

* Errors: conversion: ± 0.5-3.7%, selectivity: ± 0.2-4.4%, yield: ± 1.8-2.6%

Table. 4.5. Summary of CO_2 conversion of four 'one-pot' catalysts with 1-3 mmoles of Cr loading.

	CO_2 Conversion / %		CO Yield / %		Carbon-Balance
Catalyst	3h	10h	3h	10h	10h
1Cr/Ca-ZrO_2	1.5%	7.4%	25.6%	20.8%	93.4%
2Cr/Ca-ZrO_2	4.1%	0.7%	46.7%	32.0%	95.8%
3Cr/Ca-ZrO_2	3.3%	1.5%	46.2%	21.8%	95.1%
2Cr-ZrO_2	6.0%	3.2%	94.5%	17.8%	92.3%

*Errors: conversion: ± 3.2-4.8%, yield: ± 0.5-1.7%, carbon balance ± 0.2-0.5%. All the result data are the average of three separate identical experiments. The detailed calculation method is shown in Appendix.

4.3.3 Post-reaction analysis of one-pot catalysts, 2Cr-ZrO_2 and 2Cr/Ca-ZrO_2

For a catalytic reaction, the deactivations of the catalysts are always under consideration by scientists. In this chapter, the spent one-pot catalysts were characterised by different techniques to find out the main deactivation issue. It has been found out that the catalysts changed to black colour after the dehydrogenation process (Figure 4.14). In this case, it was assumed there would be coking formation on the catalyst's surface which block the active sites for catalytic activities.

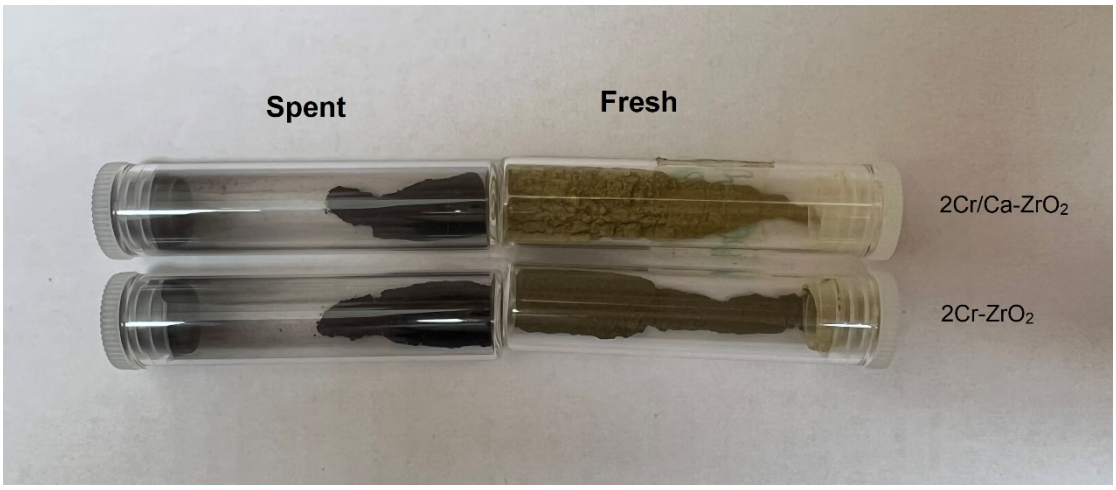


Figure 4.14. Picture of the two one-pot catalysts as their fresh and spent forms.

The TGA of two spent 'one-pot' catalysts under air is shown in Figure 4.14. The diagram shows the weight loss at 300 °C, which suggests the presence of amorphous carbon and crystalline graphite which are burnt during the analysis. This is later proved by the XRD pattern shown in Figure 4.20 (A). The TGA diagram shows that 2Cr/Ca-ZrO_2 catalyst has lower carbon loss during TGA analysis than 2Cr-ZrO_2 catalysts. This could indicate that the Ca-promoted catalyst has lower carbon coking on the catalyst's surface. Notably, the catalysts' original catalyst colour was obtained after the TGA runs under air.

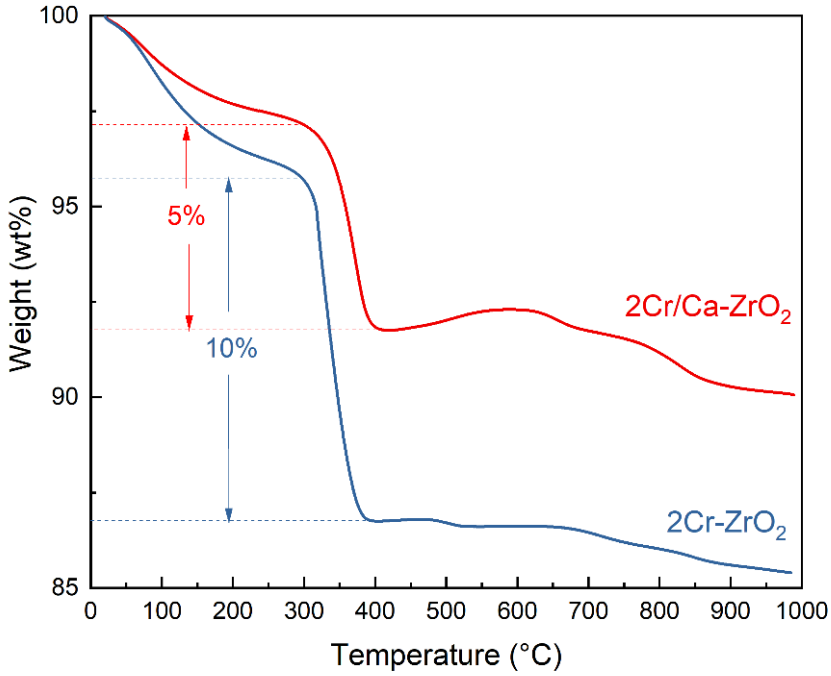


Figure 4.15. TGA diagram of two spent one-pot catalysts (Blue-2Cr-ZrO_2 and Red-2Cr/Ca-ZrO_2).

SEM images are shown in Figure 4.16 for the spent one-pot catalysts.

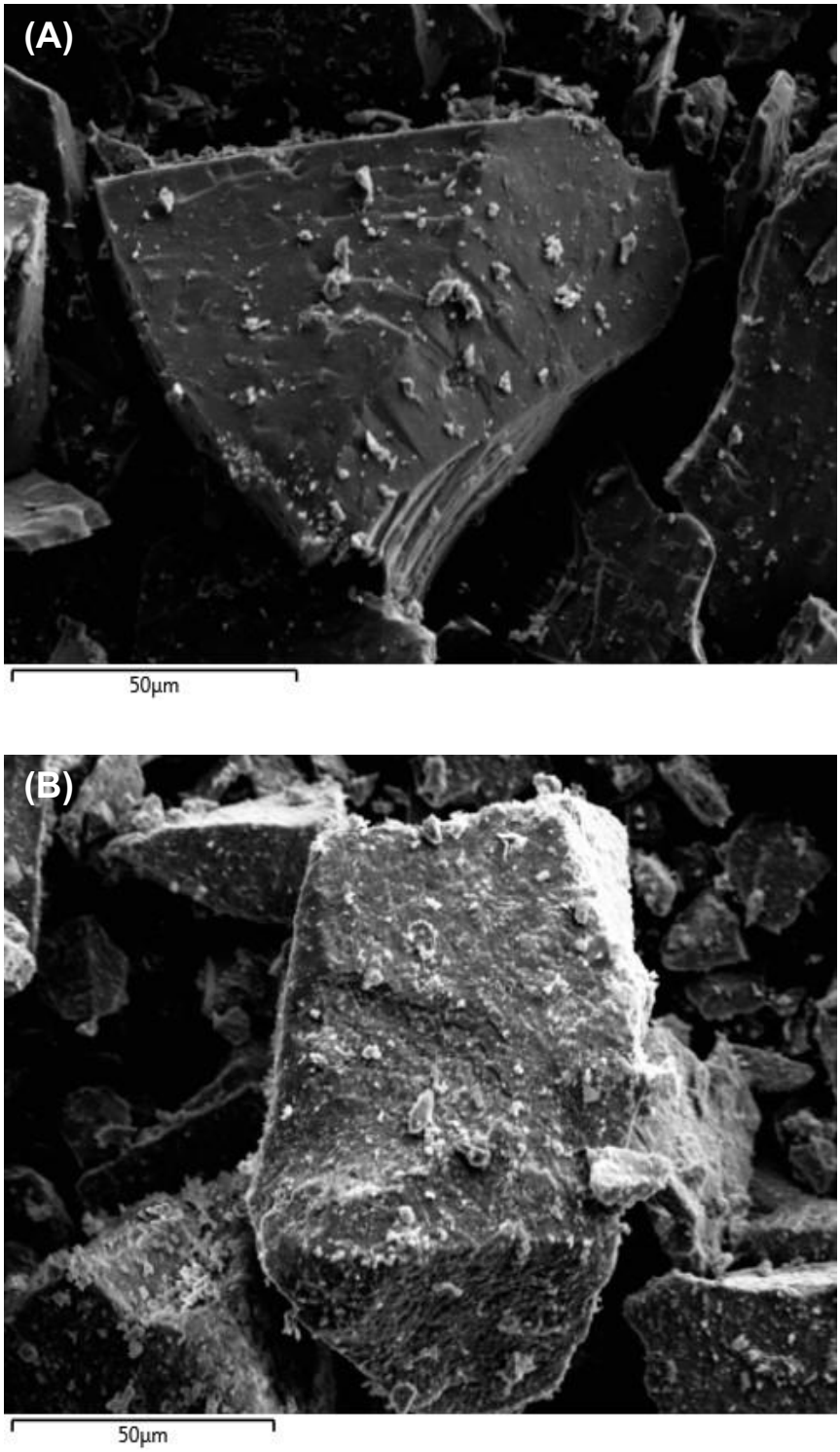


Figure 4.16. SEM images of spent (A) 2Cr-ZrO_2 and (B). 2Cr/Ca-ZrO_2 prepared by one-pot synthesis.

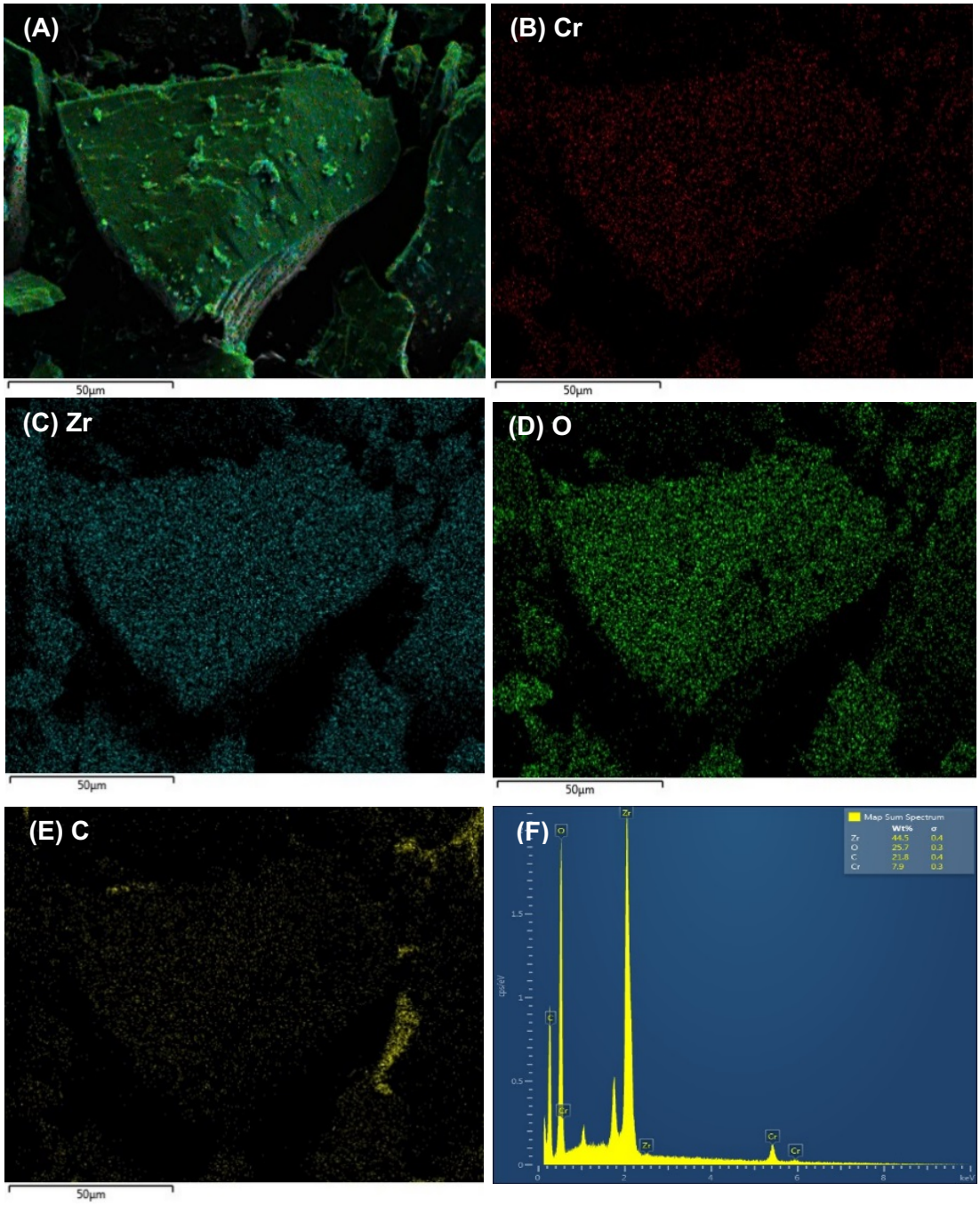
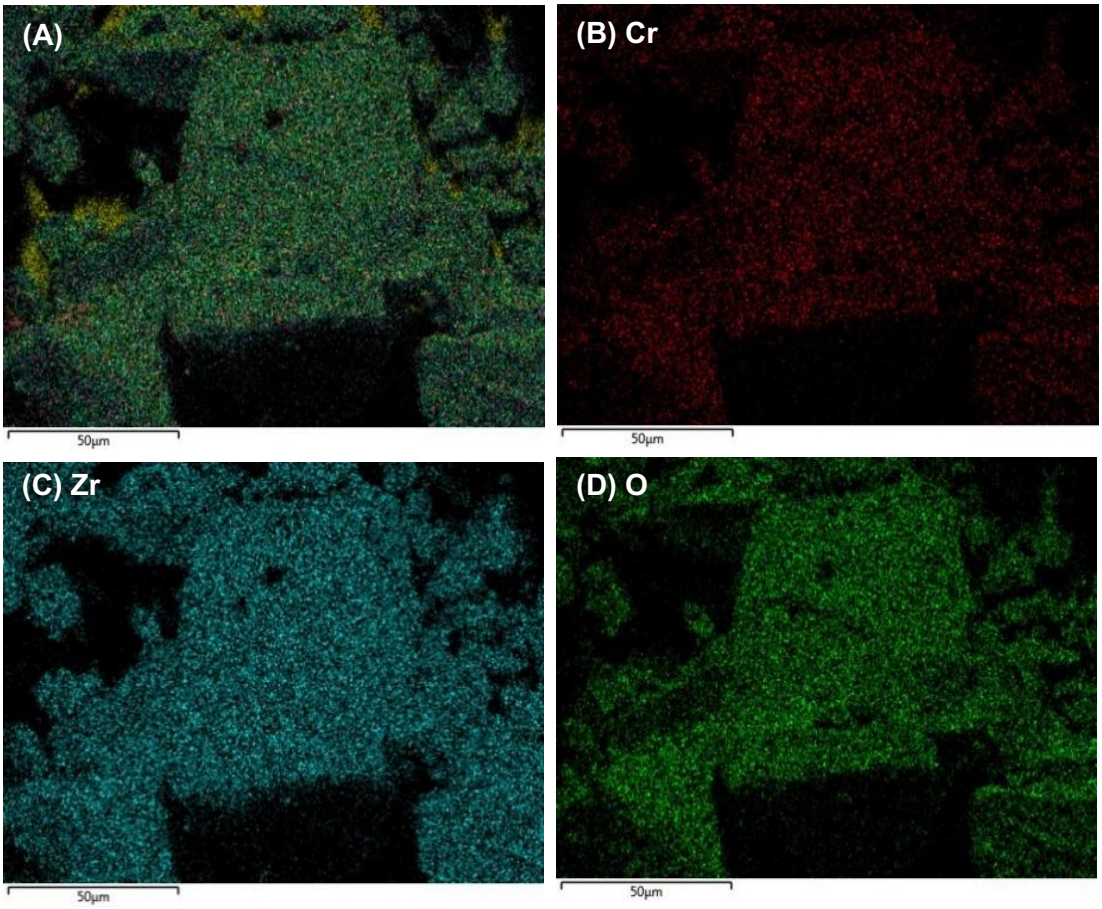


Figure 4.17. SEM images and EDS mapping of the elemental species on the surface of spent 2Cr-ZrO_2 samples prepared using one-pot synthesis. (A) SEM (backscattered electron), (B) Cr map, (C) Zr map, (D) O map, (E) C map, and (F) EDS spectrum.

The EDS mappings in Figure 4.17 show the elemental content on the spent 2Cr/Ca-ZrO_2 catalysts surface. The EDS elemental analysis suggests the carbon content is 17%, Cr content is 7.7%, Zr is 42.1%, Ca is 4.8% and O is 28.5%. For the non-promoted 2Cr-ZrO_2 catalyst, the elemental carbon content from EDS is 21.8% (Figure 4.17). The EDS result indicates that the Ca-promoted catalyst (2Cr/Ca-ZrO_2) has 25% (4.8% in amount) lower carbon content than the non-promoted 2Cr-ZrO_2 catalysts based on the EDS mapping data. But carbon is considered as light element, the X-ray signal is low and cause energy loss for detector to detect. In addition, the pumps of the vacuum system in SEM will contaminate and cause the final analysed carbon data higher than actual data. The Figure 4.15 also shows that the Ca-promoted catalysts has lower carbon loss (about 5%) during the TGA analysis, which is considered as consistent with the EDS results. As shown in the carbon SEM-EDS images (Figure 4.17 (E) and 4.18 (E)), the highlighted yellow area is indicating the carbon content on the catalysts' surface, and they are not uniformly formed and dispersed on the solid surface. Therefore, this is the challenge to determine the exact carbon content in material surface. In addition, it calculates that the carbon contents in wt% from TGA data is much higher than from carbon balance results, which is about 10%-15% higher. This is also prove the non-homogenous of the carbon formation on the calalysts.


(A)
50μm
(B) Cr
50μm
(C) Zr
50μm
(D) O
50μm

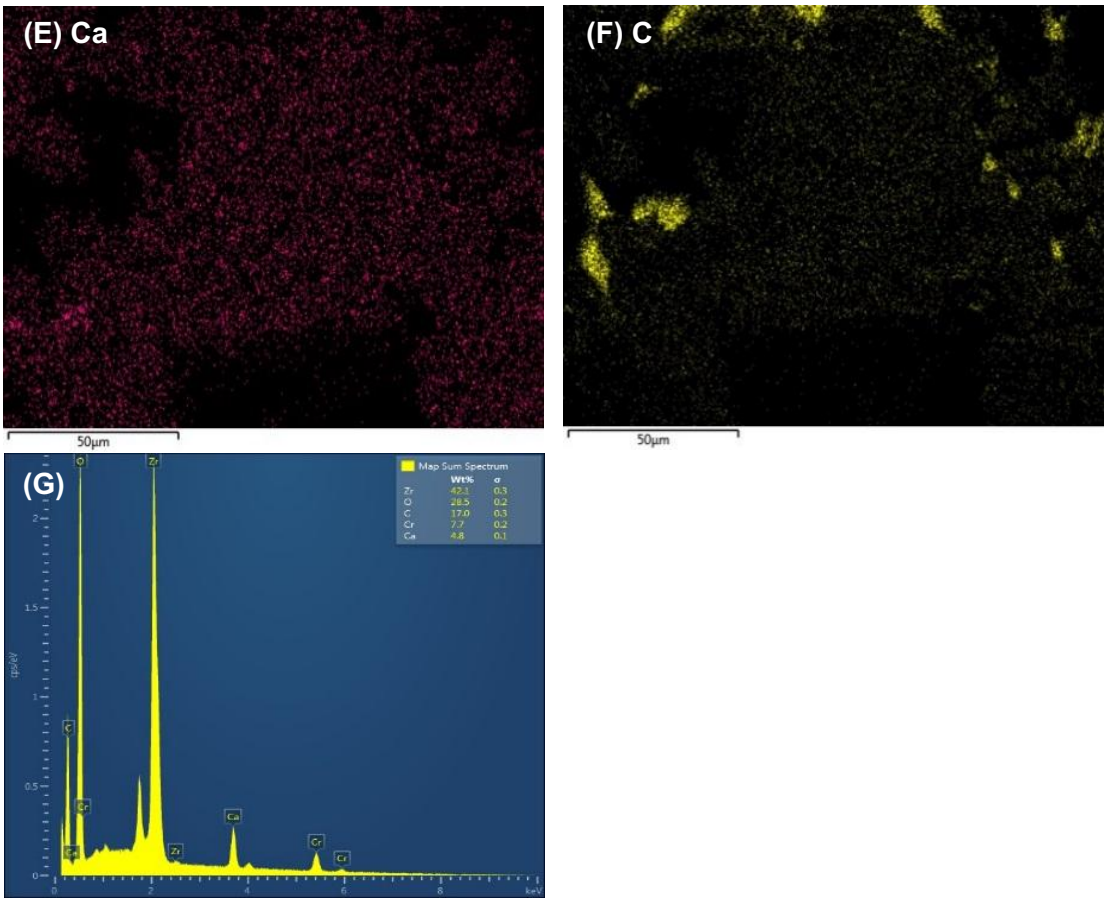


Figure 4.18. SEM images and EDS mapping of the elemental species on the surface of spent 2Cr-Ca/ZrO_2 samples prepared using one-pot synthesis. (A) SEM (backscattered electron), (B) Cr map, (C) Zr map, (D) O map, (E) Ca map, (F) C map, and (G) EDS spectrum.

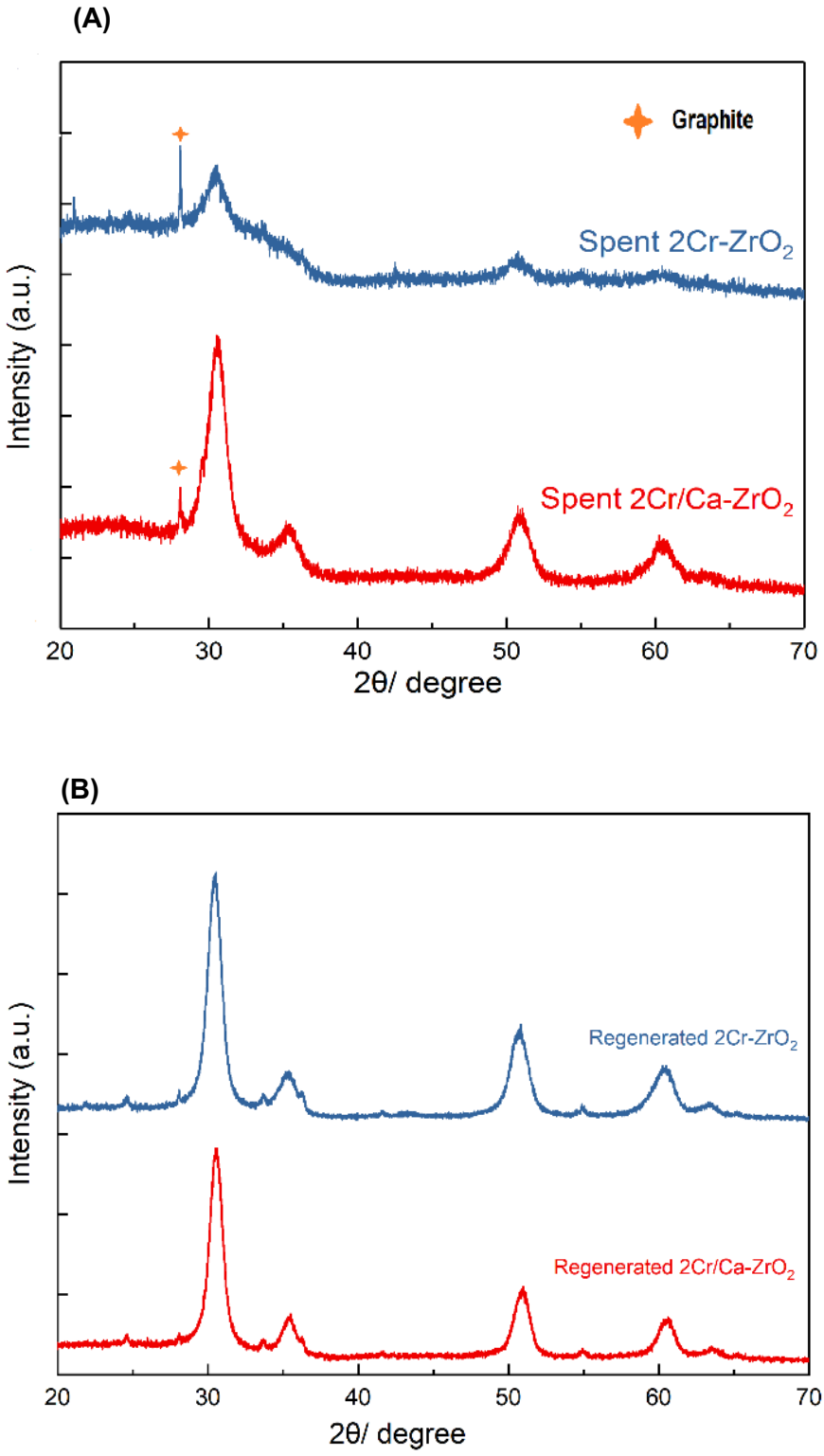


Figure 4.19. XRD patterns of (A) spent and (B) regenerated 2Cr-ZrO_2 (blue) and 2Cr/Ca-ZrO_2(red) catalysts prepared by the one-pot synthesis approach.

The X-ray diffraction pattern of spent sample is given in Figure 4.19. The XRD pattern suggests the presence of some deposited crystalline graphitic carbon (001).[27] Moreover, there is no obvious change in the diffraction peaks when compared with fresh catalysts (Figure 4.2) The ZrO_2-dominated material is still present as the tetragonal phase.

From EDS mapping and XRD patterns, it is clear that the coking formed as carbon is deposits on the catalysts' surface after the dehydrogenation process. The carbon deposition on the catalysts' surface during the reaction is considered to be the main reason for its deactivation. This has also been demonstrated by our regeneration test in Chapter 5 where the carbon was removed by combustion at 550 °C. It can be seen from the XRD patterns of regenerated catalysts (Figure 4.19. (B)) that the catalysts' structure remained unchanged indicating that the catalyst structure is stable during the dehydrogenation reaction and when the surface coking is burnt off in the TGA measurements. Compared with fresh catalysts in Figure 4.2, it seems the crystallinity increased slightly in this thermal treatment as the peaks became narrower.

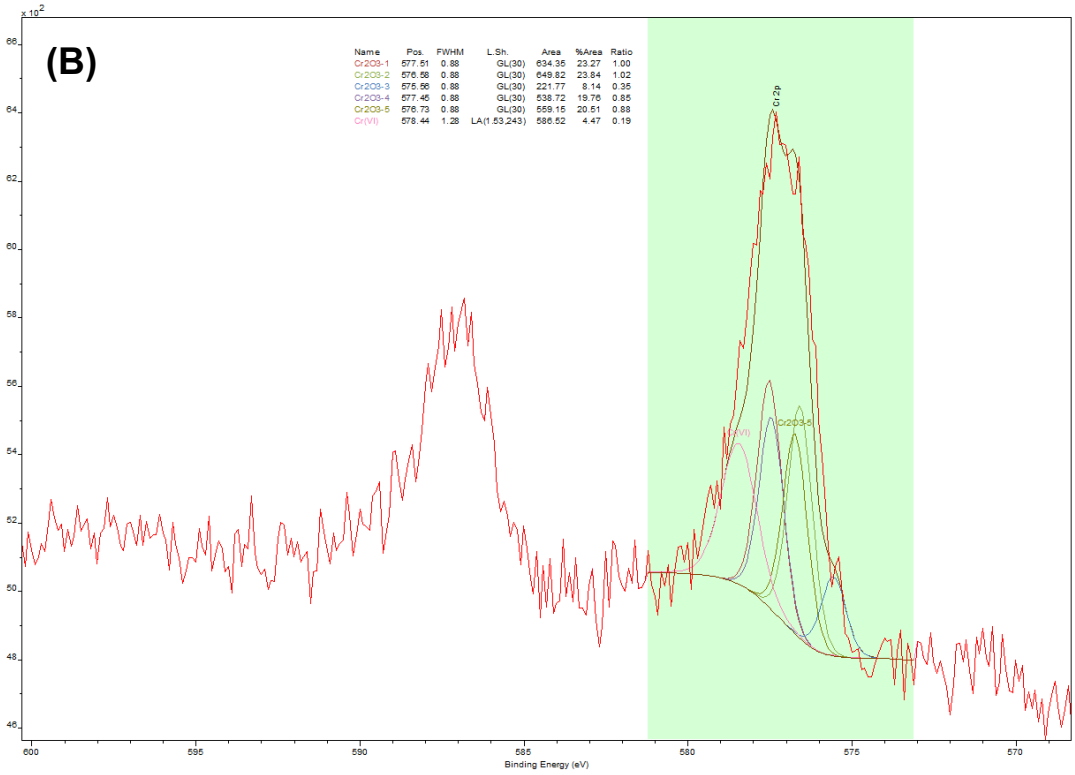
In addition, the representative XPS characterisation data from spent 2Cr-ZrO_2 and 2Cr/Ca-ZrO_2 catalysts are contained in Table 4.5. Compared with fresh 2Cr-ZrO_2 and 2Cr/Ca-ZrO_2 (Table. 4.3), a noticeable increase of Cr(III) species were observed after the dehydrogenation reaction, whilst the amount of the Cr(VI) species was found to decrease. Since the Cr(VI) ions are reported[28–30] as the most active species in the oxidative dehydrogenation of light alkanes, we therefore attribute the decrease in propane conversion to this change. Thus, the coke formation may inhibit the re-oxidation of Cr(III) to Cr(VI). A future work would be to see whether the catalytic activity can be restored after burning off the carbon (i.e. whether the Cr(VI) is restored). This will be investigated and discussed in Chapter 5.

Table. 4.6. Binding energies and relative proportions of various Cr species of spent catalysts.

Catalysts	Cr $2p_{3/2}$ Binding Energy (ev)		Cr(III)/ %	Cr(VI)/ %
	Cr(III)	Cr(VI)		
Spent 2Cr-ZrO_2	576.8	578.47	95.53	4.47
Spent 2Cr/Ca-ZrO_2	577.0	579.11	89.54	10.56



Name	Pos.	FWHM	L.Sh.	Area	%Area	Ratio
Cr2O3-1	576.62	0.88	GL(30)	727.40	18.80	1.00
Cr2O3-2	576.84	0.88	GL(30)	505.62	13.07	0.70
Cr2O3-3	577.41	0.88	GL(30)	957.03	24.73	1.32
Cr2O3-4	576.08	0.88	GL(30)	416.26	10.76	0.57
Cr2O3-5	578.07	0.88	GL(30)	854.97	22.09	1.18
Cr(VI)	579.11	1.68	LA(1.53,243)	408.80	10.56	0.56



Name	Pos.	FWHM	L.Sh.	Area	%Area	Ratio
Cr2O3-1	577.51	0.88	GL(30)	634.35	23.27	1.00
Cr2O3-2	576.58	0.88	GL(30)	649.82	23.84	1.02
Cr2O3-3	575.56	0.88	GL(30)	221.77	8.14	0.35
Cr2O3-4	577.45	0.88	GL(30)	538.72	19.76	0.85
Cr2O3-5	576.73	0.88	GL(30)	559.15	20.51	0.88
Cr(VI)	578.44	1.28	LA(1.53,243)	586.52	4.47	0.19

Figure 4.20. XPS peak fitting of Cr species of spent one-pot synthesis catalyst (A) 2Cr-ZrO_2 and (B) 2Cr/Ca-ZrO_2.

4.5 Conclusion

We have reported a detailed study of the CrO_x-based catalysts prepared by the one-pot synthesis method for the dehydrogenation of propane using CO_2. The structural information for the one-pot-synthesised CrO_x-based catalysts has been investigated. From the results-presented here, the one-pot synthesis method resulted in a different catalyst morphology and structure, and a higher mean Cr oxidation state (i.e. more Cr(VI) and less Cr(III) as compared with the conventional impregnation method. This synthetic route resulted in a marked enhancement in the CO_2 dehydrogenation of propane with high and stable propylene selectivity. The propane conversion is stable during the reaction for 4-8 hours. The SEM images show a more compact/layered structure of the one-pot catalysts. The EDS analysis shows that the one-pot catalyst contains Cr with a highly uniform distribution. Those characteristics are totally different compared with the impregnation-route catalysts which revealed a consistently lower Cr (VI)/Cr (III) ratio and less homogeneous dispersion of Cr on the catalyst surface.

We also have demonstrated the catalytic properties of two different one-pot catalysts during the propane dehydrogenation process with CO_2, the non-promoted catalyst, 2Cr-ZrO_2, and Ca-oxide-promoted catalysts, 2Cr/Ca-ZrO_2. The general activity of catalysts decreases with the time on stream. The 2Cr-ZrO_2 catalyst shows a continual decrease in conversion rate, propylene selectivity and yield. The deactivation of the catalyst was significant with an extended reaction time, which is due to the carbon coking effect. To maintain the catalytic activity of the catalyst, Ca oxide was chosen as a promoter. The results show that both the propane conversion and propylene selectivity are noticeably improved with the addition of the Ca oxide promoter. The data reveal that the promoter protects the catalysts from the time-dependent deactivation that occurs because of the depositing of carbonaceous material. This was supported by the TGA results and SEM-EDS data of the spent catalysts containing the Ca promoter which showed a lower carbon content.

The best catalyst performance reached 20% conversion of propane and 20% yield to propylene with over 90% selectivity after 180 min, and about 10% conversion, 15% product yield after 10 hours with still about 93% propylene selectivity.

The results highlight the attractiveness of the one-pot synthesis, which provides stable and active catalysts for this dehydrogenation reaction using CO_2. Also the inclusion of CaO as a promoter results in a superior catalyst selectivity and the propylene yield increases compared with the non-promoted catalyst. This is because the CaO-promoted catalyst is more resistant to carbon deposition and therefore maintains catalytic activity over an extended period. Thus, the one-pot synthesis of CaO-promoted Cr catalyst demonstrated both good stability and good catalytic performance during the dehydrogenation process.

References

1 D. Yao, H. Yang, H. Chen and P. T. Williams, *Appl. Catal. B Environ.*, 2018, **239**, 565–577.

2 Y. Yamada, T. Akita, A. Ueda, H. Shioyama and T. Kobayashi, *Rev. Sci. Instrum.*, 2005, **76**, 20129.

3 A. H. Lu and F. Schüth, *Adv. Mater.*, 2006, **18**, 1793–1805.

4 P. Michorczyk, P. Kuśtrowski, A. Kolak and M. Zimowska, *Catal. Commun.*, 2013, **35**, 95–100.

5 A. Vinu, in *Advances in Nanoporous Materials*, Elsevier B.V., 2010, vol. 1, pp. 151–235.

6 R. Wu, P. Xie, Y. Cheng, Y. Yue, S. Gu, W. Yang, C. Miao, W. Hua and Z. Gao, *Catal. Commun.*, 2013, **39**, 20–23.

7 R. K. Gautam and M. C. Chattopadhyaya, in *Nanomaterials for Wastewater Remediation*, Elsevier, 2016, pp. 139–159.

8 China Science Communication, 共沉淀法 (Coprecipitation method), https://baike.baidu.com/item/共沉淀法/5489210, (accessed 8 August 2022).

9 X. Jiang, L. Sharma, V. Fung, S. J. Park, C. W. Jones, B. G. Sumpter, J. Baltrusaitis and Z. Wu, *ACS Catal.*, 2021, **11**, 2182–2234.

10 Y. Gao, X. Jie, C. Wang, R. M. J. Jacobs, W. Li, B. Yao, J. R. Dilworth, T. Xiao and P. P. Edwards, *Ind. Eng. Chem. Res.*, 2020, **59**, 12645–12656.

11 A. M. El-Toni, A. S. Al-Awadi, A. E. Abasaeed, A. Al-Fatesh, M. Alhoshan, J. P. Labis, A. Khan and S. M. Al-Zahrani, *Ceram. Int.*, 2018, **45**, 1125–1134.

12 F. Rahmani, M. Haghighi and S. Mahboob, *Ultrason. Sonochem.*, 2016, **33**,

150–163.

13 J. F. S. de Oliveira, D. P. Volanti, J. M. C. Bueno and A. P. Ferreira, *Appl. Catal. A Gen.*, 2018, **558**, 55–66.

14 S. B. H. Farid, in *Bioceramics: For Materials Science and Engineering*, Elsevier, 2019, pp. 39–76.

15 T. Shishido, K. Shimamura, K. Teramura and T. Tanaka, *Catal. Today*, 2012, **185**, 151–156.

16 D. Qiao, G. Lu, X. Liu, Y. Guo, Y. Wang and Y. Guo, *J. Mater. Sci.*, 2011, **46**, 3500–3506.

17 J. Yu, J. Zhang and M. Jaroniec, *Green Chem.*, 2010, **12**, 1611–1614.

18 F. Nomura, Y. Liu, T. Tanabe, N. Tamura, T. Tsuda, T. Hagiwara, T. Gunji, T. Ohsaka and F. Matsumoto, *Electrochim. Acta*, 2018, **269**, 321–330.

19 E. Nowicka, C. Reece, S. M. Althahban, K. M. H. Mohammed, S. A. Kondrat, D. J. Morgan, Q. He, D. J. Willock, S. Golunski, C. J. Kiely and G. J. Hutchings, *ACS Catal.*, 2018, **8**, 3454–3468.

20 Y. Weng, S. Qiu, L. Ma, Q. Liu, M. Ding, Q. Zhang, Q. Zhang and T. Wang, *Catalysts*, 2015, **5**, 2147–2160.

21 M. Hamidzadeh, M. Ghassemzadeh, A. Tarlani and S. Far, *Orient. J. Chem.*, 2016, **32**, 481–490.

22 M. A. Atanga, F. Rezaei, A. Jawad, M. Fitch and A. A. Rownaghi, *Appl. Catal. B Environ.*, 2018, **220**, 429–445.

23 A. Samanta, X. Bai, B. Robinson, H. Chen and J. Hu, *Ind. Eng. Chem. Res.*, 2017, **56**, 11006–11012.

24 L. Le, M. Yang, C. Xiao and A. Chen, *Integr. Ferroelectr.*, 2017, **182**, 202–209.

25 B. Xu, B. Zheng, W. Hua, Y. Yue and Z. Gao, *J. Catal.*, 2006, **239**, 470–477.

26 X. Du, D.Phil thesis, University of Oxford, 2016.

27 R. Siburian, H. Sihotang, S. Lumban Raja, M. Supeno and C. Simanjuntak, *Orient. J. Chem.*, 2018, **34**, 182–187.

28 E. Asghari, M. Haghighi and F. Rahmani, *J. Mol. Catal. A Chem.*, 2016, **418**–**419**, 115–124.

29 T. A. Bugrova, V. V. Dutov, V. A. Svetlichnyi, V. Cortés Corberán and G. V. Mamontov, *Catal. Today*, 2019, **333**, 71–80.

30 Y. Cheng, F. Zhang, Y. Zhang, C. Miao, W. Hua, Y. Yue and Z. Gao, *Cuihua Xuebao/Chinese J. Catal.*, 2015, **36**, 1242–1248.

Chapter 5

Reproducibility and Life Cycle Assessment of the One-pot Catalysts

5.1 Introduction

5.1.1 Catalyst deactivation and lifetime

More than 80% of industrial chemical processes use catalysts, either to improve the reaction rates or for on-purpose synthesis of certain products.[1] There are three "virtues" for judging the catalyst performance, activity, selectivity, and productivity which is related to catalyst lifetime.[2] Catalytic activity usually draws the highest interest in academic research areas. However, in industry, the productivity is often more important which is affected by catalyst deactivation. The deactivation causes catalysts to lose their catalytic activity and product selectivity.[1,2] The low selectivity implies wasted raw materials and the need for product separations, which are costly and with a high energy requirement. In addition, the catalyst deactivation also means short catalyst lifetime, which indicates the need for frequent catalyst replacement/regeneration which results in lost production time and increases the costs. Therefore, one of the drawbacks of industrial catalysts is the unavoidable deactivation during time on stream, accompanied by the loss in catalytic activity and product selectivity.[1] Hence, for the design and operation of a catalytic process, catalyst deactivation has to be addressed carefully.

It has been found that the catalysts lifetime and economy of process are mainly related to the catalyst deactivation.[3–5] However, catalyst deactivation depends on the different catalytic processes. Some catalysts decay in seconds, as in the case of cracking catalysts, while some others have lifetimes in the order of years as for ammonia catalysts (typically 5-10 years).[6] There are many intrinsic reactions and mechanisms that could cause catalyst deactivation, they are categorised into six major types:[1,7] (1) catalyst poisoning by strong chemisorption; (2) coking effect on catalyst surface; (3) thermal degradation and sintering; (4) side reactions that produce inactive sites; (5) vapor formation with catalyst phase; (6) attrition and cracking. Some of these processes lead to permanent deactivation while others might only cause a temporary loss of catalytic activity.

Coke formation is one of most common deactivation issues for catalytic process involving organic compounds and hydrocarbons. The coke formation in the presence of a catalyst is reported to be strongly dependent on the physicochemical properties of the catalysts, including the presence of functional groups — acid-base character, porosity, the presence of metal oxides and degree of the dispersion, type of support in the case of supported catalysts, incorporation of promoters and the particle size of the metal oxides. Since different reaction pathways are possible over differing catalysts, respective intermediates formed on the catalyst species will also differ.[7,8] Formation of coke on catalysts (especially on oxides) is principally a result of cracking of hydrocarbons which is catalysed by Lewis acid sites (Metal–O sites). Dehydrogenation and cyclisation reactions of carbocation intermediates formed on acid sites leads to deposition of coke. The cokes are generally regarded as a result of the corresponding cracking/condensation reactions of hydrocarbons.[6] Dehydrogenation reactions normally have carbocation intermediates which are formed on acidic sites. These hydrocarbons can react further to higher molecular weight polynuclear aromatics that condense as coke and/or cracking further to carbons.[7] They can chemisorb strongly

as a monolayer or physically adsorb in multilayers and in either case this leads to blockage of active sites, surfaces and pores on the catalyst causing a loss in catalytic performance as illustrated in Figure 5.1.[8–10]

Therefore, they will completely deactivate that particle. On the other hand, for mesoporous catalysts, coke can also plug mesopores such that access of reactants is denied to many active sites inside these pores.[8]



Figure 5.1. A general diagram of coke formation on the catalyst surface.

There are various strategies including the modulation of metal oxidation state, increasing metal dispersion, poisoning acid sites and using cofeeding streams that have been operated to reduce coke formation. In propane dehydrogenation with CO_2, it has been reported that the specific activity of Cr-based catalysts was strongly dependent on the Cr loading and the support material which is due to the structural and redox properties of the CrO_x species.[11] By keeping the same Cr loading, a decreased order of CrO_x/SiO_2 > CrO_x/ZrO_2 > CrO_x/Al_2O_3 > CrO_x/TiO_2 was observed for the catalytic activity.[12] On the other hand, because of the propane adsorption on M–O sites in metal oxides, the acid–base pairs of metal oxide dehydrogenation catalysts are deactivated owing to coke deposition. The acidic strength and the number of acidic sites are important parameters as a higher acidity of the catalyst can result in a faster deactivation of the catalyst. In general, a faster chemical reaction due to the stronger acidic sites can cause faster retention of coke precursors and coke molecules.[13] In the PDH reaction, strong adsorption of propylene has been reported that would cause

monolayer to multilayer coke growth on the Cr-based catalysts.[14,15] Therefore, the coking processes in the PDH reactions with metal oxide as acidic sites are significantly affected by propylene chemisorption.[16,17] Moreover, the higher density of active sites can increase the probability of successive chemical reactions among the reactants within the catalysts; hence, the faster coking rate.[4]

To inhibit the coke formation and increase the catalyst lifetime, co-feeding of gas molecules during the reaction was used to reduce the adsorption strength. In a PDH process with Pt-based catalysts, the adsorption strength of C_3H_6 on the surfaces was decreased by co-feeding with hydrogen. This process increased the energy barriers for deep dehydrogenation and coking processes, thus inhibiting them.[15] In addition, the co-feeding of CO_2 is found to increase the activity and decrease the coke production over the superior 5%Ga/HZSM-5 catalyst.[13]

It has been found that the catalytic deactivation of the catalysts was mainly influenced by the coke formation on the catalyst surface in Chapter 4. The surface carbon blocked the interaction and adsorption between propane and the metal oxides in the catalysts. Therefore, the propane dehydrogenation was being stopped, and the catalyst could no longer operate. Also, the TGA results for spent catalysts in Chapter 4 showed that by reducing the surface acidity, there is less coke formed on the catalysts (Figure 4.18).

The characterisation results (figure 4.15 and 4.19) of spent catalysts shown in Chapter 4 show clearly the coke deposition, mainly carbon, on the catalysts. However, the catalysts can be recovered back to the green/yellow colour, similar to its fresh state after oxidation at 300-400 °C under air after TGA tests. Therefore, the catalysts were regenerated by oxidation under air. The method for this is described below. The XRD results (Figure 4.19 (B)) shown in Chapter 4 indicate that the surface carbon has been removed after the regeneration process. It is possible to assume that the catalysts can recover their activity after the regeneration. In this chapter, we test the catalytic activity of the regenerated catalysts and their lifetime by repeating the regeneration process.

In fact, it has been considered to use CO_2 as oxidant to remove the surface coking based on the reverse Boudouard reaction (Chapter 3, 3.5). But it was found to show a CO_2 consumption peak at 800-1000 °C, indicating the removal of coke species after catalytic tests by CO_2 or during the dehydrogenation is probably not possible due to the lower PDH reaction temperature (550 °C).

5.1.2 Life cycle assessment (LCA)

Life cycle assessment (LCA) sometimes referred to as life cycle analysis, is an important environmental management tool developed since the 1960s.[18,19] It is defined as the systematic analysis for measuring the potential environmental impacts of products or services during their entire life cycle.[19,20] During a life cycle analysis, the potential environmental burdens and benefits will be evaluated throughout the entire life cycle of a product. The entire life cycle contains several stages including extraction of materials from the environment, followed by the resource and energy consumed through manufacturing of the product, use of the product, transportation, waste management (reuse, recycle or disposal) until the end-of-life.[19–22] The evaluation of products using LCA can be from the very beginning of the life cycle to the very end or to any life cycle stages in between.[19]

With the rapid increase in urban population, large development of industrial manufacturing, concern of environmental sustainability and global climate change, LCA becomes a very important and useful tool to help manufacturers or suppliers to analyse the contribution of the life cycle stages to the overall environmental load of products. Product manufacture can then find out how the design or production process choices will affect the sustainability of the products by comparing all major environmental impacts. It is their responsibility to ensure environmental sustainability (e.g. substantial improvement on the eco-efficiency and reduced greenhouse gas

emissions to benefit human health, ecosystems and resources) during the product stewardship and to be able to prioritise improvements in products or processes.[23]

In the past few decades, the International Organization of Standards (ISO) have contributed to the development of the LCA methodology which is in a fixed structure and is practised according to international standards (ISO) 14040 and there are four stages.[23–27] The first stage is called the goal and scope analysis to assess the extent of the product life cycle. The second and third stages include inventory and impact analysis. In these stages, the description of material and energy flows within the product system and especially its interaction with environment, through consumption of raw materials and emissions to the environment, will be measured. Then these results will be used for impact assessment. The indicator results of all impact categories are detailed in the third stage. The final, fourth, stage is interpretation of a life cycle which involves critical review, determination of data sensitivity, and result presentation.[21,23,25,27,28]

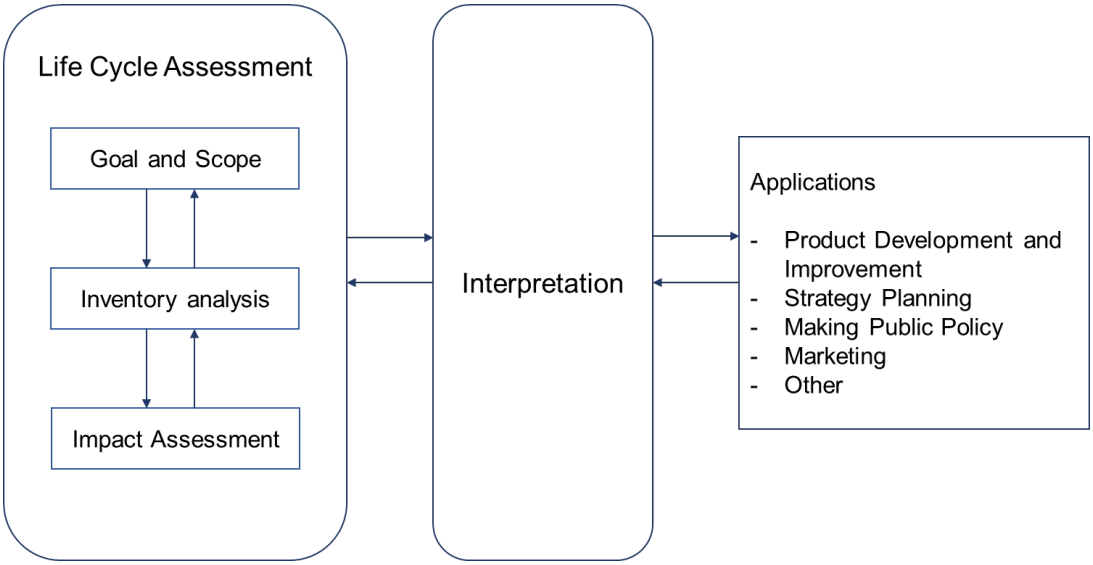


Figure 5.2. Stages of LCA based on ISO 14040.[23]

When undertaking a life cycle assessment of a product, the burdens imposed on the environment by human activities may be ascertained by accounting for the resources and energy consumed at each stage in the life cycle of a product and the resulting pollutants and wastes emitted should be addressed.[23] Once these are known, measures may be taken to mitigate the impact of the outputs on the environment.

LCA has been widely used and applied to the manufacture of many products and also in environmental areas,[24,25] for example, solid waste management, construction industry, food waste, plastic waste and also for international or national environmental studies.[24,25,29–31] For these studies, environmental impact, cost, and socially relevant unit process data are collected, impact indicators are selected, and overall sustainability is assessed.[21] For example, LCA analysis of biodiesel production with various feedstocks and catalysts has been performed. The LCA results by Sieira of biodiesel production from soybean, showed that the process can reduce about 99% equivalent CO_2 emission compared to the conventional biodiesel production.[32] 25% of CO_2 emissions can be reduced by using microalgae-produced biodiesel.[33] Life cycle

assessment (LCA) is a favourite approach to evaluate the environmental burdens of chemical manufacturing. For example, Zhao et al. quantitatively compared the energy consumption and greenhouse gas emissions per ton of propylene produced via different processes[34]. Xiang et al. evaluated the life-cycle environmental friendliness of propylene production by replacing oil feedstock with coal or natural gas.[35] In the development of ethylene production from shale gas, LCA helps to evaluate different synthesis route and procedures to reduce greenhouse gas (GHG) emissions, water consumption and energy consumption.[36] It shows that about 6-10% CO_2-equiv/kg ethylene can be saved by using a corn-stover-based pathway (stover is residual leaves, stalks, and cobs of corn plants) or a corn-grain-based pathway compared to ethylene produced via the shale-gas-based pathway.[36] Other researchers have examined the life cycle environmental impacts of ethylene manufacturing from biomass.[37–39] Besides, environmental impacts of ethylene produced from sugar cane, corn grain, corn stover, and naphtha were analyzed and compared.[40] The researchers also used LCA to evaluate the olefin production in Germany and indicated that olefin production via waste gasification is associated with significant benefits in terms of greenhouse gas emissions.[41] There are also LCA studies on propylene production processes to find the best green pathway.[42–44]

In general, Life cycle assessment (LCA) is the steady-state, global/regional, comprehensive and quantitative analysis of a product and/or process from its entire life cycle.[22] The LCA provides results that may be used to compare products and processes on common grounds and to make improvement for reducing environmental impacts. In a commercial area, LCA assists environmental assessments, such as ecolabeling, environmental product declarations, so-called carbon footprints and GHG accounting and management. It also aims to develop ecoefficiency for industrial ecology which tries to mimic the natural ecology process.[21]

5.2 Chapter Overview

Due to the global climate issues especially in carbon emission, the sustainability of product manufacture become more and more important. In our study on propane dehydrogenation, CO_2 has been chosen at the beginning as mild oxidant rather than O_2 to reduce the net carbon emission and provide a new carbon utilisation pathway. On the other hand, the development of the catalytic system for CO_2-PDH is not only to improve the catalyst's performance or efficiency, but also to reduce the overall energy consumption and carbon (CO_2) emission of the entire process. This will be related to the greenhouse gas (GHG) emission of chemical process and industrial manufacture. Therefore, during the research of the catalysts, whether the whole system would be able to achieve green and sustainable process or not is highly important and requires evaluation.[45]

During the CO_2-PDH, the catalyst deactivation becomes an important issue due to the side reactions and competing adsorption. This affects the sustainability of the whole process as we would need to change and produce the catalysts very often to keep the process running. Therefore, it would be better to keep the catalysts active or investigate if they can be regenerated. In Chapter 4, we have found out that the main reason for catalyst deactivation is coke formation on the catalyst surface. This will block the interaction between the active site and reactants.

In this chapter, the spent one-pot catalysts are recovered by a re-oxidation process to remove the surface cokes and hence recover their catalytic activity. This oxidation process is applied to remove the surface carbon formed from side reactions during the CO_2-PDH process which blocks the adsorption during the dehydrogenation process. This is then followed by catalytic activity tests to check their catalytic activity for CO_2-PDH after regeneration. In the final part of the chapter we discuss the life cycle assessment for the process with and without regeneration.

5.3 Experimental Methods

5.3.1 Regeneration process of spent catalysts and catalytic tests of regenerated catalysts

For a permanently deactivated catalyst, to recover the catalytic activity with standard regeneration procedures is difficult.[1] Fortunately, catalyst deactivation caused by the coking effect is usually reversible, and the surface coke can easily be removed by oxidation with air (O_2). Indeed, in most industrial processes, coke is typically burned off with air to reactivate the spent catalyst.[1] High temperature can lead to the sintering of the active component. Hence, the control of the burning temperature of coke is of great importance.[46]

The current regeneration methods are oxidation (using air, ozone and NO_x species), gasification (using carbon dioxide and water steam) and hydrogenation (using hydrogen). *Zhou et al* have summarised all regeneration methods to indicate how catalysts and their related processes can be further optimized. Catalyst type, coke property and location of the coke are important parameters that affect catalyst regeneration.[1] As noted above, there have been suggestions to remove coke using CO_2 via the reverse Boudouard reaction (3.5). However, the coke was found to hardly be removed by CO_2 at reasonable temperatures since the temperature of CO_2 consumption by the process appears at very high temperature (800 °C-1000 °C).[13]

In this chapter, the spent one-pot catalysts were treated under air with flow rate 20 ml/min for 3 hours at 400°C straight after the catalytic activity test in an M-R-10A fixed-bed micro reactor (Kun-Lun Yong-Tai Company, China) to remove the surface coke.

After the treatment, the catalysts were tested for their catalytic activity for CO_2-PDH under the same conditions as the tests for fresh catalysts. The performance of catalysts for propane dehydrogenation with CO_2 were examined at a temperature of

550 °C in a fixed-bed microreactor at atmospheric pressure for a period of 10 hours. The feedstock gases were a mixture of propane, carbon dioxide with mole ratio of C_3H_8: CO_2 = 1:3. Due to the instrument limitation noted in earlier chapters, the minimum stable gas flow rate is 25 mL/min. The emerging reaction products were analysed through a direct link to an on-line gas chromatograph (GC, Perkin Elmer, Clarus 580) with a flame ionization detector (FID) and a thermal conductivity detector (TCD). The catalysts were treated under these conditions for six cycles and there was regeneration between each cycle. The overall number of full regenerations – CO_2-PDH cycles was six for each catalyst.

5.4 Results and Discussion

5.4.1 The regeneration of the spent one-pot catalysts and their catalytic activity after regeneration

In Chapter 4, it was noted that the spent one-pot catalysts changed colour from green to black after the activity tests. The TGA in air of the spent catalysts shows a weight loss at 300-400°C (Figure 4.18) which suggests the presence of carbon which has been burnt during the analysis. This is also indicated by the XRD pattern with the typical graphitic peak at around 28º shown in Figure 4.16. (A). Notably, the catalysts' original green colour returned after the regeneration process. The carbon loss observed in our TGA experiments is consistent with the EDX analysis data between two one-pot catalysts. In addition, the carbon balance results of these catalysts shown in table 4.5 also indicated the formation of carbon on the catalysts' surfaces.

Based on the characterisation results (Figure 4.15 and Figure 4.19 (A)) of spent and regenerated catalysts (Figure 4.19 (B)) in Chapter 4, it was considered that the coking effect could be the main reason of the deactivation of catalysts. Figure 4.15 also showed that the carbon would be the main coking form as there isn't any other weight loss during TGA analysis. Hence, if the carbon deposition on the catalysts surface can be reduced or removed, the catalyst could be reactivated and able to carry out further propane dehydrogenation. Therefore, the spent one-pot catalysts were treated by air to remove the surface coke.

As mentioned above, the colour changed after the regeneration process, suggesting the carbon removal. After the regeneration process, the performances of regenerated catalysts for propane dehydrogenation with CO_2 were examined using the same experimental method and conditions as for fresh catalysts described in Chapter 2. The results for the 2Cr-ZrO_2 catalyst made by the one-pot method are shown in Figure 5.3.

It is known that the catalytic conversion of propane generally decreases during the dehydrogenation process as discussed in Chapter 4 due to the coking effect.

The conversion results show a consistent decrease in performance during each cycle of CO_2-PDH (regeneration is carried out between each cycle), i.e. for each cycle the performance decreases with elapsed time. In addition, the results also show that the propane conversion decreased as the catalyst undergoes more cycles of regeneration (numbers labelled on each bar). i.e. the performance at a given elapsed time is not recovered in subsequent cycles. Figure. 5.3. (B) shows the propylene selectivity and yield at the 6-hour reaction time during each of the six cycles separated by the regeneration processes and similar decreases are evident.

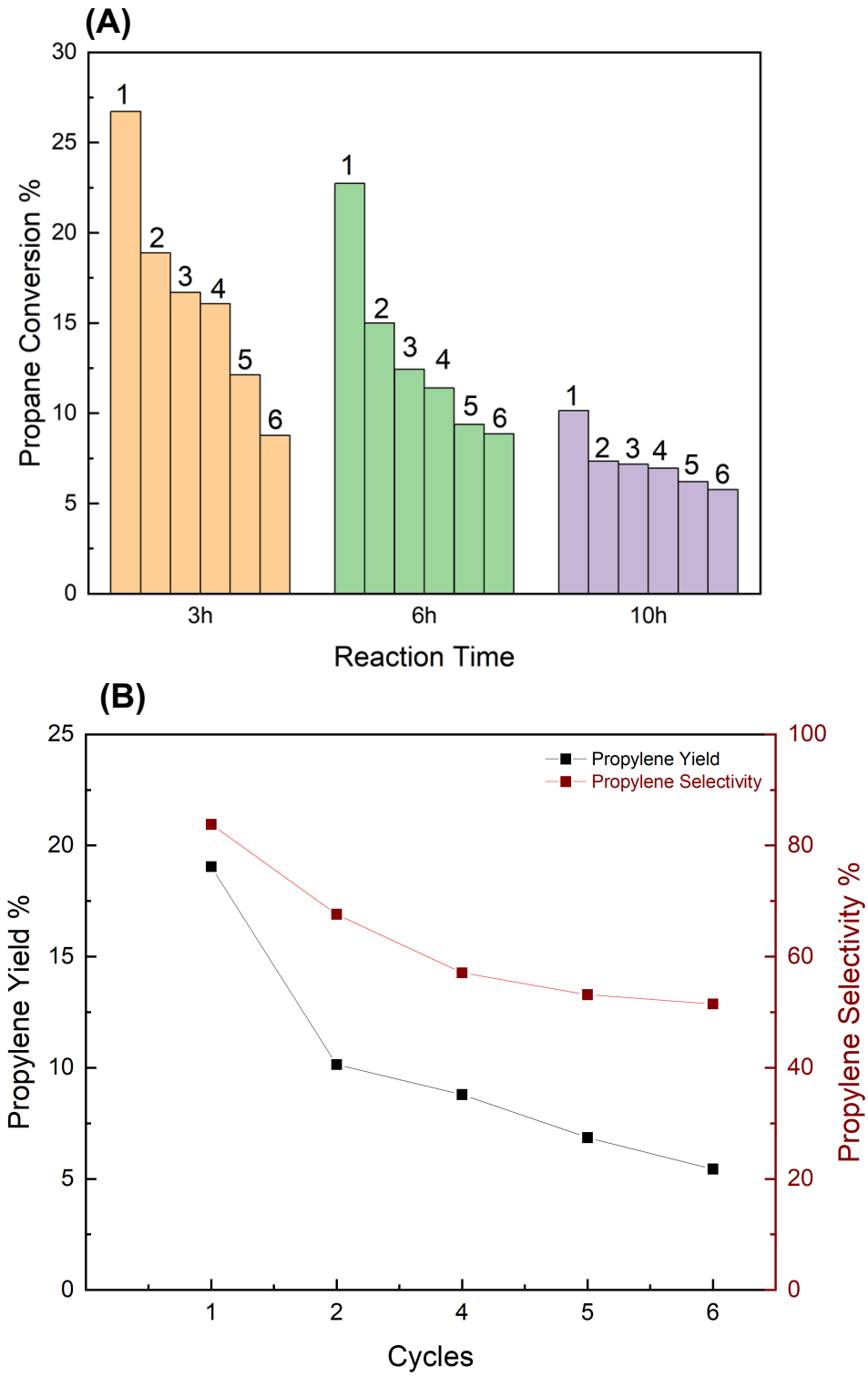


Figure 5.3. Results obtained for regenerated 2Cr-ZrO_2 catalyst (A) The propane conversions at reaction times of 3h, 6h and 10h during each of six cycles with regeneration between each cycle, (B) the percentage yield and selectivity of propylene after the treatments at the six-hour point during each cycle. (%Error: conversion: ± 2.1-4.3%, yield: ± 1.2-2.0%, selectivity: ± 0.2-1.6%)

These results in Figure 5.3 show that the activity of the 2Cr-ZrO_2 catalysts decreases after each cycle of regeneration process. It is noted that the catalytic activity can only be partially recovered after each regeneration. The propane conversion quickly decreases after the first regeneration cycle and there is a gentler decrease from the second to the sixth cycle. After 10 hours of reaction, results suggest a small difference in activity between each cycle. The propane conversion falls from 22.7% in the first run at 6h to 8.5% in the sixth run. The propylene selectivity decreases as well, from 83.8% to 51.5%. Clearly, the spent catalysts can be partially regenerated by combustion of the surface coking: the performance is enhanced at the start of each cycle, after the regeneration process, compared with the end of the previous cycle. So the catalysts were still able to catalyse the propane dehydrogenation reaction to some extent, after regeneration, although the deactivation is not completely reversed by the regeneration process. It could suggest that coking formation may not be the only cause of the catalysts' deactivation. In addition to the coking effect, loss of activity through sintering is possible, and this could also occur during the exothermic regeneration step. Therefore, even though the catalysts recover most of their activity after each reaction–regeneration cycle, the loss of activity due to the sintering or catalyst cracking during the regeneration process is not entirely reversible. Sintering is also one of the main factors that causes catalyst deactivation induced by loss of catalytic surface area as small particles aggregate to form larger ones.[10] Moreover, the other issue in air regeneration is avoiding hot spots or overtemperatures which could further deactivate the catalyst.[7] For example, McCulloch suggested that in the regeneration of hydrotreating catalysts, the temperature should be kept at below 450 °C. In that case it was to avoid several undesirable processes: γ- to α-alumina conversion, MoO_3 sublimation, and cobalt or nickel aluminate formation which would occur at 815, 700, and 500-600 °C.[47]

In Chapter 4, the XRD patterns of regenerated catalysts in Figure 4.16 do not show any obvious structural change after the first cycle of regeneration of the catalysts. A possible future experiment would be to perform X-ray diffraction during the full series of catalysis and regeneration cycles, to investigate the effect of more and more regeneration cycles on crystallinity and show whether there was crystallisation of phases. However, it should be noted that the information from XRD for these samples was rather limited. In addition, it has been suggested that due to the reducibility of some metal oxides, the metal oxides can be reduced to the lower oxidation state or even the metallic state during the reactions, which may contribute to the deactivation.[48] However in this case reduction of Cr to the metal is not favourable. In theory, considering the facile redox of CrO_x at high temperatures, it is generally accepted that CO_2-PDH over supported CrO_x catalysts may follow the redox mechanism shown in Figure 4.12. In this case, the activated propane molecules abstract the active oxygen over Cr species with a higher oxidation number to give propylene and water.[11] Simultaneously, Cr(III) is re-oxidised by the activated CO_2 molecules to complete the redox cycle of Cr species with the release of CO molecules. As shown in the Table 4.5 in Chapter 4, the amount of Cr(VI) is decreased in spent catalysts, which means Cr(VI) was reduced to the Cr(III) during the dehydrogenation process but not fully re-oxidised back to Cr(VI), or the direct PDH reaction occurs as the proposed PDH mechanism showed in Figure 3.2. Hence the full redox cycle of Cr species might not occur during the propane dehydrogenation process. Besides coke formation, the reduction of Cr(VI) to Cr(III) is responsible for deactivation of chromium-based catalysts. Therefore, whether the reduced Cr species could be fully re-oxidised with oxygen during regeneration as the amount in the fresh catalysts is unknown. The continuous net reduction of Cr(VI) may be what causes the general decrease of propane conversion and propylene yield along each cycle. Thus, deactivation caused by regeneration is another deactivation phenomenon.[48] More characterisations on the oxidation states of Cr species, such as XPS, will be required for further study.

According to the propane dehydrogenation mechanisms on the metal oxides, the supports, promoters and coverage of the reactants can therefore help inhibit the deactivation of metal oxide-based catalysts.[48] Previously, it has been investigated that by adding Ca (as CaO) as promoter, the Cr-based one-pot catalyst showed a better and more stable catalytic performance compared with the non-promoted catalyst in Chapter 4. In addition, the Ca-promoted catalyst also shows less coking on the catalyst surface due to the lower surface acidity. The reproducibility of the 2Cr-Ca/ZrO_2 catalyst has also been tested under regeneration cycles. The results in Figure 5.4 show an increase in propane conversion and propylene yield after the first five cycles. The propylene selectivity was kept stable and didn't show many changes after each cycle.

It is very interesting that instead of propane conversion and propylene yield decreasing with each regeneration cycle as found for the Ca-free catalyst, it shows the increase in these two aspects in the first five cycles. The propane conversion increased from 10.4% after the first cycle to 30.6% after the fifth cycle. The propylene yield increased from 5.4% to 20.3% with a constant propylene selectivity around 82-85%. It is not quite clear why the results are so different between the Ca-promoted and non-promoted catalysts and no literatures seem to have reported similar results. It is shown in the previous investigations in Chapter 4 that the Ca-promoter produced good catalytic performance due to there being fewer acidic sites.[49]

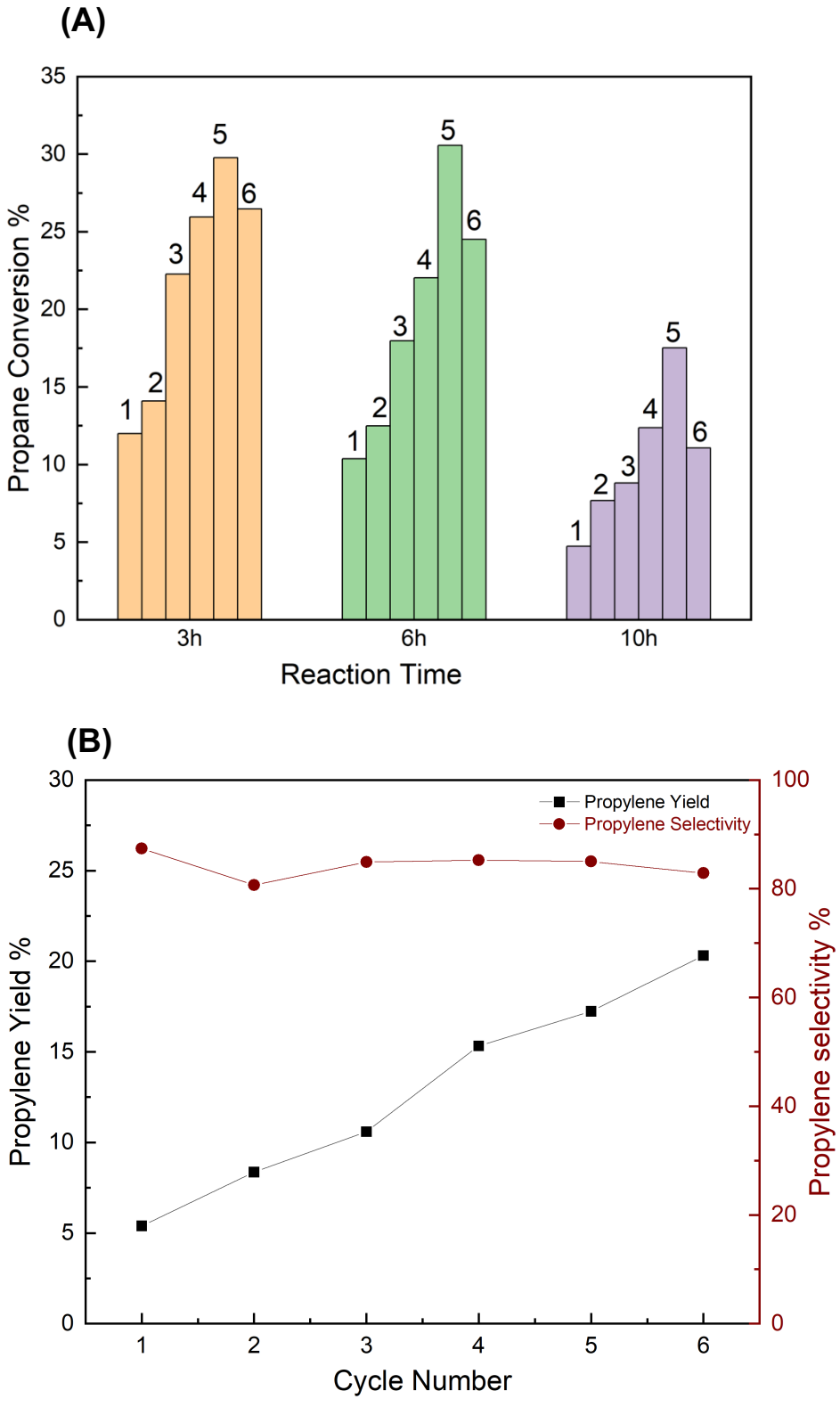


Figure 5.4. (A) The propane conversions rate at reaction time 3h, 6h and 10h after 6 cycles of regeneration, (B) the percentage yield and selectivity of propylene after the treatments using 2Cr-Ca/ZrO_2. (%Error: conversion: ± 1.5-3.1%, yield: ± 0.8-1.7%, selectivity: ± 0.2-0.8%)

In fact, the acidic sites could affect coke removal during regenerations.[1] Jong's group has reported the regeneration of coked HZSM-5 ethylbenzene conversion catalysts in air. They found that coke deposited in the inter-crystalline channels near the acid sites was removed prior to that on the external surface.[50] Guisnet et al. also showed similar results showing that increase the density of acid sites could rapid the rate of coke oxidation.[51] Moreover, coke located close to the metal or metal oxides, which are recognised as acidic sites, is much easier to remove, while coke located on the support requires longer regeneration time and higher temperatures to be removed.[52] In this case, we can predict that, although the regeneration of the spent catalysts removes most of the surface coke, there might still be a small amount of carbon remaining and possible to act as activated carbons, which are possible active sites for oxidative PDH.[48]

In the previous study, the XRD pattern in Figure 4.19 suggests the presence of some deposited crystalline graphitic carbon in the spent catalyst and the activated carbon is known as a crude form of graphite. Dai et al. has discussed the regeneration process of Co/Al_2O_3 catalyst for propane dehydrogenation.[53] They said that the regeneration process not only includes the removal of large amounts of coke species, but the redox cycle of metal oxide species also occurs on the catalyst surfaces. In my research, such redox process of surface Cr species presumably determines the extent to which the catalytic activity of the regenerated catalyst can recover to the initial level before the next reaction run. During the regeneration process, there may be a trend to form Cr sites in a locally stable structure containing Cr, Ca and Zr. This may make the surface structure more stable and active for CO_2-PDH.

In conclusion, to regenerate coked catalysts with air combustion as used in this chapter is often the preferred and most practical route. However, high exothermicity can easily cause overheating, leading to metal sintering, and catalyst degradation. The work in this chapter has shown that the catalytic activity of spent catalysts can be recovered

through combustion of the surface cokes, which is considered to be the main cause of catalysts deactivation. But the extent to which this is possible depends on the catalytic system. After the regeneration cycle followed by the CO_2-PDH process, both spent one-pot catalysts showed the recovery of their catalytic activity for CO_2-PDH.

The spent 2Cr-ZrO_2 catalyst showed overall decrease in propane conversion, propylene yield and selectivity after each regeneration-PDH cycle. These results suggested that even though the coke can be at least partially removed to recover the catalyst's performance, there is some irreversible deactivation with more and more regeneration cycles. Therefore, developing an efficient but milder regeneration method is of particular interest. The other one-pot catalyst, 2Cr-Ca/ZrO_2 showed an increase in catalytic performance in the first five regeneration cycles and started decrease from the sixth one. However, the reasons for this observation require further investigation. We could assume that the alkaline CaO promoter might play a very important role during the regeneration process, especially affect the surface acidity of the catalyst. This may account for the difference in behaviour.

5.4.2 Environmental and sustainable considerations of the one-pot catalysts

Referring to Chapter 1, the global propylene demand has increased because propylene is an extreme important intermediate chemical and building block of the chemical industry and propylene is widely used in the synthesis of polypropylene, acrylonitrile, and other valuable chemical products.[54] Most propylene is produced by traditional routes of light oil steam cracking and fluid catalytic cracking in petrochemical plants, which will be gradually limited by increasingly scarcity of crude oil resources.[55] With the increasing demand for propylene, the traditional processes have been unable to meet the demand of propylene market. Propane dehydrogenation (PDH) for

propylene production has broad practical prospect, which has received extensive attention worldwide.[54,56]

In addition to environmental and sustainable issues that have received increasing attention, a comprehensive analysis simultaneously considering technical, economic, and environmental aspects must be conducted. The current most widely used industrial PDH plants and technologies are CATOFIN and OLEFLEX.[56] However, both techniques require large amounts of energy input to reach the high temperature as the dehydrogenation is an endothermic process (1.1) and the heating causes a large amount of CO_2 emission. In comparison, the PDH in our research uses CO_2 as a mild oxidant, which is more environmentally friendly, sustainable and potentially able to decrease net carbon dioxide emission in general. This is because instead of only producing CO_2 and increasing the CO_2 emission, CO_2-PDH consumes the CO_2 and thus reduces the overall CO_2 emission. Rigamonti et al. reported that CO_2 capture from industrial flue gas is 0.70 kg CO_2 equivalent per kg of CO_2 less than the direct propane dehydrogenation.[57] The molecular transformation of carbon dioxide into value-added products such as CO is also an important goal for modern chemistry.[58] In the work presented here it has been shown that the propylene selectivity and propane conversion can reach similar levels as in the CATOFIN and OLEFLEX processes. However, as the results shown in this work are all on the lab scale, how the behaviour would change as we enlarge into an industrial scale requires further study.

During the investigation of one-pot catalysts, the determination of catalytic performance has been focused on propane conversion and propylene yield during CO_2-PDH process. The sustainability of the catalysts including the preparation process, also needs consideration. Based on the ISO 14040 for LCA, catalysts will be counted in the inventory stage as they can be considered as raw material for the process and the energy consumed to making them has to be considered. Hence the catalyst performance, with any specific environmental benefit of such performance

enhancement (such as total energy consumption and CO_2 emission), the cost of disposal of spent catalysts and manufacturing wastes are also very important.[45]

Edwards's group in collaboration with that of Sir David King. introduced the Catalyst Sensitivity Index (CSI) in 2015 which is an entirely new measurable and comparable index to show how the efficiency or performance of a heterogeneous catalyst will directly impact the carbon emission across industrial and manufacturing technologies.[45] CSI is considered as a factor between catalytic efficiency (CE) of the entire manufacturing or industrial process and the total fossil fuel energy consumptions which is related to the CO_2 emission. Therefore, for a catalytic process, the change in CE compared with the current best-performing catalyst will result in a CSI factor. The CE is catalyst efficiency and given by the following expression:

$$\text{Catalyst efficiency CE} = (Cn/Co + Sn/So + Ln/Lo)/3 \qquad (5.1)$$

where Cn is the conversion of the new or improved catalyst, Co is the conversion of the benchmark catalyst, which representing the best-performing catalyst to-date (CE for the benchmark catalyst = 1.0); Sn is the new or improved catalyst selectivity, and So is the benchmark catalyst selectivity; Ln is the life time of the catalyst and Lo is the benchmark catalyst life time.

At present, the CO_2-assisted dehydrogenation of propane has no industrial application. Therefore, there will be many assumptions when using the CSI to evaluate the one-pot catalysts. However, if we compare catalysts from the two different preparation methods used in this thesis, impregnation and one-pot synthesis, and set CE=1.0 for impregnation catalysts, i.e. 2Cr-Ca/ZrO_2. As shown in Chapter 4, the one-pot catalyst showed a better catalytic performance (higher and stable propane conversion, higher propylene yield and selectivity) compared with impregnation catalyst overall. Comparing the impregnated 2Cr-Ca/ZrO_2 catalysts and the one-pot catalyst, the

catalyst efficiency of one-pot 2Cr-Ca/ZrO_2 has CE about 1.18-1.3. During the CE calculation, there are several assumptions that have been made:

1. The lifetime of two kind of catalysts are the same;

2. The propane conversions data at three different reaction times, 3h, 6h and 10h, being used for the calculation;

3. The average propylene selectivity was calculated for CE.

As both catalysts were used under the same conditions through the same reaction route, the total CO_2 emission due to the process energy be assumed as the same. Hence, one-pot catalysts, especially the Ca-promoted catalysts would have a lower CSI value than the equivalent impregnation catalysts. Compared with O_2-PDH, CO_2-PDH is able to utilise CO_2 as feedstock and converts it into CO which is an important platform chemical. This CO_2 utilisation process can be believed as a more sustainable process and able to reduce total carbon emission.

The Catalyst Sensitivity Index (CSI) with assist life cycle assessment study would be able to evaluate what efficiency gains or energy and CO_2 emission reductions could be expected with higher efficiency catalysts. This approach will help to identify catalytic processes where the energy/CO_2 emissions improvement gain would be the greatest from higher efficiency in operating catalysts.

5.5 Conclusion

It has been found out that one of the main issues that causes catalyst deactivation is surface coke formation. This coke presents mainly carbon deposition on catalyst surfaces that blocks the catalytic active sites and cause them to lose their catalytic activity for CO_2-PDH. Therefore, to recover their activity, the spent catalysts were regenerated by combustion of the surface carbon deposit under air. The results show that both 2Cr-ZrO_2 and 2Cr/Ca-ZrO_2 catalysts can recover their catalytic activity by regeneration process. The 2Cr-ZrO_2 catalyst shows a general decrease of propane conversion, propylene yield and selectivity after each regeneration cycle. These decreases indicate that there are other deactivation issues such as catalyst sintering and cracking apart from coking formation, which cannot be reversed by the regeneration process. However, 2Cr/Ca-ZrO_2 shows an opposite result with an increase in propane conversion and propylene yield in the first five cycles. In fact, these unexpected results are not fully understood yet. More characterisation of regenerated catalysts especially after each cycle will be required for further study.

The regeneration process helps to extend the catalyst lifetime and reduce the time and energy consumption for preparing and changing new catalysts to keep the PDH process running, providing a more sustainable and green process in some aspect. However, the regeneration process requires energy input, and the overall cost of adding the regeneration process should be considered: for example, by burning off the surface coking, CO_2 will be produced.

Catalysts continue to have an enormous beneficial impact on the chemical, energy, manufacturing and environmental industries. Often the performances of catalysts are characterised by their activity, selectivity and life-time (or stability). However, the precise association—and with that the quantification—of a catalyst performance with any specific environmental benefit of such performance enhancement, such as total

energy consumption and CO_2 emission footprint, has not previously been correlated. Therefore, it was not always clear which catalytic process to target in making the most significant environmental improvement in developing and applying a heterogeneous catalyst to reduce total energy usage and concomitant CO_2 emissions. Edwards et al. have developed the CSI. This is a new concept for correlating the industrial process energy input and CO_2 emission saving with a measurable improvement in CE. [45] They suggested using this concept in combination with a complete LCA methodology for analysing catalytic conversion processes, to assist scientists and engineers in the design of high efficiency catalysts to reduce total energy consumption and total CO_2 emissions in manufacturing processes.

References

1 J. Zhou, J. Zhao, J. Zhang, T. Zhang, M. Ye and Z. Liu, *Chinese J. Catal.*, 2020, **41**, 1048–1061.

2 S. L. Scott, *ACS Catal.*, 2018, **8**, 8597–8599.

3 M. Guisnet and P. Magnoux, *Stud. Surf. Sci. Catal.*, 1994, **88**, 53–68.

4 M. S. Ahmad, C. K. Cheng, P. Bhuyar, A. E. Atabani, A. Pugazhendhi, N. T. L. Chi, T. Witoon, J. W. Lim and J. C. Juan, *Fuel*, 2021, **283**, 118851.

5 G. F. Froment, *Stud. Surf. Sci. Catal.*, 1980, **6**, 1–19.

6 C. H. Bartholomew, *Appl. Catal. A Gen.*, 2001, **212**, 17–60.

7 M. D. Argyle and C. H. Bartholomew, *Catalysts*, 2015, **5**, 145–269.

8 J. Grams and A. M. Ruppert, *Catalysts*, 2021, **11**, 1–24.

9 K. Wittich, M. Krämer, N. Bottke and S. A. Schunk, *ChemCatChem*, 2020, **12**, 2130–2147.

10 D. Pham Minh, X. H. Pham, T. J. Siang and D. V. N. Vo, *Appl. Catal. A Gen.*, 2021, **621**, 118202.

11 J. Wang, Y. H. Song, Z. T. Z. W. Liu and Z. T. Z. W. Liu, *Appl. Catal. B Environ.*, 2021, **297**, 120400.

12 G. Li, C. Liu, X. Cui, Y. Yang and F. Shi, *Green Chem.*, 2021, **23**, 689–707.

13 Y. Zhang and M. Aly, *Appl. Catal. A Gen.*, 2022, **643**, 118795.

14 M. Guisnet and P. Magnoux, *Appl. Catal. A Gen.*, 2001, **212**, 83–96.

15 Y. Dai, Y. Wu, H. Dai, X. Gao, S. Tian, J. Gu, X. Yi, A. Zheng and Y. Yang, *J. Catal.*, 2021, **395**, 105–116.

16 Z. Han, S. Li, F. Jiang, T. Wang, X. Ma and J. Gong, *Nanoscale*, 2014, **6**, 10000–10008.

17 T. Wang, F. Jiang, G. Liu, L. Zeng, Z. J. Zhao and J. Gong, *AIChE J.*, 2016, **62**, 4365–4376.

18 生命周期评估 (Life Cycle Assessment), https://baike.baidu.com/item/生命周期评估/8286658?fromtitle=Life Cycle Assessment&fromid=11298535&fr=aladdin, (accessed 16 August 2022).

19 L. Golsteinjn, Life Cycle Azsessment (LCA) explained, https://pre-sustainability.com/articles/life-cycle-assessment-lca-basics/, (accessed 16 August 2022).

20 Sphera's Editorial Team, What is Life Cycle Assessment (LCA)?, https://sphera.com/glossary/what-is-a-life-cycle-assessment-lca/, (accessed 16 August 2022).

21 N. Haque, in *Future Energy: Improved, Sustainable and Clean Options for Our Planet*, Elsevier, 2020, pp. 633–647.

22 S. H. Farjana, M. A. P. Mahmud and N. Huda, *Life Cycle Assessment for Sustainable Mining*, Candice Janco, 2021.

23 I. V. Muralikrishna and V. Manickam, in *Environmental Management*, Elsevier, 2017, pp. 57–75.

24 H. Khandelwal, H. Dhar, A. K. Thalla and S. Kumar, *J. Clean. Prod.*, 2019, **209**, 630–654.

25 A. Azapagic and R. Clift, *Comput. Chem. Eng.*, 1999, **23**, 1509–1526.

26 T. Terlouw, C. Bauer, L. Rosa and M. Mazzotti, *Energy Environ. Sci.*, 2021, **14**, 1701–1721.

27 P. R. Yaashikaa, P. S. Kumar and S. Karishma, *Fuel*, 2022, **316**, 123379.

28 K. Walter, *Environ. Sci. Pollut. Res.*, 1997, **4**, 223–228.

29 H. Lei, L. Li, W. Yang, Y. Bian and C. Q. Li, *J. Build. Eng.*, 2021, **44**, 103374.

30 J. Laso, M. Margallo, I. García-Herrero, P. Fullana, A. Bala, C. Gazulla, A. Polettini, R. Kahhat, I. Vázquez-Rowe, A. Irabien and R. Aldaco, *Waste Manag.*, 2018, **80**, 186–197.

31 M. G. Davidson, R. A. Furlong and M. C. McManus, *J. Clean. Prod.*, 2021, **293**, 126163.

32 P. Sieira, *Am. J. Chem. Eng.*, 2015, **3**, 25.

33 P. K. Campbell, T. Beer and D. Batten, *Bioresour. Technol.*, 2011, **102**, 50–56.

34 Z. Zhao, Y. Liu, F. Wang, X. Li, S. Deng, J. Xu, W. Wei and F. Wang, *J. Clean. Prod.*, 2017, **163**, 285–292.

35 D. Xiang, S. Yang, X. Li and Y. Qian, *Energy Convers. Manag.*, 2015, **90**, 12–20.

36 M. Yang, X. Tian and F. You, *Ind. Eng. Chem. Res.*, 2018, **57**, 5980–5998.

37 D. Humbird, R. Davis, L. Tao, C. Kinchin, D. Hsu, A. Aden, P. Schoen, J. Lukas, B. Olthof, M. Worley, D. Sexton and D. Dudgeon, *Process design and economics for conversion of lignocellulosic biomass to ethanol*, 2011, vol. 303.

38 A. Mohsenzadeh, A. Zamani and M. J. Taherzadeh, *ChemBioEng Rev.*, 2017, **4**, 75–91.

39 J. Hong, Y. Zhang, X. Xu and X. Li, *Biomass and Bioenergy*, 2014, **67**, 304–311.

40 M. K. Patel, M. Crank, V. Dornburg, B. Hermann, A. L. Roes, B. Hüsing, L. S. van Overbeek, F. Terragni and E. Recchia, *The BREW Project - Medium and*

Long-term Opportunities and Risks of the Biotechnological Production of Bulk Chemicals from Renewable Resources - The Potential of White Biotechnology, 2006.

41 F. Keller, R. P. Lee and B. Meyer, *J. Clean. Prod.*, 2020, **250**, 119484.

42 L. Lv, G. Song, X. Zhao and J. Chen, *Sci. Total Environ.*, 2021, **799**, 149451.

43 H. Kim, B. Lee, D. Lim, C. Choe and H. Lim, *Green Chem.*, 2021, **23**, 7635–7645.

44 D. Liu, R. V Chaudhari and B. Subramaniam, *ACS Sustain. Chem. Eng.*, 2020, **8**, 5140–5146.

45 T. Xiao, T. Shirvani, O. Inderwildi, S. Gonzalez-Cortes, H. AlMegren, D. King and P. P. Edwards, *Top. Catal.*, 2015, **58**, 682–695.

46 Z. Lian, C. Si, F. Jan, S. Zhi and B. Li, *ACS Catal.*, 2021, **11**, 9279–9292.

47 D. C. McCulloch, in *Applied Industrial Catalysis*, ed. B. E. Leach, Academic Press Inc., New York, 1983, pp. 69–121.

48 S. Chen, X. Chang, G. Sun, T. Zhang, Y. Xu, Y. Wang, C. Pei and J. Gong, *Chem. Soc. Rev.*, 2021, **50**, 3315–3354.

49 Y. Gao, X. Jie, C. Wang, R. M. J. Jacobs, W. Li, B. Yao, J. R. Dilworth, T. Xiao and P. P. Edwards, *Ind. Eng. Chem. Res.*, 2020, **59**, 12645–12656.

50 S. J. Jong, A. R. Pradhan, J. F. Wu, T. C. Tsai and S. Bin Liu, *J. Catal.*, 1998, **174**, 210–218.

51 K. Moljord, P. Magnoux and M. Guisnet, *Top. Catal.*, 1995, **121**, 245–259.

52 A. T. Aguayo, J. Ereña, I. Sierra, M. Olazar and J. Bilbao, in *Catalysis Today*, 2005, vol. 106, pp. 265–270.

53 Y. Dai, J. Gu, S. Tian, Y. Wu, J. Chen, F. Li, Y. Du, L. Peng, W. Ding and Y. Yang, *J. Catal.*, 2020, **381**, 482–492.

54 D. Xiang, P. Li and X. Yuan, *J. Clean. Prod.*, 2022, **367**, 133024.

55 I. Kainthla, G. V. R. Babu, J. T. Bhanushali, K. S. R. Rao and B. M. Nagaraja, *J. CO2 Util.*, 2017, **18**, 309–317.

56 H. A. Maddah, *Am. Sci. Res. J. Eng. Technol. Sci.*, 2018, **45**, 49–63.

57 M. G. Rigamonti, M. Shah, T. G. Gambu, M. Saeys and M. Dusselier, *ACS Catal.*, 2022, **12**, 9339–9358.

58 J. Artz, T. E. Müller, K. Thenert, J. Kleinekorte, R. Meys, A. Sternberg, A. Bardow and W. Leitner, *Chem. Rev.*, 2018, **118**, 434–504.

Chapter 6

Conclusions and Outlook

6.1 Catalyst Development for CO_2-PDH

When looking back my four-year study on the development and investigation on heterogeneous catalysts for propane dehydrogenation using CO_2, the properties of catalysts and their catalytic performance are the things that drew the most attraction during the research. CrO_x-based catalysts are known as some of the best catalysts for propane dehydrogenation and have been extensively investigated. ZrO_2 is also widely used as a support for heterogeneous catalysts. Hence, my project was conceived to continue development and investigation on this important class of material.

Firstly, it has been found out that different metal oxides can act as promoters which can have large effects on the catalytic performance of CrO_x-based catalysts.[1] Therefore, different transition metals were chosen as promoters added to the Cr-based catalysts and their catalytic performances in CO_2-PDH have been compared. The results indeed showed the different abilities of these promoters. Ca, as a Group 2 metal was chosen due to the basicity of its oxide which is able to control the acidity and basicity on the catalyst surface. In Chapter 3, we have reported the catalytic performance of several metal oxide-promoted catalysts. Ca-promoted catalysts showed a better performance than the catalyst without promoter and other transition-metal-oxide-promoted catalysts. This would be a good direction for further research and investigations on the dehydrogenation process. Then, based on the study and

reading of previous related literatures, we tried a new preparation method for CrO_x-based catalysts, named 'One-pot Synthesis'.

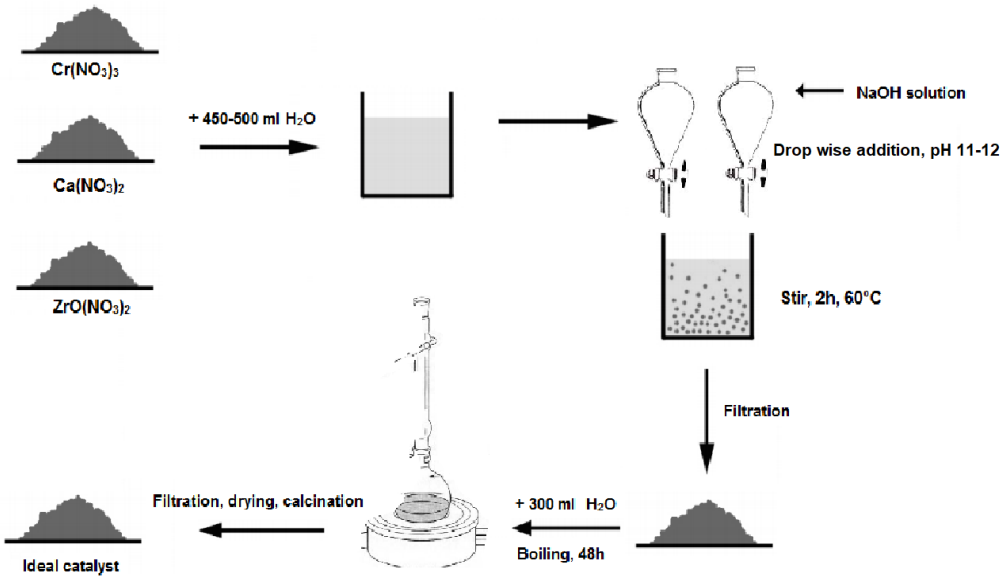


Figure 6.1. The experimental procedures diagram of the one-pot synthesis.

The different preparation method in which the support and the CrO_x were co-precipitated presented a new catalytic system with different surface properties and structure with a good catalytic performance compared with impregnation method. The results in Chapter 4 highlight the attractiveness of this one-pot synthesis method, which produced stable and active catalysts for this dehydrogenation reaction using CO_2. The one-pot synthesis method resulted in a different catalyst morphology and crystal structure and a greater Cr(VI) to Cr (III) ratio compared to the catalyst prepared via the conventional impregnation method as shown in Table 4.2. This synthetic route resulted in a marked enhancement in the CO_2 dehydrogenation of propane with high and stable propylene selectivity. The 2Cr/Ca-ZrO_2 has the best catalytic performance. In CO_2-PDH reaction, it helped the process to reach 18% of the total propane converted to get propylene 20%. The yield of propylene was about 20% with over 90% selectivity after

2 hours. After 10-hour reaction, the propane conversion reduced to about 10%, 15% product yield but with still about 93% propylene selectivity. All these results are calculated by equations 4.1, 4.2 and 4.3, shown in Table 4.4 in Chapter 4. In a comparison of 2Cr-ZrO_2 and 2Cr/Ca-ZrO_2 prepared by impregnation method, both catalysts show a rapid drop in propane conversion after 30 min of the reaction and a continuous decrease with further reaction. The 2Cr/Ca-ZrO_2 in Chapter 3 shows a slightly higher propane conversion, higher propylene selectivity and better stability compare with 2Cr-ZrO_2. But in general, the impregnation catalysts didn't performance as well as the one-pot catalysts.

Furthermore, for sustainable, environmental, and economic aspects, it is also very important to improve the catalyst efficiency during the reaction. In other words, to keep the system catalytically active for a longer time. This will also lower the initial costs and be more profitable in an industrial context. For this reason, a process that would recycle and regenerate the spent catalysts has been developed and discussed in Chapter 5. By re-oxidising the spent catalysts (remove the surface coking), they can be reused as "fresh" catalysts with good propane conversion and propylene selectivity. Due to the catalyst sintering or cracking which lead to some irreversible catalyst deactivation, the catalysts often cannot attain their initial catalytic ability after each regeneration cycle. In investigating catalyst regeneration, the catalytic performances of two regenerated one-pot catalysts have been studied. The results in Figures 5.3 and 5.4 indicate that the spent catalysts can recover their catalytic performance for CO_2-PDH by combustion of the surface coking: the catalytic performance is better with better propane conversion and propylene yield at the start of each cycle after the regeneration process, compared with the end of the previous cycle. This behaviour depended on the catalyst system. The 2Cr-ZrO_2 catalyst showed the decrease in propane conversion and yield not only along with the reaction time but also with the regeneration cycles. The propane conversion falls from 22.7% at 6h of dehydrogenation process after the first

regeneration to 8.5% in the sixth run. The propylene selectivity decreases from 83.8% to 51.5% and the yield dropped from about 20% to 5% after six cycles. However, the propane conversion of 2Cr-Ca/ZrO_2 shows an increase from 10.4% to 30.6% from the first cycle until the fifth cycle. The propylene yield increased from 5.4% to 20.3% with a constant higher propylene selectivity around 82-85%. We predict and assume that the activated carbon could be present in the catalytic system after regeneration and this might help improve the dehydrogenation reaction. There have been studies on PDH using activated carbon as a support.[2,3] More investigation and characterisation are planned for the activated and non-activated catalysts including TGA in air to follow the amounts of C deposited. The planned tests could also include addition of activated carbon to the catalyst to check if this improves the propane conversion, propylene yield and selectivity. In addition, under such oxidative conditions, solid carbon also could be partially or completely gasified to regenerate the catalyst's active surface.[4] Therefore, such reaction tests that check whether the carbon added and burn off would have effects on the catalysts or not would be preferred in further studies.

In this thesis, efforts have been made to improve the performances of CrO_x-based catalysts by changing preparation method and adding promoters. However, further improvements with lower Cr metal loadings or using other transition metals in order to reduce deactivation rates are highly desirable. Research on alternative catalysts to conventional metal and metal oxide-based catalysts remains a great challenge. Catalysts containing other metal oxides such as those of Co and Ga have been widely developed with the expectation that they could be superior alternatives to CrO_x-based catalysts.[1] However, their catalytic performances are still unsatisfactory compared with the CrO_x-based systems. In addition, different types of supports, promoters and preparation methods significantly influence the catalyst structures. Therefore, developing novel efficient methods to further improve their dehydrogenation performance is required.

Moreover, advanced characterisation and deep and detailed discussion of the nature of the active sites and reaction mechanisms during dehydrogenation process and regeneration process are still inadequate. In situ characterisation techniques and spectroscopy techniques should be encouraged and operated. These characterisation methods, such as XRD, XPS, Raman spectroscopy, would help to understand the surface and structural information of regenerated catalysts. Metal oxide-based catalysts have various species on their surfaces. For example, it is expected that there are various kinds of Cr species on the surface of the CrO_x-based catalysts, which makes it challenging to identify the actual active sites, especially under PDH reaction conditions. In situ X-ray absorption near edge spectroscopy (XANES) measurements can be used to conducted in order to identify the local environment of the metals under reaction conditions.[5] In-situ Diffuse reflectance infrared Fourier transform spectroscopy (DRIFTS) has been widely used in heterogeneous catalytic reactions in order to get insights into the catalytic reaction mechanism. It is one of the most powerful charaterisation technologies for identifying the adsorption species and intermediates on catalysts surface during the reactions.

Based on the results shown in Chapter 5, the regeneration of catalytic activity through combustion of the cokes can be used to regenerate the catalysts, but the extent to which this is possible depends on the catalytic system. Therefore, developing an efficient but milder regeneration method is of particular interest. Finally, further studies should examine the scale-up of promising dehydrogenation catalysts to scales closer to those relevant in the industrial context. During the scale-up towards an industrial process, the life cycle assessment (LCA) of the whole process should be fully contained to meet the sustainable and “green” goal. In addition, for the promising one-pot catalysts for CO_2-PDH described here, more research and calculations are required to determine the total energy consumption during the catalyst’s preparation and regeneration, carbon emission, waste catalyst disposal and so on. With these data,

we can fully and accurately evaluate the catalysts compared with the industrial catalysts by CSI.

6.2 CO_2 in Future

There are two main reasons to develop novel materials to catalyse propane dehydrogenation using CO_2. The first is due to the high demand for propylene as it is an important chemical feedstock. Propane dehydrogenation (PDH) is a promising catalytic technology utilised for the conversion of propane into propylene which is involved in many petrochemical applications.[6] The other reason is CO_2, as one of the most well-known greenhouse gases. It contributes over 60% to greenhouse gas (GHG) emission which is the main reason of the global warming.[7]

As mentioned in Chapter 1, the CO_2 content of the atmosphere has a significant impact on climate and ocean environment. The increase in global CO_2 emissions more than 2.1 Gt was the largest in modern history in absolute terms from the IEA analysis.[8] The removal of CO_2 from the atmosphere becomes one of the most urgent issues around the world. It is commonly accepted that people need to reduce the uses of fossil fuels as the energy resources to reduced CO_2 net emission. The Kyoto Protocol in April 2005 and the Paris Agreement in 2016 have been agreed by different countries around the world as the official arrangements for attempting to control the CO_2 emission and reach a “Carbon Neutral” state.

In Chapter 1, it has been mentioned about the development of renewable energies (mostly carbon-free) to take place of fossil fuels, but they cannot reach the large energy demand. The other route is the development of CCU, carbon capture and utilisation. This method is to use CO_2 as a feedstock and to convert CO_2 into useful chemical products. There are many studies, research and techniques have been focusing and

developed on CO_2 involved chemical manufacture which already been described in Chapter 1. However, the process or method to remove and collect CO_2 is very costly. Due to the thermodynamic limitation, most of the processes involving CO_2 are endothermic and require high temperatures. This encourages the development of different processes in the use of CO_2 and the development of different useful catalysts to provide the lowest energy pathways possible.

In the recent studies in CO_2 reduction, scientists and engineers combine CCS and CCU technologies together as CCUS, carbon capture, utilisation and storage, for CO_2 reduction. From IEA report, CCUS facilities around the world have the capacity to capture more than 40 Mt of CO_2 each year and the global anthropogenic CO_2 emissions over 32 billion tonnes per year.[9] Nowadays, around 230 Mt of CO_2 are used globally each year, around 125 Mt/year to produce fertilisers and 70-80 Mt/year for enhanced oil recovery.[10] There are also being developed new CO_2 utilisation pathways including using CO_2 to convert hydrogen into a synthetic hydrocarbon fuel, chemicals manufacture (using carbon in CO_2 as an alternative to fossil fuels in the production of some chemicals); and building materials (using CO_2 in the production of building materials to replace water in concrete or as a raw material in its constituents).[10] CCUS technologies can provide a means of removing CO_2 from the atmosphere, or called “negative net carbon emissions”. The reduce of total CO_2 emissions from industrial sectors to reach zero emissions may not be economically or technically feasible.

From my point of view, reduction of CO_2 emission will be the continuous main research area in the coming decades. It is important that the global scientific community should be combining all the different methods together to face the CO_2 challenge. In some of the area such as vehicles, we can use clean and carbon-free energy resources, for example, electricity or hydrogen instead of petroleum from fossil fuel; in chemical manufacturing industries, CO_2 from exhaust gas streams should be separated, removed and collected instead of just being released into the atmosphere. Efforts

should go into developing more processes which make use of CO_2. An example studied in this thesis is the propane dehydrogenation process using CO_2 as oxidant instead of oxygen. This has the potential to convert this greenhouse gas into CO which is an important platform chemical.[11] However, the catalysts for this process is still under research and development for scale up to industrial level. In biological view, CO_2 reduction can also be achieved by planting more trees or plants. As we know that trees and plants rely on CO_2 in the atmosphere to convert CO_2 into sugars via photosynthesis. A study published in July 2019, led by Thomas Crowther estimated the world has room for an extra 0.9 billion hectares of forest. Once those trees had matured, they could store 752 billion tonnes of CO_2.[12] But it is still much less than the total amount of annual CO_2 emission globally. In the end, all the countries should collaborate and cooperate for the aim of becoming “Carbon Neutral”, to create a more sustainable global environment.

References

1 S. Chen, X. Chang, G. Sun, T. Zhang, Y. Xu, Y. Wang, C. Pei and J. Gong, *Chem. Soc. Rev.*, 2021, **50**, 3315–3354.

2 P. Kuśtrowski, P. Michorczyk, L. Chmielarz, Z. Piwowarska, B. Dudek, J. Ogonowski and R. Dziembaj, *Thermochim. Acta*, 2008, **471**, 26–32.

3 S. F. Pan, J. L. Yin, X. L. Zhu, X. J. Guo, P. Hu, X. Yan, W. Z. Lang and Y. J. Guo, *Carbon N. Y.*, 2019, **152**, 855–864.

4 D. Pham Minh, X. H. Pham, T. J. Siang and D. V. N. Vo, *Appl. Catal. A Gen.*, 2021, **621**, 118202.

5 E. Gomez, S. Kattel, B. Yan, S. Yao, P. Liu and J. G. Chen, *Nat. Commun.*, 2018, **9**, 1–6.

6 H. A. Maddah, *Am. Sci. Res. J. Eng. Technol. Sci.*, 2018, **45**, 49–63.

7 C.-H. Huang and C.-S. Tan, *Aerosol Air Qual. Res.*, 2014, **14**, 480–499.

8 International Energy Agency, *Global CO_2 emissions rebounded to their highest level in history in 2021*, Paris, 2022.

9 M. Fajardy, *CCUS in Industry and Transformation*, Paris, 2021.

10 IEA (2021), About CCUS, IEA, Paris, https://www.iea.org/reports/about-ccus, (acessed by 20 Sept 2022).

11 B. Zhu, J. Meng, W. Yuan, X. Zhang, H. Yang, Y. Wang and Y. Gao, *Angew. Chemie - Int. Ed.*, 2020, **59**, 2171–2180.

12 S. L. Lewis, E. T. A. Mitchard, C. Prentice, M. Maslin and B. Poulter, *Science*, 2019, **366**, 1–3.

Appendix

Estimation of Errors

The assessment of the possible errors from all catalytic test results are the fundamental by important in this thesis.

Experimental error, also called observational error, is the difference between a measured quantity and its true value. It includes random error which is the naturally occurring errors that are to be expected with any experiment, and systematic error caused by particular instrument that will affect all measurements.

During the catalytic tests, if only a single measurement of a catalytic analysis is taken, any estimation of the error from that measured data may widely wrong. Because there may be a large personal or a large accidental error, as well as the systematic error. To help reduce, or revel the accidental errors occurred from a single measurement, repeated measurements of the same quantity was made during this study.

If a quantity X is measured n times and record as X_1, X_2, X_3…, X_n, the arithmetic mean $\bar{X}$ of n measurements is then,

$$\bar{X} = \frac{(X_1 + X_2 + X_3 + \ldots + X_n)}{n} \qquad (A.1)$$

n is the number of measurements was taken for the same quantity. Thus, the larger the value of n (number of times a measurement is made) the nearer $\bar{X}$ (the arithmetic mean) approaches the actual true value of the quantity. Therefore, we note that by repeated measurements of the same quantity, the experimental errors can be reduced in some degree, but systematic errors cannot be ruled out. Hence in general $\bar{X}$ will be taken as the actual or “theoretical” value of the measured quantity which the

measurements provide. The experimental errors, e_n, in each measurement can be written as follows:

$$e_n = | X_n - \bar{X} | \qquad \text{(A.2)}$$

During the actual measurements, the error from each measured quantity may be positive and/or negative. In any case e_n must be a positive number for calculate the percentage error and the average error, $\bar{e}$, is calculated using following equation:

$$\bar{e} = \frac{(e_1 + e_2 + e_3 + \ldots + e_n)}{n} \qquad \text{(A.3)}$$

In summary, in this thesis, each catalytic activity tests are taken at least 3 independents repeated measurements and all the experimental results with error less than 5%. So that to be considered as precise and reliable data for that measured quantity. The percentage errors are calculated by following:

$$\text{Percent error} = \frac{\bar{e}}{\bar{X}} \times 100\ \% \qquad \text{(A.4)}$$

There is a distinction between the terms of accuracy and precision. Accuracy refers to the closeness of the measurement to the “actual” or “real” value of any physical quantity, whereas, precision is used to indicate the closeness with which the measurements agree with one another quite independently of any systematic error involve.

Reference

J. Topping, *“Errors of observation and their treatment”*, 4th Edition, 1972, Chapman and Hall, Great Britain.